# SOME OPTIMIZATION PROBLEMS IN

# POWER SYSTEM RELIABILITY ANALYSIS

A Dissertation

by

PANIDA JIRUTITIJAROEN

Submitted to the Office of Graduate Studies of
Texas A&M University
in partial fulfillment of the requirements for the degree of

DOCTOR OF PHILOSOPHY

August 2007

Major Subject: Electrical Engineering

# SOME OPTIMIZATION PROBLEMS IN

# POWER SYSTEM RELIABILITY ANALYSIS

A Dissertation

by

PANIDA JIRUTITIJAROEN

Submitted to the Office of Graduate Studies of
Texas A&M University
in partial fulfillment of the requirements for the degree of

DOCTOR OF PHILOSOPHY

Approved by:

| | |
|---|---|
| Chair of Committee, | Chanan Singh |
| Committee Members, | Prasad Enjeti |
| | Andrew K. Chan |
| | Sergiy Butenko |
| Head of Department, | Costas N. Georghiades |

August 2007

Major Subject: Electrical Engineering

# ABSTRACT

Some Optimization Problems in Power System Reliability Analysis.

(August 2007)

Panida Jirutitijaroen,

B.Eng., Chulalongkorn University, Bangkok, Thailand

Chair of Advisory Committee: Dr. Chanan Singh

This dissertation aims to address two optimization problems involving power system reliabilty analysis, namely multi-area power system adequacy planning and transformer maintenance optimization. A new simulation method for power system reliability evaluation is proposed. The proposed method provides reliability indexes and distributions which can be used for risk assessment. Several solution methods for the planning problem are also proposed. The first method employs sensitivity analysis with Monte Carlo simulation. The procedure is simple yet effective and can be used as a guideline to quantify effectiveness of additional capacity. The second method applies scenario analysis with a state-space decomposition approach called global decomposition. The algorithm requires less memory usage and converges with fewer stages of decomposition. A system reliability equation is derived that leads to the development of the third method using dynamic programming. The main contribution of the third method is the approximation of reliability equation. The fourth method is the stochastic programming framework. This method offers modeling flexibility. The implementation of the solution techniques is presented and discussed. Finally, a probabilistic maintenance model of the transformer is proposed where mathematical

equations relating maintenance practice and equipment lifetime and cost are derived. The closed-form expressions insightfully explain how the transformer parameters relate to reliability. This mathematical model facilitates an optimum, cost-effective maintenance scheme for the transformer.

To My Late Grandmother, อาม่า สุ่ยฟ้า แซ่คิ้ว, and My Beloved Family

## ACKNOWLEDGMENTS

Thank you all who have helped me during my doctoral studies.

I especially want to thank my mentor, Dr. Chanan Singh, for his advice, guidance, and encouragement on academic as well as personal life for the past five years. His life and work philosophy have inspired me and shaped my way of thinking. I would also like to acknowledge Mrs. Singh for her thoughtful and kind support. I will always think of them fondly as my parents in College Station.

I would like to express my sincere appreciation to the committee members, Dr. Sergiy Butenko, Dr. Prasad Enjeti, and Dr. Andrew K. Chan, for their valuable comments and time. Thanks to Tammy Carda, Lisa Allen, and Nancy Reichart for their help related to the department. To Xu Bei, Satish Natti, and other colleagues in the Electric Power & Power Electronics Institute, I appreciate your valuable friendship and assistance. Thanks to the Power System Engineering Research Center and the National Science Foundation Grant No. ECS0406794 for their financial support.

My deepest gratitude goes to my wonderful parents, Pairat and Karuna Jirutitijaroen, and my brother, Panin Jirutitijaroen, for their everlasting love and support, to my grandmother, Yin Sae-Khiw, for her endless admiration and devotion. I also thank Wasu Glankwamdee whose constant encouragement gives me strength to go through my difficult times.

## TABLE OF CONTENTS

CHAPTER Page

I INTRODUCTION ..... 1

1.1 Introduction ..... 1
1.2 Objectives and Organization ..... 4

II SIMULATION METHODS FOR POWER SYSTEM RELIABILITY INDEXES AND THEIR DISTRIBUTIONS ..... 5

2.1 Introduction ..... 5
2.2 Latin Hypercube Sampling ..... 10
2.3 Discrete Latin Hypercube Sampling ..... 13
2.4 Comparison of the Sampled Distributions ..... 15
2.4.1 Sampled Generation Distribution ..... 17
2.4.2 Sampled Combined Generation and Load Distribution ..... 18
2.4.3 Sampled Unserved Energy Distribution ..... 21
2.5 Comparison of Reliability Indexes ..... 23
2.5.1 Loss of Load Probability Estimation ..... 23
2.5.2 Expected Unserved Energy Estimation ..... 25
2.6 Discussion and Conclusions ..... 27

III MULTI-AREA POWER SYSTEM ADEQUACY PLANNING USING MONTE CARLO SIMULATION WITH SENSITIVITY ANALYSIS ..... 30

3.1 Introduction ..... 30
3.2 System Modeling ..... 30
3.2.1 Area Generation Model ..... 31
3.2.2 Tie Line Model ..... 32
3.2.3 Area Load Model ..... 32
3.3 Purturbation Procedure ..... 33
3.3.1 Sequential Simulaion ..... 33
3.3.1.1 Fixed Time Interval ..... 34
3.3.1.2 Next Event Method ..... 35
3.3.2 State Sampling Simulation ..... 37
3.4 Computational Results ..... 37
3.5 Discussion and Conclusions ..... 39

IV MULTI-AREA POWER SYSTEM ADEQUACY PLANNING USING GLOBAL DECOMPOSITION WITH SCENARIO ANALYSIS ..... 41

CHAPTER Page

4.1 Introduction ..... 41
4.2 Review of Decomposition Approach for Reliability Evaluation ..... 42
4.2.1 Network Capacity Flow Model ..... 43
4.2.2 State Space Representation ..... 43
4.2.3 Partition an Unclassified Set ..... 44
4.2.4 Probability Calculation ..... 47
4.3 Scenario Analysis ..... 48
4.3.1 Comparison Algorithm for Generation Planning ..... 49
4.3.2 Comparison Algorithm for Transmission Line Planning ..... 52
4.4 Computational Results ..... 54
4.4.1 Generation Planning ..... 52
4.4.2 Transmission Line Planning ..... 56
4.5 Discussion and Conclusions ..... 58

V MULTI-AREA POWER SYSTEM ADEQUACY PLANNING USING GLOBAL DECOMPOSITION WITH DYNAMIC PROGRAMMING ..... 60

5.1 Introduction ..... 60
5.2 Problem Formulation ..... 62
5.2.1 Generation Probability Distribution Equation Incorporating Identical Additional Units ..... 65
5.2.2 Generation Probability Distribution Equation Incorporating Non-Identical Additional Units ..... 66
5.2.3 Reliability Equation and Approximation after Global Decomposition ..... 67
5.2.3.1 The First *A* Set Equation ..... 71
5.2.3.2 The First *L* Set Equation ..... 72
5.3 Dynamic Programming Application to the Problem ..... 75
5.3.1 Recursive Function of the First *A* Set Optimization ..... 77
5.3.2 Recursive Function of the First *L* Set Optimization ..... 79
5.4 Illustration on Three-Area Test System ..... 80
5.4.1 Illustration of the First *A* Set Optimization ..... 81
5.4.2 Illustration of the First *L* Set Optimization ..... 86
5.5 Implementation on Twelve-Area Test System ..... 93
5.6 Improvements Using Heuristic Search ..... 98
5.7 Discussion and Conclusions ..... 103

VI MULTI-AREA POWER SYSTEM ADEQUACY PLANNING USING STOCHASTIC PROGRAMMING ..... 108

6.1 Introduction ..... 108

CHAPTER Page

6.2 Problem Formulation ..... 109
6.3 Solution Procedures ..... 113
6.3.1 L-Shaped Algorithm ..... 115
6.3.2 Sampled Average Approximation ..... 117
6.3.2.1 Lower Bound Estimates ..... 119
6.3.2.2 Upper Bound Estimates ..... 120
6.3.2.3 Optimal Solution Approximation ..... 121
6.3.3 Sampling Techniques ..... 121
6.3.3.1 Mote Carlo Simulation ..... 122
6.3.3.2 Latin Hypercube Simulation ..... 122
6.4 Computational Results ..... 123
6.4.1 L-Shaped Algorithm ..... 123
6.4.2 Sampled Average Approximation ..... 124
6.5 Unit Availability Consideration ..... 132
6.6 Discussion and Conclusions ..... 139

VII TRANSFORMER MAINTENANCE OPTIMIZATION: A PROBABILISTIC MODEL ..... 142

7.1 Introduction ..... 142
7.1.1 Deterioration Process of a Transformer ..... 143
7.1.1.1 Deterioration Process of the Winding ..... 143
7.1.1.2 Deterioration Process of the Oil ..... 144
7.1.2 Maintenance Process of a Transformer ..... 144
7.1.2.1 Oil Filtering ..... 144
7.1.2.2 Oil Replacement ..... 145
7.1.3 Transformer Inspection Tests ..... 145
7.2 Transformer Maintenance Model ..... 149
7.3 Sensitivity Analysis ..... 153
7.4 Equivalent Models for Mathematical Analysis ..... 174
7.4.1 Perfect Maintenance Model ..... 175
7.4.2 Imperfect Maintenance Model ..... 175
7.5 Mean Time to the First Failure Analysis ..... 176
7.5.1 MTTFF for Perfect Maintenance Model ..... 177
7.5.2 MTTFF for Imperfect Maintenance Model ..... 179
7.6 Cost Analysis ..... 182
7.6.1 Cost Analysis for Perfect Maintenance Model ..... 183
7.6.2 Cost Analysis for Imperfect Maintenance Model ..... 186
7.7 Inspection Model ..... 189
7.8 Discussion and Conclusions ..... 194

VIII CONCLUSIONS ..... 195

Page

8.1 Conclusions ..... 195
8.2 Suggestions of Future Work ..... 197

REFERENCES ..... 199

APPENDIX A ..... 213

APPENDIX B ..... 216

APPENDIX C ..... 219

APPENDIX D ..... 222

VITA ..... 224

## LIST OF FIGURES

FIGURE Page


3.1 Area LOLP after Generation Addition ..... 38

4.1 Power System Network: Capacity Flow Model ..... 43

5.1 State Diagram of the Problem ..... 76

5.2 Stage Diagram of Three Area System ..... 81

5.3 Comparison of Algorithm Efficiency Produced by Different Initial Solutions ..... 102

6.1 Upper Bound and Lower Bound of Objective Function ..... 124

6.2 Bounds of SAA Solution with Monte Carlo Sampling ..... 131

6.3 Bounds of SAA Solution with Latin Hypercube Sampling ..... 132

7.1 Transformer Maintenance Model ..... 151

7.2 Relationship between MTTFF and Inspection Rate of Stage 1 ..... 154

7.3 Relationship between MTTFF and Inspection Rate of Stage 2 ..... 155

7.4 Relationship between MTTFF and Inspection Rate of Stage 3 ..... 156

7.5 Relationship between MTTFF and Inspection Rate of Stage 1 with Three Sub-Stages in Stage 1 ..... 158

7.6 Relationship between MTTFF and Inspection Rate of Stage 2 with Three Sub-Stages in Stage 1 ..... 159

7.7 Relationship between MTTFF and Inspection Rate of Stage 3 with Three Sub-Stages in Stage 1 ..... 160

7.8 Relationship between Expected Annual Failure Cost and Inspection Rate of Stage 1 ..... 162

7.9 Relationship between Expected Annual Maintenance Cost and Inspection Rate of Stage 1 ..... 163

7.10 Relationship between Expected Annual Inspection Cost and Inspection Rate of Stage 1 ..... 164

7.11 Relationship between Expected Annual Total Cost and Inspection Rate of Stage 1 ..... 165

7.12 Relationship between Expected Annual Failure Cost and Inspection Rate of Stage 2 ..... 166

FIGURE Page

7.13 Relationship between Expected Annual Maintenance Cost and Inspection Rate of Stage 2 ..... 167

7.14 Relationship between Expected Annual Inspection Cost and Inspection Rate of Stage 2 ..... 168

7.15 Relationship between Expected Annual Total Cost and Inspection Rate of Stage 2 ..... 169

7.16 Relationship between Expected Annual Failure Cost and Inspection Rate of Stage 3 ..... 170

7.17 Relationship between Expected Annual Maintenance Cost and Inspection Rate of Stage 3 ..... 171

7.18 Relationship between Expected Annual Inspection Cost and Inspection Rate of Stage 3 ..... 172

7.19 Relationship between Expected Annual Total Cost and Inspection Rate of Stage 3 ..... 173

7.20 Perfect Maintenance Equivalent Model ..... 175

7.21 Imperfect Maintenance Equivalent Model ..... 176

7.22 Inspection Model ..... 189

## LIST OF TABLES


| TABLE | | Page |
|---|---|---|
| 2.1 | Storage Comparison between DLHS and LHS | 15 |
| 2.2 | Number of States of Selected Area Generation Distribution for LHS | 17 |
| 2.3 | Performance Index of Sampled Generation Distribution from Monte Carlo Sampling | 18 |
| 2.4 | Performance Index of Sampled Combined Generation and Load Distribution from Monte Carlo Sampling | 19 |
| 2.5 | Performance Index of Sampled Combined Generation and Load Distribution from Latin Hypercube Sampling | 20 |
| 2.6 | Performance Index of Sampled Combined Generation and Load Distribution from Discrete Latin Hypercube Sampling | 20 |
| 2.7 | Performance Index of Sampled Unserved Energy Distribution from Monte Carlo Sampling | 21 |
| 2.8 | Performance Index of Sampled Unserved Energy Distribution from Latin Hypercube Sampling | 22 |
| 2.9 | Performance Index of Sampled Unserved Energy Distribution from Discrete Latin Hypercube Sampling | 22 |
| 2.10 | Percentage Error of Estimated LOLP from Monte Carlo Sampling | 24 |
| 2.11 | Percentage Error of Estimated LOLP from Latin Hypercube Sampling | 24 |
| 2.12 | Percentage Error of Estimated LOLP from Discrete Latin Hypercube Sampling | 25 |
| 2.13 | Percentage Error of Estimated EUE from Monte Carlo Sampling | 26 |
| 2.14 | Percentage Error of Estimated EUE from Latin Hypercube Sampling | 26 |
| 2.15 | Percentage Error of Estimated EUE from Discrete Latin Hypercube Sampling | 27 |
| 3.1 | Area LOLP before Generation Addition | 38 |
| 4.1 | Generation and Load Parameters | 55 |
| 4.2 | Number of Possible and Omitted Scenarios at Each Decomposition Stage for Generation Planning | 56 |
| 4.3 | Transfer Capability and Additional Capacity | 57 |

TABLE Page


4.4 Number of Possible and Omitted Scenarios at Each Decomposition Stage for Transmission Line Planning ..... 58

5.1 Three Area Addition Unit Parameters ..... 81

5.2 Available Budget and Modified Probability with Additional Units for the First *A* Set Optimization ..... 83

5.3 Optimal Decision at Stage 3 for the First *A* Set Optimization ..... 84

5.4 Optimal Decision at Stage 2 for the First *A* Set Optimization ..... 85

5.5 Optimal Decision at Stage 1 for the First *A* Set Optimization ..... 86

5.6 Available Budget and Modified Probability with Additional Units for the First *L* Set Optimization ..... 88

5.7 Optimal Decision at Stage 3 for the First *L* Set Optimization ..... 89

5.8 Optimal Decision at Stage 2 for the First *L* Set Optimization ..... 90

5.9 Optimal Decision at Stage 1 for the First *L* Set Optimization ..... 91

5.10 Comparison between Solutions from the First *L* Set Optimization and Enumerations ..... 91

5.11 Comparison between Solutions from the First *L* Set Optimization and Enumerations with System Load of 400, 500, and 400 in Areas 1, 2 and 3 ..... 92

5.12 Comparison between Solutions from the First *L* Set Optimization and Enumerations with System Load of 300, 400, and 300 in Areas 1, 2 and 3 ..... 93

5.13 Generation and Load Parameters of a Twelve Area Test System ..... 94

5.14 Solution with $0.5 Billion Budget ..... 95

5.15 Solution with $0.5 Billion Budget and 10% Increased Load ..... 95

5.16 Solution with $1 Billion Budget ..... 96

5.17 Solution with $1 Billion Budget and 10% Increased Load ..... 96

5.18 Comparison between the Solutions from the Proposed Method and the Optimal Solution ..... 96

5.19 Solution from an Optimization Method and Random Sampling ..... 101

TABLE Page

5.20 Comparison of Number of Computations between Exhaustive Search and Dynamic Programming ..... 104

6.1 Lower Bound Estimate from Monte Carlo Sampling ..... 126

6.2 Lower Bound Estimate from Latin Hypercube Sampling..... 126

6.3 Upper Bound Estimate and Approximate Solutions from Monte Carlo Sampling ..... 127

6.4 Upper Bound Estimate and Approximate Solutions from Latin Hypercube Sampling..... 128

6.5 Comparison between Possible Optimal Solutions ..... 129

6.6 Three Area Additional Unit Parameters with Unit Availability Consideration ..... 138

6.7 Upper Bound and Lower Bound of Objective Function with Unit Availability Consideration ..... 138

7.1 IEEE Std. C57.100-1986 Suggested Limits for In-Service Oil Group 1 by Voltage Class ..... 146

7.2 IEEE Std. C57.100-1986 Suggested Limits for Oil to Be Reconditioned or Reclaimed ..... 146

7.3 IEEE Std. C57.104-1991 Dissolved Gas Concentrations ..... 147

7.4 IEEE Std. C57.104-1991 Action Based on TDCG Analysis ..... 148

# CHAPTER I

# INTRODUCTION

## 1.1 Introduction

Electric power systems in the United States have been going through a restructuring process that transforms electric market from integrated utility to privately owned generation, transmission, and distribution units [21] [25]-[27] [30]. The key driving force of deregulation is to increase efficiency by introducing competitiveness to the energy market. To oversee system operation and ensure reliability, Independent System Operator (ISO), a public regional company, is established to monitor the market and provide congestion management. ISO is also responsible for power exchange market that determines real-time market clearing price in its service region, and several other auxiliary markets, including Installed Capacity Market (ICAP).

Several issues arise with deregulations since the market is now operating in an increasingly competitive environment that demands high reliability with the least expensive cost. The need for optimizing available resources in the market to maximize system reliability has assumed an increased importance. This research aims to address some optimization problems involving power system reliability in the new market structure namely, capacity expansion planning, and maintenance optimization.

Capacity expansion problem is one of the major optimization problems in the literature. Previously, utilities projected generation and transmission investment

---

This dissertation follows the style and format of *IEEE Transactions on Power Systems*.

concurrently and correlatively with the assumption of one bus model where all generating units and loads are connected into a single bus. Only generation requirement is evaluated while transmission lines were planned to ensure energy delivery ahead of time, consequently, the system is well balanced and stabilized. Under the deregulated environment, Independent Power Producers (IPPs) can install new generations virtually in any area which may results in imbalances between generation and transmission.

Installed Capacity Market (ICAP) is a capacity market such that firm capacities are procured as required by the ISO while the rest of the capacity can be paper traded. ICAP is established to guarantee long term system adequacy in the face of future increasing future demand. The requirement also helps prevent the power producers from limiting their power supplies, which reduce their ability to exercise market power. Long term adequacy analysis does not only benefit the consumers for affordable, efficient and reliable electricity but also serves the IPPs as a tool for minimum cost generation investment.

At the time of writing this dissertation, the capacity requirement is calculated by simulation and ad hoc methods. In particular, ISO--New England (ISO-NE) utilizes Multi-Area Reliability Simulation Program (MARS) for the calculation [15]. An optimization procedure along with MARS is proposed to determine an excess or deficient amount of generation in each area. One of the contributions of this paper is to show the relationship between each area risk level and load changes. The analysis pointed out that an exponential approximation of risk level [89] can be applied to multi-area systems. The major drawback of [15] is that the method requires iterations between

optimization and risk calculation which is obtained from several MARS runs. In a single MARS run, the outage of each component in the system is simulated chronologically by Monte Carlo sampling which may demand long history to produce converged results.

Optimization methods have been applied to solve capacity expansion problem without reliability considerations [10] [14] [31] [56] [67] [71] [79]. Mixed-integer programming [24] and dynamic programming have been proposed to incorporate the discrete decision of additional capacity and to obtain the sequence of optimal decisions respectively. Various optimization algorithms; such as, Branch and Bound and Bender's decomposition, have been applied to the problem. Heuristic techniques such as Fuzzy logic [12], greedy adaptive search [38], genetic algorithm [32], simulated annealing, and Tabu search have also beeen used [11] [51] [63]. This research aims to develop optimization techniques incorporating reliability constraints to the solution of capacity expansion problem, in particular, for multi-area power systems.

In addition to the multi-area adequacy problem, another important issue in the current aging infrastructure is the performance of a device since the system is now forced economically to operate at its limit that accelerates the aging process of most of the devices in the system. Electric supply utilities are now pursuing maintenance scheme in a cost effective fashion [35]. Transformers are considered one of the most common equipment in power systems. Their deterioration failures cause system interruption as well as high cost of load loss. Preventive maintenance can prevent this type of failure and help extend transformer lifetime. Too little or too much maintenance may lead to poor reliability or high maintenance cost. System reliability and cost should be balanced

to achieve cost effective maintenance. This study is intended to devise methodology for the optimal maintenance schedule for a transformer.

## 1.2 Objectives and Organization

The objective of this research is to develop optimization techniques and computational tools that systematically incorporate reliability aspects. The problem of interest is multi-area power system adequacy planning and transformer maintenance optimization. The organization of this dissertation is given below.

Chapter II proposes a new simulation method for power system reliability evaluation. Chapters III, IV, V, and VI propose different solution methods to multi-area power system adequacy planning problem. Chapter VII proposes a probabilistic model for transformer maintenance problem with equivalent mathematical equations relating maintenance practice and equipment lifetime and cost.

# CHAPTER II

# SIMULATION METHODS FOR POWER SYSTEM RELIABILITY INDEXES AND THEIR DISTRIBUTIONS*

## 2.1 Introduction

Mathematical models for computing reliability indices can be solved either by direct analytical methods or using a simulation approach. Although the analytical solutions are exact within the assumptions made, they are sometimes difficult to derive for a large power system. While the simulation methods produce only estimates of reliability indexes, they generally provide more flexibility in dealing with complex systems and conditions. Most of current simulation methods evolve from Monte Carlo simulation (MC). The principal advantage of this approach is its simplicity to implement at any levels of reliability analysis. However, MC can require long computation time to produce converged results. Thus, there is a need for efficient simulation methods for reliability analysis of large power systems.

There are two basic approaches in Monte Carlo – sequential simulation and random sampling. In the remainder of this chapter, MC refers to the sampling technique where the basic concept is to draw random samples of system states. Reliability indexes are then statistically estimated from these samples. The converged results are found when the normalized variance of an estimate lies within an acceptable level. The

---

* Reprinted with permission from "Comparison of Simulation Methods for Power System Reliability Indexes and Their Distribution" by P. Jirutitijaroen and C. Singh, *IEEE Transactions on Power Systems,* to be published. © 2007 IEEE

convergence of the estimate depends heavily on the occurrence of loss of load events. As a result, the efficiency of MC deteriorates for the power system having a high level of reliability. In other words, when the power system is highly reliable, the probability of loss of load states becomes small and estimating the rare-event probability is very time consuming.

To overcome this problem, one approach is to employ variance reduction techniques such as Importance Sampling (IS), Control Variate, and Antithetic Variate methods [33] [59] [75]. The main idea of IS is to make the rare-events more frequently sampled by modifying the probability distribution function of system components so that loss of load events are more likely to occur [18] [41] [58] [74]. Control Variate and Antithetic Variate methods exploit correlations among random variables to achieve variance reduction [75]. Convergence in these methods is based on a new random variable whose mean value is the same as of the original but has lower variance. These variance reduction methods are generally found to successfully reduce simulation time; however, the probability distribution functions of predictor variables are altered from that of the original even though the mean values stay the same. Therefore, these methods are suitable for the analysis when mean values of the indices are of primary interest. However, it may become less attractive to apply these methods when the integrity of the actual distribution functions needs to be preserved such as in risk analysis and in the optimization framework.

An integration of reliability evaluation and optimization procedures is used in many types of problems; for example, planning [4] [6] [15] and design [19] problems.

These problems often search for the best solution that maximizes system reliability while minimizing cost and can be considered as stochastic programming problems due to system uncertainties in reliability evaluation. In order to describe the stochastic behavior of system components, their probability distribution functions need to be taken into account. The available solution algorithms of stochastic programming, such as the L-shaped algorithm, are based on enumeration of states [46] [60] [62]. When components possess continuous probability distribution function or discrete probability distribution function with a large number of states, the algorithm may become computationally intractable. To overcome this problem, algorithms employing sampling techniques, for example, SAA (Sample-Average approximation) [9] [29] [60] and Stochastic Decomposition [62] are proposed. These algorithms require that the fidelity of probability distribution function be maintained while the sampling is carried out. Details of available stochastic algorithms are beyond the scope of this chapter. Interested readers are referred to [60].

Latin Hypercube Sampling (LHS), developed by McKay, Conover, and Beckman in 1979, is a marriage between stratified and random sampling [28] [85]. The sample size, n, is pre-selected and the probability distribution function is divided into n intervals with equal probability of occurrence. Random sampling is then performed for each interval corresponding to the probability distribution function in that interval. This means that LHS is a constrained version of MC sampling that can produce estimates more precise than MC with the same sample size. LHS is thus considered as one of the variance reduction techniques. This major advantage can be exploited when combining

reliability evaluation with optimization. LHS is currently used in the stochastic optimization framework in comparison with MC sampling. The results show that the method produces tighter bounds of the optimal solution than MC [9] [29]. In addition, the approximate distributions of the reliability indexes are also generated which may be used as a risk assessment tool since reliability index itself only represents the mean value.

In general, stochastic nature of components of a power system is modeled in terms of discrete probability distribution functions based on their failure and repair rates. In order to perform LHS, discrete probability distribution functions of area generation and load need to be constructed prior to sampling. This means that LHS uses some extra computation time during the equivalent distribution function construction while MC can sample states according to the failure and repair rates of a unit. To reduce this computation time, Discrete Latin Hypercube Sampling (DLHS) is proposed in this study. DLHS is a modified version of LHS that is done at the component level based on its failure and repair rate without creating an equivalent discrete distribution function. DLHS not only saves computation time and storage to construct the equivalent distribution functions, but also requires less storage than LHS during sampling. Other modifications of LHS are tailored to fit particular applications and can be found in [45].

Multi-area reliability analysis has two major approaches; Monte-Carlo simulation and state-space decomposition. In Monte-Carlo simulation, failure and repair history of components are created using their probability distributions. Reliability indices are estimated by statistical inferences. The basic concept of state-space decomposition,

originally proposed in [46], is to classify the system state space into three sets; acceptable sets (A sets), unacceptable sets (L sets), and unclassified sets (U sets) while the reliability indices are calculated concurrently. Advanced versions of decomposition such as simultaneous-decomposition for including load and planned outages in a computationally efficient manner are described in [19], [29], [33], [39].

This research proposes LHS and DLHS for reliability evaluation of power systems and illustrates the process using a single area power system. It should be pointed out that LHS and DLHS can be used for a multi-area power system as well as single area. Single area is chosen for illustration since the correct distributions for single area can be readily obtained using enumeration for the purposes of comparison. Reliability indexes in this study are loss of load probability and expected unserved energy. Both sampling techniques produce approximated distribution function for unserved energy. The comparisons among LHS, DLHS and conventional MC sampling are presented including analysis of efficiency and accuracy of each method. More specifically, a performance index is used to determine the accuracy of the approximated distribution functions from LHS, DLHS and MC to the actual ones found from enumerations. Several comparisons of the sampled distribution functions are made at generation level, combined generation and load level, and finally, unserved energy. The test system is an actual twelve-area power system with a variety of unit types in terms of capacity, availability, and quantity.

This chapter is organized as the following. Section 2.2 explains mechanism of LHS in detail. DLHS is then proposed in section 2.3. A comparison of approximated

distribution produced by three sampling techniques is presented in section 2.4 while that of reliability indexes, namely unserved energy and loss of load probability, is given in section 2.5. Finally, conclusions are given in section 2.6.

## 2.2 Latin Hypercube Sampling

LHS was invented to estimate uncertainty in a problem where the variable of interest is expressed as a function of random variables [28] as follow.

$$y = f(\mathbf{x}) \tag{2.1}$$

where

$y$ = The variable of interest

$\mathbf{x}$ = Random variables

When the function to be evaluated is complicated and computation intensive, investigation of interaction of variable of interest with other stochastic variables (in multi-dimension) is inevitably cumbersome. LHS has been developed as a probabilistic risk assessment tool to specifically assist this type of investigation. The very first application of LHS was a reactor safety study of nuclear power plants [9]. Recently, LHS has been applied in the stochastic optimization framework. The test problems include vehicle routing [29], aircraft allocation, electric power planning, telecom network design, and cargo flight scheduling problems [9]. The problem uncertainties represented by probability distribution functions are incorporated into the model. Due to numerous system states, sampling techniques are employed to reduce the states to be evaluated in the optimization algorithm. The results show that LHS outperforms MC

sampling by producing tighter upper and lower bounds of the optimal objective values with the same sample size. LHS has been also applied to statistical modeling of microwave devices [39].

While MC is conventionally applied for power system reliability problems, LHS can yield relatively better estimate of the distribution of the variable of interest than MC [28], [85]. This is due to the fact that prior to sampling, LHS divides a distribution function into intervals of equal probability. The number of intervals is equal to sample size. Then LHS randomly chooses one value from each and every subinterval with respect to its distribution in that subinterval. This means that LHS is done over the entire spectrum of the distribution function, including the tail-end values. The sampled values thus represent the actual distribution better than MC especially for the extreme region of the distribution. The variance of a sample from LHS is considered smaller than that from MC since LHS yields a stratified sample of the random variables.

With multi-dimensional random variables, LHS creates a system state by pairing the values after sampling each random variable individually. The pairing scheme is rather simple in the case of uncorrelated random variables. A system state is found by randomly choosing one value out of the sampled values from each component without replacement. However, in case of random variables with certain correlation among them, a strategy of pairing scheme will involve use of optimization. A full description of the pairing scheme in such cases is beyond the scope of this chapter. Interested readers are referred to [3] for detailed procedure in the presence of correlations between random variables. LHS as applied in this dissertation is described as follows.

The sample size, n, is specified in advance. Next, the equivalent probability distribution functions of area generation and load are divided into n subintervals with equal probability, . A value is randomly chosen from each and every subinterval. At this point, there are n generation values and n load values from each area. Then, a system state is constructed from randomly pairing area generation to area load. This constitutes n samples of system state for each area. Steps of LHS are presented as follows.

1. Specify sample size, n.
2. Construct discrete distribution function of area load and generation.
3. Divide equivalent area generation and load distribution functions into n subintervals with equal probability.
4. Randomly sample without replacement and record a value from each and every subinterval corresponding to its distribution in that subinterval.
5. Perform random permutations to produce pairs of generation and load.
6. Use each pair as a system state for reliability analysis.

Note that in step 4, the n sampled values of each component need to be stored for the pairing in step 5. Then, after random pairing, reliability can be evaluated from each pair of area generation and load. MC, on the contrary, samples generation capacity state by randomly choosing capacity of each unit according to its failure and repair rates, and then summarizing over all available units in that area. Reliability evaluation is done without storing all sampled values of area generation and load. This means that LHS requires extra space to store samples of generation and load for pairing. In addition, the

equivalent distribution functions of area generation need to be constructed before sampling.

To reduce the storage requirement for pairing and the extra computation time for constructing equivalent distribution functions, DLHS is proposed in this dissertation. The detailed procedure is presented in the next section.

## 2.3 Discrete Latin Hypercube Sampling

DLHS is a special case of LHS proposed specifically for a random variable with discrete distribution function. DLHS is performed at the unit level based on its failure and repair rates or its state probabilities to avoid constructing equivalent distribution function. Generally, a unit is represented by two-stage Markov model. This assumption can be relaxed and the same procedure can also apply to a multi-stage Markov model. Probability of a unit being in up and down states can be found from the following formula.

$$p_i^U = \frac{\mu_i}{\mu_i + \lambda_i} \tag{2.2}$$

$$p_i^D = \frac{\lambda_i}{\mu_i + \lambda_i} \tag{2.3}$$

where

$p_i^U$ = Probability of a unit *i* being in up state

$p_i^D$ = Probability of a unit *i* being in down state

$\mu_i$ = Repair rate of a unit *i*

$\lambda_i$ = Failure rate of a unit *i*

For a pre-selected sample size, *n*, number of times that a unit will stay in up or down state is proportional to its probability in (2.2) and (2.3), respectively. Random sampling is performed to choose a state of each unit. Then, an area generation state is found by summing capacities of all available units. This means that instead of storing sampled state capacity as in LHS, DLHS stores only number of up or down states of a unit. DLHS also does not require constructing equivalent distribution function of area generation. Steps of DLHS are presented as follows.

1. Specify sample size, *n*.
2. For all units, compute and record number of times unit *i* is in up state.
3. Randomly sample status of each generating unit without replacement.
4. Summarize generation capacity from all available units.
5. Choose load state by LHS and randomly pair with generation states.
6. Use each pair as a system state for reliability analysis.

It can be seen that DLHS requires recording only number of up states for all units while LHS requires storing *n* sampled values of generation states before pairing. This storage reduction is significant when the sample size is considerably large. Additionally, DLHS reduces storage space of tens of thousand of generation states resulting from equivalent discrete distribution function of area generation. If an area possesses *m* generating units with different capacity and a sample size is *n*, Table 2.1 shows the comparison of storage required between DLHS and LHS for a single area reliability analysis.

Table 2.1 Storage Comparison between DLHS and LHS

| Space required when | LHS | DLHS |
|---|---|---|
| Creating equivalent PDF | At most $2^m$ | - |
| Selecting a generation state | $n$ | $m$ |

Since DLHS is applied at the component level, the resulting sampled distribution of DLHS is somewhat less representative of the actual distribution than that of LHS. However, the computation efficiency is increased and the storage space is reduced. Later analysis will show that the gain from reducing storage and computation time exceeds the loss in accuracy.

## 2.4 Comparison of the Sampled Distributions

The test system as shown in Appendix A is a multi-area representation of an actual power system [6] [17]. Single area reliability analysis is performed for all areas except area 6, 7, and 8 which have no load. Area generating unit statistics are given in Table A.1. Generating unit failure and repair rate data are from IEEE Reliability Test System 1996. Area loads are grouped into eight clusters each; the peak value is shown in Table A.2. Hourly load models can also be used. Reliability indexes of each area are also shown in Table A.2**.** Frequency and duration indices can be calculated using the formulas given in [43] [58] [64]. It can be seen that each area possesses a variety of generating units. This diversity in capacity and number of units affects smoothness of the equivalent generation distribution functions, which, in turn, affects the efficiency of

the sampling techniques. Next, the comparison of sampled distribution function is made among MC, LHS, and DLHS.

In single area reliability analysis, area generation and load states are sampled to determine if the area suffers loss of load or not. Thus, the analysis can be divided into three parts; generation, combined generation and load, and then unserved energy. This chapter investigates the effect of sampling techniques, MC, LHS and DLHS on the distribution of all three parts of single area reliability analysis.

In order to measure the accuracy among MC, LHS, and DLHS, the sampled distributions are compared with the actual ones found from enumeration. It may be difficult to compare the sampled distributions visually, thus a performance index is used to determine the closeness of sampled distribution to the actual one. The index is adopted from chi-square test and is shown in (2.4). The actual distributions are divided into intervals such that the expected number of occurrences in each interval is at least five.

$$\text{Performance Index} = \sum_{j=1}^{k} \frac{\left(\text{Observed}_j - \text{Expected}_j\right)^2}{\text{Expected}_j} \tag{2.4}$$

where

$\text{Observed}_j$ = Observed frequency of interval $j$

$\text{Expected}_j$ = Expected frequency of interval $j$

$k$ = Number of interval

The analysis is performed with five sample sizes, 1000, 2000, 5000, 10000, and 20000 and repeated ten times for each sample size. The performance index is statistically inferred by averaging over 10 batches of samples to handle randomness in the sampling.

Table 2.2 Number of States of Selected Area Generation Distribution for LHS

| Area | 1 | 2 | 3 | 9 | 10 | 11 |
|---|---|---|---|---|---|---|
| No. of States | 1777 | 21860 | 13513 | 1576 | 2276 | 3422 |

In case of LHS, the distributions need to be stored during sampling while DLHS does not even require distribution construction. Table 2.2 gives the number of storage entries for LHS. From this table, it can be appreciated that the computational space would be dramatically reduced in case of DLHS as it would not require this storage. DLHS also reduces storage required during the course of sampling. For example, when the sample size is 1000 for area 2, LHS requires 1000 spaces while DLHS requires only 32, which is number of units in area 2. When the sample size increases to 5000 for area 2, LHS would require 5000 spaces while space requirement for DLHS remains at 32.

### 2.4.1 Sampled Generation Distribution

For LHS and DLHS, the performance indexes of sampled generation distribution of all areas are zero regardless of the sample size. Performance index of MC in this case is shown in Table 2.3. The sampled generation distributions from MC tend to approach the actual ones as sample size increases. In particular, the generation distributions in

area 5 and 12 are closer to the actual ones than other areas. This may be due to the fact that their unit quantities are small and their capacities are evenly distributed. This would indicate that generating unit variety in each area contributes to the sampling accuracy.

Table 2.3 Performance Index of Sampled Generation Distribution from Monte Carlo Sampling

| Area | Sample size | | | | |
|---|---|---|---|---|---|
| | 1000 | 2000 | 5000 | 10000 | 20000 |
| 1 | 2.90 | 2.72 | 2.95 | 2.26 | 4.21 |
| 2 | 11.12 | 12.58 | 12.22 | 11.48 | 9.99 |
| 3 | 9.36 | 12.35 | 10.24 | 9.48 | 9.52 |
| 4 | 4.55 | 3.58 | 4.47 | 4.11 | 3.69 |
| 5 | 0.33 | 0.38 | 0.29 | 0.22 | 0.22 |
| 9 | 2.08 | 0.88 | 1.21 | 1.48 | 1.42 |
| 10 | 7.19 | 5.79 | 6.09 | 7.04 | 5.50 |
| 11 | 3.38 | 5.01 | 5.34 | 3.45 | 6.80 |
| 12 | 0.31 | 0.16 | 0.11 | 0.10 | 0.08 |

The sampled generation distributions from both LHS and DLHS perfectly represent the actual generation distribution. This means that DLHS performs as well as LHS in terms of accuracy but requires less computation time and storage.

### 2.4.2 Sampled Combined Generation and Load Distribution

Performance indexes of MC, LHS, and DLHS are shown in Table 2.4, Table 2.5, and Table 2.6 respectively. It can be seen that the performance indexes in the case of LHS and DLHS are smaller than those of MC. This would indicate a closer fit to the

actual distribution for LHS and DLHS. By examining the equation of the performance index, this means that that MC would give higher deviation of observed interval frequency from the expected frequency, indicating a higher degree of randomness.

Table 2.4 Performance Index of Sampled Combined Generation and Load Distribution from Monte Carlo Sampling

| Area | Sample size | | | | |
|---|---|---|---|---|---|
| | 1000 | 2000 | 5000 | 10000 | 20000 |
| 1 | 27.27 | 36.97 | 72.10 | 127.67 | 240.54 |
| 2 | 20.08 | 28.50 | 50.63 | 74.35 | 140.96 |
| 3 | 19.83 | 26.03 | 39.83 | 62.63 | 111.58 |
| 4 | 14.09 | 15.86 | 27.83 | 41.06 | 67.69 |
| 5 | 27.47 | 36.18 | 87.65 | 153.24 | 285.43 |
| 9 | 21.24 | 32.62 | 70.21 | 119.08 | 222.75 |
| 10 | 24.01 | 32.47 | 67.09 | 113.96 | 226.34 |
| 11 | 14.28 | 23.86 | 32.75 | 68.03 | 95.85 |
| 12 | 23.83 | 36.66 | 88.21 | 149.47 | 286.22 |

Table 2.5 Performance Index of Sampled Combined Generation and Load Distribution from Latin Hypercube Sampling

| Area | Sample size | | | | |
|---|---|---|---|---|---|
| | 1000 | 2000 | 5000 | 10000 | 20000 |
| 1 | 8.84 | 7.80 | 8.90 | 5.50 | 7.72 |
| 2 | 9.05 | 10.73 | 11.31 | 13.67 | 11.40 |
| 3 | 10.35 | 9.97 | 14.53 | 11.93 | 14.01 |
| 4 | 7.61 | 7.92 | 8.61 | 8.00 | 7.17 |
| 5 | 4.21 | 2.70 | 2.62 | 3.65 | 3.09 |
| 9 | 5.92 | 6.76 | 7.76 | 3.54 | 6.28 |
| 10 | 9.32 | 9.69 | 9.99 | 8.72 | 7.29 |
| 11 | 9.65 | 10.56 | 7.56 | 8.51 | 7.26 |
| 12 | 2.57 | 4.18 | 2.34 | 2.22 | 5.02 |

Table 2.6 Performance Index of Sampled Combined Generation and Load Distribution from Discrete Latin Hypercube Sampling

| Area | Sample size | | | | |
|---|---|---|---|---|---|
| | 1000 | 2000 | 5000 | 10000 | 20000 |
| 1 | 7.58 | 9.10 | 9.93 | 10.26 | 9.05 |
| 2 | 11.96 | 15.19 | 14.67 | 12.14 | 11.87 |
| 3 | 8.73 | 16.68 | 11.93 | 11.41 | 12.09 |
| 4 | 8.13 | 8.46 | 7.34 | 10.33 | 7.61 |
| 5 | 3.17 | 3.22 | 3.03 | 4.01 | 4.65 |
| 9 | 5.06 | 6.72 | 4.46 | 4.87 | 4.62 |
| 10 | 9.07 | 7.70 | 10.80 | 7.27 | 11.95 |
| 11 | 9.10 | 8.56 | 9.46 | 9.45 | 12.46 |
| 12 | 2.83 | 2.69 | 3.27 | 3.23 | 2.44 |

It can be seen from Table 2.5 and Table 2.6 that the distributions obtained using DLHS, represent the actual ones as closely as LHS.

### 2.4.3 Sampled Unserved Energy Distribution

Unserved energy distribution is the conditional probability distribution function of combined generation and load when the system load is not satisfied. Performance indexes of MC, LHS, and DLHS are shown in Table 2.7, Table 2.8 and Table 2.9 respectively. Performance index of MC is higher than LHS and DLHS in all areas, especially in area 10 and 12, which have high LOLP. This indicates that LHS and DLHS represent unserved energy distribution better than MC. In addition, sample distribution from DLHS, again, represents the actual ones as well as that from LHS.

Table 2.7 Performance Index of Sampled Unserved Energy Distribution from Monte Carlo Sampling

| Area | Sample size | | | | |
|---|---|---|---|---|---|
| | 1000 | 2000 | 5000 | 10000 | 20000 |
| 1 | 2.50 | 1.99 | 4.69 | 3.43 | 2.31 |
| 2 | 1.45 | 1.21 | 1.68 | 2.26 | 0.81 |
| 3 | 1.61 | 1.25 | 1.01 | 1.91 | 1.96 |
| 4 | 3.16 | 4.95 | 2.44 | 4.03 | 4.33 |
| 5 | 0.78 | 1.06 | 1.01 | 0.90 | 1.08 |
| 9 | 2.86 | 3.26 | 2.59 | 5.33 | 2.24 |
| 10 | 11.19 | 11.22 | 13.90 | 13.67 | 18.17 |
| 11 | 0.80 | 1.43 | 1.22 | 1.37 | 1.32 |
| 12 | 13.28 | 12.60 | 15.42 | 25.31 | 20.67 |

Table 2.8 Performance Index of Sampled Unserved Energy Distribution from Latin Hypercube Sampling

| Area | Sample size | | | | |
|---|---|---|---|---|---|
| | 1000 | 2000 | 5000 | 10000 | 20000 |
| 1 | 3.01 | 2.60 | 2.83 | 2.92 | 1.93 |
| 2 | 0.55 | 0.58 | 0.58 | 0.99 | 0.69 |
| 3 | 0.97 | 0.41 | 1.15 | 0.82 | 0.33 |
| 4 | 1.50 | 1.60 | 3.34 | 2.07 | 2.02 |
| 5 | 0.40 | 1.10 | 0.76 | 0.88 | 0.34 |
| 9 | 1.92 | 4.11 | 2.85 | 2.49 | 1.47 |
| 10 | 9.77 | 9.80 | 11.70 | 8.07 | 12.75 |
| 11 | 0.46 | 0.44 | 0.73 | 0.43 | 0.69 |
| 12 | 8.48 | 10.01 | 8.79 | 7.45 | 9.58 |

Table 2.9 Performance Index of Sampled Unserved Energy Distribution from Discrete Latin Hypercube Sampling

| Area | Sample size | | | | |
|---|---|---|---|---|---|
| | 1000 | 2000 | 5000 | 10000 | 20000 |
| 1 | 2.09 | 1.81 | 3.13 | 2.62 | 3.90 |
| 2 | 3.28 | 0.85 | 1.44 | 0.52 | 1.74 |
| 3 | 0.74 | 1.29 | 1.19 | 0.91 | 0.82 |
| 4 | 3.45 | 3.41 | 3.21 | 3.93 | 3.50 |
| 5 | 1.07 | 1.23 | 1.01 | 0.99 | 1.31 |
| 9 | 2.19 | 2.84 | 3.19 | 2.23 | 2.67 |
| 10 | 9.98 | 9.84 | 13.30 | 10.71 | 13.87 |
| 11 | 0.75 | 0.64 | 2.00 | 1.08 | 0.99 |
| 12 | 10.09 | 8.62 | 10.15 | 10.05 | 9.35 |

It should be noted that unserved energy distribution represents tail-end region of combined generation and load distribution. The expected number of occurrences is quite small in this region especially in areas 2, 3, 5, and 11 where LOLP is small. The

performance indexes for these areas seem to be small, or equivalently, the sampled distributions are very close to the actual ones; however, the reliability estimates in the next section will show otherwise. This behavior of performance index is due to the small occurrence of values of actual distribution.

## 2.5 Comparison of Reliability Indexes

Reliability indexes in this study are loss of load probability and expected unserved energy. Percentage error of the estimates is found from averaging the percentage absolute deviation from the actual value, over all ten batches of sample. The formula is shown in the following.

$$\text{Error} = \frac{1}{m}\sum_{i=1}^{m}\frac{\left|\text{Estimate}_i - \text{Actual}\right|}{\text{Actual}} \times 100\% \tag{2.5}$$

where

$\text{Estimate}_i$ = Reliability index of batch *i*

Actual = Reliability index from enumeration

*m* = Number of batch

The resulting percentage errors from different sampling techniques are shown in the following.

### 2.5.1 Loss of Load Probability Estimation

Percentage error of LOLP estimates are shown in Table 2.10, Table 2.11, and Table 2.12. As sample size increases, the estimates are closer to the actual values for all

sampling techniques. In addition, LHS and DLHS produce closer LOLP estimates than MC, especially for areas 10 and 12 where LOLP is comparatively high. Percentage error of the estimates shows that LHS and DLHS outperform MC for all areas. Overall LHS appears to be the best predictor for LOLP, especially in areas with small LOLP such as area 2, 3, 5, and 11.

Table 2.10 Percentage Error of Estimated LOLP from Monte Carlo Sampling

| Area | Sample size | | | | |
|---|---|---|---|---|---|
| | 1000 | 2000 | 5000 | 10000 | 20000 |
| 1 | 25.60 | 16.99 | 8.93 | 11.03 | 5.84 |
| 2 | 58.76 | 32.29 | 31.40 | 22.28 | 10.45 |
| 3 | 110.03 | 69.24 | 38.46 | 42.32 | 31.36 |
| 4 | 26.62 | 27.27 | 8.26 | 9.21 | 5.39 |
| 5 | 45.23 | 35.08 | 22.03 | 15.81 | 10.83 |
| 9 | 19.13 | 16.81 | 8.72 | 8.75 | 5.99 |
| 10 | 07.27 | 8.37 | 6.61 | 5.67 | 4.41 |
| 11 | 40.00 | 32.56 | 24.86 | 15.18 | 11.82 |
| 12 | 7.17 | 4.84 | 5.24 | 6.16 | 4.89 |

Table 2.11 Percentage Error of Estimated LOLP from Latin Hypercube Sampling

| Area | Sample size | | | | |
|---|---|---|---|---|---|
| | 1000 | 2000 | 5000 | 10000 | 20000 |
| 1 | 24.01 | 11.40 | 12.62 | 8.41 | 4.53 |
| 2 | 37.98 | 29.38 | 16.46 | 16.70 | 10.50 |
| 3 | 80.78 | 38.09 | 47.69 | 25.77 | 8.86 |
| 4 | 19.66 | 13.50 | 9.01 | 4.76 | 2.98 |
| 5 | 28.61 | 38.46 | 19.26 | 14.52 | 7.14 |
| 9 | 15.82 | 10.94 | 9.25 | 4.02 | 3.51 |
| 10 | 5.74 | 3.71 | 2.80 | 1.69 | 1.55 |
| 11 | 30.31 | 19.24 | 15.52 | 9.18 | 8.14 |
| 12 | 2.99 | 2.19 | 1.25 | 0.72 | 0.58 |

Table 2.12 Percentage Error of Estimated LOLP from Discrete Latin Hypercube Sampling

| Area | Sample size | | | | |
|---|---|---|---|---|---|
| | 1000 | 2000 | 5000 | 10000 | 20000 |
| 1 | 13.49 | 14.47 | 6.66 | 6.85 | 6.53 |
| 2 | 75.97 | 34.07 | 29.12 | 10.88 | 13.94 |
| 3 | 80.78 | 69.64 | 42.32 | 30.01 | 19.81 |
| 4 | 21.30 | 13.58 | 10.45 | 4.97 | 5.19 |
| 5 | 53.23 | 36.62 | 24.31 | 17.05 | 13.97 |
| 9 | 16.22 | 13.27 | 6.13 | 3.88 | 4.48 |
| 10 | 9.02 | 4.89 | 3.30 | 1.87 | 1.99 |
| 11 | 41.44 | 25.16 | 28.29 | 15.22 | 10.76 |
| 12 | 3.84 | 2.09 | 1.93 | 1.02 | 0.55 |

### 2.5.2 Expected Unserved Energy Estimation

Percentage errors of EUE estimates are shown in Table 2.13, Table 2.14, and Table 2.15. As sample size increases, the estimates are closer to the actual values for all sampling techniques. In general, LHS and DLHS perform better than MC. More specifically, LHS predicts EUE better than MC almost in all areas except in area 3, where DLHS produces the best EUE estimates in areas 2 and 3. LHS predicts EUE the best in areas with high LOLP (area 10 and 12) where DLHS predicts EUE the best in areas with low LOLP (area 2 and 3).

Table 2.13 Percentage Error of Estimated EUE from Monte Carlo Sampling

| Area | Sample size | | | | |
|---|---|---|---|---|---|
| | 1000 | 2000 | 5000 | 10000 | 20000 |
| 1 | 16.34 | 8.93 | 5.73 | 6.77 | 3.63 |
| 2 | 43.02 | 42.16 | 20.75 | 15.06 | 11.95 |
| 3 | 90.21 | 54.63 | 61.83 | 28.47 | 23.37 |
| 4 | 18.77 | 18.34 | 14.72 | 8.32 | 5.19 |
| 5 | 53.66 | 41.01 | 23.76 | 13.07 | 7.02 |
| 9 | 10.45 | 7.00 | 6.80 | 4.63 | 3.29 |
| 10 | 9.11 | 7.71 | 5.25 | 1.94 | 2.60 |
| 11 | 48.30 | 28.53 | 15.23 | 5.81 | 8.79 |
| 12 | 5.91 | 4.65 | 3.16 | 2.48 | 1.88 |

Table 2.14 Percentage Error of Estimated EUE from Latin Hypercube Sampling

| Area | Sample size | | | | |
|---|---|---|---|---|---|
| | 1000 | 2000 | 5000 | 10000 | 20000 |
| 1 | 11.72 | 13.59 | 6.47 | 7.40 | 2.20 |
| 2 | 52.36 | 28.87 | 16.24 | 16.96 | 9.58 |
| 3 | 104.84 | 46.10 | 56.66 | 21.43 | 25.34 |
| 4 | 15.41 | 11.61 | 11.09 | 9.01 | 4.14 |
| 5 | 31.12 | 36.67 | 19.25 | 13.04 | 8.26 |
| 9 | 8.77 | 15.57 | 5.73 | 4.96 | 2.08 |
| 10 | 9.40 | 4.80 | 3.50 | 2.42 | 1.94 |
| 11 | 25.80 | 15.72 | 11.85 | 14.24 | 4.27 |
| 12 | 4.10 | 3.40 | 1.75 | 0.92 | 0.87 |

Table 2.15 Percentage Error of Estimated EUE from Discrete Latin Hypercube Sampling

| Area | Sample size | | | | |
|---|---|---|---|---|---|
| | 1000 | 2000 | 5000 | 10000 | 20000 |
| 1 | 18.72 | 13.30 | 13.04 | 5.37 | 4.54 |
| 2 | 56.59 | 28.11 | 20.55 | 14.84 | 6.44 |
| 3 | 79.79 | 49.79 | 41.93 | 20.45 | 18.51 |
| 4 | 19.52 | 15.47 | 8.83 | 11.20 | 6.38 |
| 5 | 46.32 | 16.53 | 16.02 | 8.22 | 8.66 |
| 9 | 17.29 | 14.30 | 6.98 | 4.38 | 4.06 |
| 10 | 8.21 | 6.60 | 3.54 | 3.40 | 2.64 |
| 11 | 46.50 | 36.88 | 19.49 | 13.00 | 8.84 |
| 12 | 5.88 | 4.30 | 2.89 | 1.77 | 1.27 |

Reliability indices, as generally used, are the mean values of the distributions of these indices. It appears that LHS and DLHS are able to predict these distributions more accurately but the differences in the mean values of indexes are not that significant. This is because the mean values are generally dominated by the high probability region of the distribution which can be captured effectively by all three methods, especially when the sample size is large. On the other hand, the comparison of the distributions requires consideration of the entire spectrum including low probability regions where the LHS and DLHS appear to perform better by virtue of the constrained sampling from all strata.

## 2.6 Discussion and Conclusions

Latin Hypercube Sampling (LHS) has been investigated for reliability evaluation of power systems. Due to its storage requirement during the sampling and extra computation time for equivalent distribution construction, a new sampling technique

called Discrete Latin Hypercube Sampling (DLHS) is proposed. Both sampling techniques are applied to a single area reliability analysis in comparison with traditional Monte Carlo (MC) simulation. Generation distribution, combined generation and load distribution and unserved energy distribution resulting from LHS, DLHS and MC are analyzed and compared with the actual distribution from enumeration.

The results indicate that LHS and DLHS represent sampled distribution better than MC. In addition, DLHS performs as well as LHS but with less computation time and storage. The distribution of unserved energy provides the spectrum of potential load loss even with small probability; thus, the information can be helpful for risk assessment since EUE tells only the expected value. The comparison between estimated reliability indexes; LOLP and EUE, from all sampling techniques to the actual one from enumeration is made. Percentage error is used to show deviation of sampled indexes from actual indexes. The results show that LHS and DLHS generally predict both indexes slightly better than MC.

It should be noted that LHS and DLHS are also able to provide distributions that are close representations of the actual ones. Therefore, these techniques are especially important when we need sampled states in the optimization process rather than simply computing the indexes. This information would also be useful in risk analysis. Furthermore, DLHS can be considered as a mixed sampling technique between MC and LHS. The level of randomness of DLHS is smaller than MC yet higher than LHS since it puts constraints on how many failure states each unit can be in, not on the distribution. DLHS needs less storage requirement than LHS. On the other hand, the distribution is

less representative than LHS since LHS uses a constrained sampling from the actual distribution. Finally the objective of this study is not to universally promote one method over the others. All the three methods have their respective strengths and can be used where appropriate.

# CHAPTER III

# MULTI-AREA POWER SYSTEM ADEQUACY PLANNING USING MONTE CARLO SIMULATION WITH SENSITIVITY ANALYSIS

## 3.1 Introduction

In this chapter, sensitivity analysis of the effect of additional generation in each area on system reliability is conducted utilizing Monte Carlo simulation and a perturbation procedure. The analysis is a preliminary test for the prospective location in which the additional generation has the most effect on system reliability. System loss of load probability is used as a reliability index to quantify this effect in different locations. A benefit of installing new capacity in a certain area is measured as a decrement of system loss of load probability. A candidate location will be determined from this benefit. The proposed simulation procedure is a perturbation analysis of generation addition in each area along with Monte Carlo simulation in the presence of system loss of load.

This chapter is organized as follows. Section 3.1 presents system modeling. Perturbation procedures are proposed in section 3.3. Section 3.4 shows computational results. Discussion and conclusions are given in the last section.

## 3.2 System Modeling

Multi-area power systems can be formulated as a network flow problem where each node in the network represents an area in the system and each arc represents tie line

connection between areas. Source and sink nodes are introduced to represent generation capacity and load. Discrete probability distribution function of each generation system and transmission line is constructed from the capacity and forced outage rates. System load vectors are constructed based on hourly forecasted data in each area utilizing K-mean clustering algorithm. Discrete joint probability function of system load is then derived. It is assumed that the additional generation is 100% reliable for all areas. In this analysis, capacity flow model and Ford Fulkerson algorithm is employed to determine loss of load state. The following presents detailed modeling of area generation, area load, and tie lines correspondingly.

### 3.2.1 Area Generation Model

Generation units in each area are given forced outage rate, repair time and their capacities. Discrete probability distribution function is constructed based on unit parameters assuming two stage Markov process, up and down states. The distribution function construction utilizes unit addition algorithm approach. The probability table contains numbers of state capacity including zero and its corresponding probability. Let

$\vec{c}_i$ = Capacity vector of area *i*

$\vec{p}_i$ = Probability vector of area *i* such that $\Pr(\vec{c}_i) = \vec{p}_i$

For computational efficiency, the generation state capacity will be rounded off to a fixed increment so that only minimum capacity state and number of states in each area are stored. A state with very small probability will be neglected.

### 3.2.2 Tie Line Model

It is assumed that transmission line capacity, forced outage rate and repair rate are given. Discrete probability distribution of tie-line capacity between areas is constructed based on the given parameters using two stage Markov process. The tie-line model is represented by (3.1), which contains the connection areas (from area, to area), its capacity and its corresponding probability (3.2).

$$\vec{t}_{ij} = \left(\vec{f}_{ij}, \vec{b}_{ij}\right) \tag{3.1}$$

$$\vec{p}_{ij}^{\,t} = \Pr\left(\vec{t}_{ij}\right) \tag{3.2}$$

where

$\vec{t}_{ij}$ = Tie-line capacity vector from area *i* to area *j*

$\vec{f}_{ij}$ = Tie-line capacity vector from area *i* to area *j* in forward direction

$\vec{b}_{ij}$ = Tie-line capacity vector from area *i* to area *j* in backward direction

$\vec{p}_{ij}^{\,t}$ = Probability vector of tie-line capacity from area *i* to area *j*

### 3.2.3 Area Load Model

Discrete joint distribution of area load is composed employing hourly load data in each area to preserve the correlation between area loads and is presented in (3.3)

$$\vec{L}^h = \left(L_1^h, L_2^h, \ldots, L_n^h\right) \tag{3.3}$$

where

$\vec{L}^h$ = Load vector for the hour *h*

$L_i^h$ = Load for the hour *h* in area *i*

*n* = Number of areas in the system

Due to numerous load states, they are grouped together utilizing clustering algorithm to an appropriate number of states. To simplify this, peak load will also be assumed in some applications.

## 3.3 Perturbation Procedure

Perturbation analysis is applied to estimate the derivatives of generation reliability indices in Monte Carlo simulation with respect to generation parameters such as mean up time and mean down time in [54] [64]. The analysis requires single Monte Carlo simulation followed by the sensitivity analysis of reliability indices, which is obtained from the derivative estimation. Perturbation concept is extended in this context to account for changes in generation capacity in each area independently. The possibility to apply this procedure mathematically to both sequential simulation and state sampling Monte Carlo simulation is explored. The objective of this procedure is to determine the derivative of loss of load probability with respect to addition capacity in each area.

### 3.3.1 Sequential Simulation

This simulation can be completed by advancing time in two cases; fixed step or by the next event.

#### 3.3.1.1 Fixed Time Interval

Time in each stage is constant over the simulation period. Let

$T$ = Time duration of each state

$N$ = Number of simulation periods

$G_{is}$ = Generation in area $i$ for state $s$

$n$ = Number of area

$TTF_{is}$ = Total transfer flow to area $i$ for state $s$ [55] [70]

$L_{is}$ = Load at area $i$ for state $s$

Loss of load at state $s$ occurs when

$$G_{is} + TTF_{is} - L_{is} < 0 \tag{3.4}$$

Let

$P_i(G_{is}, TTF_{is}, L_{is})$

= Loss of load probability for area $i$ obtained from simulation

$P(G_{is}, TTF_{is}, L_{is})$

= System loss of load probability

Then,

$$P_i(G_{is}, TTF_{is}, L_{is}) = \frac{1}{N}\sum_{s=1}^{N} \max\left(0, \frac{L_{is} - G_{is} - TTF_{is}}{\left|L_{is} - G_{is} - TTF_{is}\right|}\right) \tag{3.5}$$

$$P(G_{is}, TTF_{is}, L_{is}) = \frac{1}{N}\sum_{s=1}^{N} \max_{i\in\{1,2,..,n\}}\left(0, \frac{L_{is} - G_{is} - TTF_{is}}{\left|L_{is} - G_{is} - TTF_{is}\right|}\right) \tag{3.6}$$

Using perturbation analysis, generation in each area is perturbed by $\Delta G_i$ individually, loss of load probability in area $i$ becomes (3.7).

$$P_i'(G_{is}, TTF_{is}, L_{is}) = \frac{1}{N}\sum_{s=1}^{N} \max\left(0, \frac{L_{is} - G_{is} - TTF_{is}}{\left|L_{is} - G_{is} - TTF_{is}\right|}\right) - \Delta P_i \tag{3.7}$$

and,

$$\Delta P_i = -\frac{1}{N}\sum_{s=1}^{N} \max\left(0, \frac{L_{is} - G_{is} - \Delta G_i - TTF_{is}}{\left|L_{is} - G_{is} - \Delta G_i - TTF_{is}\right|}\right) \tag{3.8}$$

where

$\Delta P_i$ = Change in loss of load probability

Likewise, change in system of loss of load probability is (3.9).

$$\Delta P = -\frac{1}{N}\sum_{s=1}^{N} \max_{i\in\{1,2,..,n\}}\left(0, \frac{L_{is} - G_{is} - \Delta G_i - TTF_{is}}{\left|L_{is} - G_{is} - \Delta G_i - TTF_{is}\right|}\right) \tag{3.9}$$

#### 3.3.1.2 Next Event Method

Time in each stage is advanced by the next event. Let

$T_s$ = Time duration of state *s*

$T_{tot}$ = Total simulation time

$N$ = Number of simulation periods

$G_{is}$ = Generation in area *i* for state *s*

$n$ = Number of area

$TTF_{is}$ = Total transfer flow to area *i* for state *s*

$L_{is}$ = Load at area *i* for state *s*

The same concept is applied here. Loss of load probability in each area *i* can be written as (3.10).

$$P_i\left(G_{is}, TTF_{is}, L_{is}\right) = \frac{1}{T_{tot}} \sum_{s=1}^{N} T_s \times \max\left(0, \frac{L_{is} - G_{is} - TTF_{is}}{\left|L_{is} - G_{is} - TTF_{is}\right|}\right) \tag{3.10}$$

System loss of load probability is (3.11).

$$P\left(G_{is}, TTF_{is}, L_{is}\right) = \frac{1}{T_{tot}} \sum_{s=1}^{N} T_s \times \max_{i \in \{1,2,..,n\}}\left(0, \frac{L_{is} - G_{is} - TTF_{is}}{\left|L_{is} - G_{is} - TTF_{is}\right|}\right) \tag{3.11}$$

By perturbation analysis, generation in each area is perturbed by $\Delta G_i$ individually, loss of load probability in area *i* becomes (3.12).

$$P_i'\left(G_{is}, TTF_{is}, L_{is}\right) = \frac{1}{T_{tot}} \sum_{s=1}^{N} T_s \times \max\left(0, \frac{L_{is} - G_{is} - TTF_{is}}{\left|L_{is} - G_{is} - TTF_{is}\right|}\right) - \Delta P_i \tag{3.12}$$

And,

$$\Delta P_i = -\frac{1}{T_{tot}} \sum_{s=1}^{N} T_s \times \max\left(0, \frac{L_{is} - G_{is} - \Delta G_i - TTF_{is}}{\left|L_{is} - G_{is} - \Delta G_i - TTF_{is}\right|}\right) \tag{3.13}$$

where

$\Delta P_i$ = Change in loss of load probability

Then, change in system of loss of load probability is (3.14).

$$\Delta P = -\frac{1}{T_{tot}} \sum_{s=1}^{N} T_s \times \max_{i \in \{1,2,..,n\}}\left(0, \frac{L_{is} - G_{is} - \Delta G_i - TTF_{is}}{\left|L_{is} - G_{is} - \Delta G_i - TTF_{is}\right|}\right) \tag{3.14}$$

Since the change in loss of load probability as a function of addition generation is not continuous, derivative with respect to $\Delta G_i$ does not exist. Mathematical analysis may not be directly applied to the problem. However, this perturbation concept can simply be implemented by artificially increasing generation in each area when loss of load exists in state sampling simulation.

### 3.3.2 State Sampling Simulation

The proposed simulation utilizes state sampling method because of its simple implementation. Whenever loss of load state is encountered, perturbation analysis module is activated. The process will explicitly add generation in each area with assumption of full availability of the additional unit. Then, the flow calculation is determined to identify loss of load state. Major drawback of this procedure is its convergence criteria. Perturbation analysis of additional generation in each area (when system suffers loss of load) produces more uncertainty in the simulation. Therefore, the simulation bound for nominal loss of load probability should be tighter than a commonly used bound of 5 %. In this chapter, convergence criteria of 3 % is used which should provide reasonable accuracy. It should be emphasized here that this simulation requires single extended Monte Carlo simulation instead of one Monte Carlo simulation for each area.

## 3.4 Computational Results

The test system is thirteen-area power system given in Appendix B. Loss of load probability (LOLP) of individual areas before generation is shown in Table 3.1. Generating unit failure and repair rate data are from IEEE Reliability Test System 1996. System peak load is assumed to be increased by 1.275 times the original load for area 1-3, and 10-12, by 1.2 times the original load for area 4, 5, 8 and 13. The system LOLP before generation addition is 0.004419. Simulation result is shown in Fig. 3.1.

Table 3.1 Area LOLP before Generation Addition

| Area | LOLP |
|---|---|
| 1 | 0 |
| 2 | 0.000020 |
| 3 | 0.000010 |
| 4 | 0.000173 |
| 5 | 0 |
| 8 | 0.002477 |
| 10 | 0 |
| 11 | 0 |
| 12 | 0.000026 |
| 13 | 0.001713 |

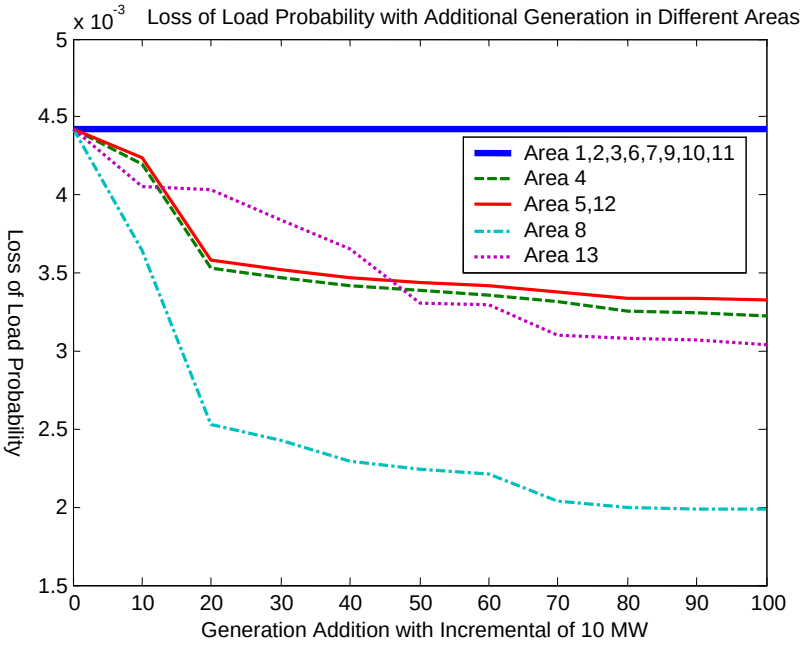


Fig. 3.1 Area LOLP after Generation Addition

As seen from Table 3.1, area 8, with LOLP of 0.002477, suffers most from loss of load and contributes most to system loss of load probability. Therefore, one should

expect that generation addition in this area would improve system LOLP the most. System LOLP with additional generation from each area is shown in Fig. 3.1.

System LOLP declines with the highest slope when new generation is added to area 8 while it remains unchanged when generation is added to areas 1-3, 6-7, and 9-11. Generation addition to area 4, 5, and 12 also improve system LOLP to a certain degree. It can be seen from the system diagram in Appendix B that the areas 4-5, and 12 are closely located and connected to area 8 and 13 that suffer most from loss of load, the affected areas thus receive capacity assistance from their neighborhood areas. The simulation suggests that additional generation should be located in area 13. The amount of power that should be produced depends on the desired system reliability level and can be found from Fig. 3.1.

### 3.5 Discussion and Conclusions

The simulation procedure proposed here can be used as a guideline to quantify the effectiveness of additional generation in each area. The procedure is simple yet effective enough to provide a relationship of reliability index of interest and generation after one Monte Carlo simulation. The assumption of 100% reliable generation unit can be relaxed in the simulation phase. Furthermore, each area can have different forced outage rates which will represent a more realistic system.

However, the procedure is limited since it can only quantify the effect of one area generation. In real applications, it would be more reliable and applicable to locate generation in more than one area. Therefore, the effect of combination of generation

from many areas should is studied in further chapters. Moreover, after the effect of reliability index and generation is analyzed, the optimization scheme should be proposed and applied to make a decision based on the cost and benefit of the additional units.

# CHAPTER IV

# MULTI-AREA POWER SYSTEM ADEQUACY PLANNING USING GLOBAL DECOMPOSITION WITH SCENARIO ANALYSIS*

## 4.1 Introduction

Multi-area reliability analysis is performed using two major approaches; Monte-Carlo simulation and state-space decomposition. In Monte-Carlo simulation, failure and repair history of components are created using their probability distributions. Reliability indices are estimated by statistical inferences. The basic concept of state-space decomposition, originally proposed in [87], is to classify the system state space into three sets; acceptable sets (*A* sets), unacceptable sets (*L* sets), and unclassified sets (*U* sets) while the reliability indices are calculated concurrently. Advanced versions of decomposition such as simultaneous-decomposition for including load and planned outages in a computationally efficient manner are described in [72], [76], [78], [80]. One of many applications of this method is multi-area production costing [61] with the objective of determining the optimal sets of unit addition.

Previously, in Chapter III, the sensitivity analysis along with Monte Carlo simulation is proposed to the solution of multi-area power system adequacy planning problem. One of the main drawbacks of MC is that the method may require a long history to produce a converged result. This study develops a comparative algorithm for

---

* Reprinted with permission from "A Global Decomposition Algorithm for Reliability Constrained Generation Planning and Placement" by P. Jirutitijaroen and C. Singh, *Proceedings of the 9th International Conference on Probabilistic Methods Applied to Power Systems*, Stockholm, Sweden, June 2006. © 2006 IEEE

selecting the best generation combination utilizing a technique called global decomposition method for reliability calculation. The prospective additional units are included in the system and the decomposition process is performed once. The reliability indices were then calculated by extracting only the states of interest. Even though global decomposition is involved with large number of states, it did not significantly affect the computation time. Scenario analysis is proposed to determine the best generation combination. The comparison is made concurrently with global decomposition process to improve computational efficiency and reduce memory required.

The chapter is organized as follows. Section 4.2 reviews concepts of decomposition approach for multi-area power system reliability evaluation. Scenario analysis is given in section 4.3. Discussion and conclusions are given in the last section.

## 4.2 Review of Decomposition Approach for Reliability Evaluation

A multi-area power system is modeled as given in section 3.2. The system state space consists of area generation states, tie line capacity states, and area load states. Decomposition approach analytically partitions the state spaces into the following three different sets of states.

1. Sets of acceptable states (*A* sets): The success states that all area load is satisfied.
2. Sets of unacceptable states (*L* sets): The failure states or Loss of load states that some load areas are not satisfied.
3. Sets of unclassified states (*U* sets): The states that have not been classified into *A* or *L* sets.

The state space is first categorized as a *U* set and then further decomposed into *A* sets, *L* sets, and *U* sets. The process of decomposition is presented in the following.

### 4.2.1 Network Capacity Flow Model

The system is transformed into network capacity flow model as shown in Figure 4.1. Each node in the network represents an area and each arc connecting between nodes represents tie line capacity in multi-area power systems. Artificial source and sink nodes are created to represent area generation and load. An area generation arc connects source node to its area while an area load arc connects its area to sink node. Every arc in the network is associated with capacity states and corresponding probabilities.

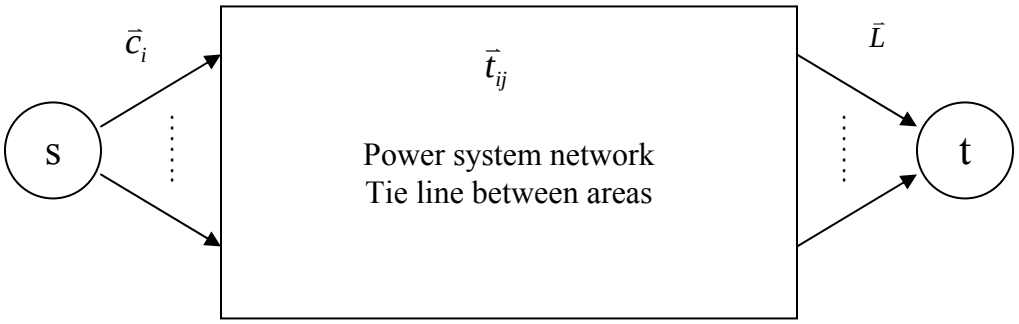


Fig. 4.1 Power System Network: Capacity Flow Model

### 4.2.2 State Space Representation

The state space is defined as equation (4.1).

$$S = \begin{bmatrix} M_1 & M_2 & \dots & M_N \\ m_1 & m_2 & \dots & m_N \end{bmatrix} \tag{4.1}$$

where

$M_k$ = Maximum state of arc *k*.

$m_k$ = Minimum state of arc *k*.

$N$ = Number of arcs in the network

A system state, *X*, can assume any value between its minimum and maximum state as shown in (4.2).

$$X = \begin{bmatrix} x_1 & x_2 & \dots & x_N \end{bmatrix} \tag{4.2}$$

where $m_k \le x_k \le M_k$, and

$x_k$ = State of arc *k*.

The process of partitioning the state space to *A* and *L* sets involves determining maximum flow in the network.

### 4.2.3 Partitioning an Unclassified Set

A maximum flow from artificial source to sink node is found in order to classify system loss of load state. Ford-Fulkerson algorithm is implemented with breadth-first search to find an existing flow in the network. Given a *U* set, unclassified set or state space (*S* set, as in (4.1)) at the beginning of the decomposition, the process of partitioning into *A* and *L* sets is explained in the following.

The capacity of each arc in the network is assigned to be the capacity of maximum state in the set. After the maximum flow is performed, the resulting flow is expressed as (4.3).

$$F = \begin{bmatrix} f_1 & f_2 & \dots & f_N \end{bmatrix} \tag{4.3}$$

where

$f_k$ = Flow in arc *k* from the maximum flow calculation

If the resulting maximum flow is less than the sum of area loads, then obviously the *U* set does not have any success state in it. On the other hand, if the maximum flow from the calculation is equal to the sum of area loads, then any state above the resulting flow in the network ( $f_k$ ) will result in success state, let

$u_k$ = State of arc *k* that has capacity equal to or just greater than $f_k$

Then, the *A* set can be obtained from (4.4).

$$A = \begin{bmatrix} M_1 & M_2 & \dots & M_N \\ u_1 & u_2 & \dots & u_N \end{bmatrix} \tag{4.4}$$

In order to extract loss of load sets, a systematic approach is to reduce each capacity arc until system reach loss of load state given that all other arcs are at its maximum states in *U* set. With this approach, the number of *L* sets is equal to the number of arcs in the network (*N*). The construction of L sets is found from the '*v*' vector. Let

$v_k$ = The minimum state of arc *k* that will produce system success when all other arcs are kept at its maximum capacity in the *U* set.

This means that if the capacity of arc *k* is below $v_k$, the system will suffer loss of load in any area irrespective of all other arcs capacity. The direct calculation of '*v*' vector would require many flow calculations with reduced capacity of arc *k* until the system reaches loss of load state. However, this procedure would require so much time and thus reduce computational efficiency.

The efficient procedure of evaluating '*v*' vector is described in the following. Instead of making flow calculation every time the capacity of each arc is reduced, this vector can be found from the flow calculation of the residual network. Let

$e_k$ = The assisting flow from the residual network when arc *k* is removed

The value of $e_k$ is evaluated from maximum flow calculation of the residual network with arc *k* removed. The source and sink node for the flow calculation is defined from the direction of arc *k*. This means that if arc *k* is removed from the system, the assisting flow of capacity $e_k$ will be delivered, or equivalently, the system will still remain in success state with this assistance level $e_k$ from other arcs.

Then, '*v*' vector is calculated from (4.5)

$$v_k = \begin{cases} x_k : f_k - e_k & \text{if} \quad f_k - e_k \geq 0 \\ m_k & \text{if} \quad f_k - e_k < 0 \end{cases} \tag{4.5}$$

where

$x_k$ = State of arc *k*.

$f_k$ = Flow in arc *k* from the maximum flow calculation

$e_k$ = The assisting flow from the residual network when arc *k* is removed

$m_k$ = Minimum state of arc $k$ in $U$ set

$L$ sets are also constructed to make them disjointed sets. The general formulation of $L$ set is (4.6).

$$L_k = \begin{bmatrix} M_1 & M_2 & \cdots & M_{k-1} & v_k - 1 & M_{k+1} & \cdots & M_N \\ v_1 & v_2 & \cdots & v_{k-1} & m_k & m_{k+1} & \cdots & m_N \end{bmatrix} \tag{4.6}$$

Based on $A$ and $L$ sets, the next $U$ sets can be constructed as (2.10)

$$U_k = \begin{bmatrix} M_1 & M_2 & \cdots & M_{k-1} & u_k - 1 & M_{k+1} & \cdots & M_N \\ u_1 & u_2 & \cdots & u_{k-1} & v_k & v_{k+1} & \cdots & v_N \end{bmatrix} \tag{2.10}$$

The decomposition process creates $N$ numbers of $L$ sets and $N$ numbers of $U$ sets each time and will continue until the probability of $U$ sets is insignificant. Some of these sets may be null sets.

### 4.2.4 Probability Calculation

Let $X$ be any set in the form (4.7),

$$X = \begin{bmatrix} M_1^X & M_2^X & \dots & M_N^X \\ m_1^X & m_2^X & \dots & m_N^X \end{bmatrix} \tag{4.7}$$

where

$M_k^X$ = Maximum state of arc $k$ in set $X$

$m_k$ = Minimum state of arc $k$ in set $X$

$N$ = Number of every arc in the network

Probability of any set is calculated from (4.8).

$$\Pr(X) = \prod_{k=1}^{N} \sum_{m_k^X \le x_k \le M_k^X} p_{x_k} \tag{4.8}$$

where

$x_k$ = State of arc $k$

$p_{x_k}$ = Probability of state $x_k$ of arc $k$

Equation (4.8) can be simplified by utilizing cumulative probabilities in (4.9).

$$\Pr(X) = \prod_{k=1}^{N} \left( \overline{p}_{M_k^X} - \overline{p}_{m_k^X - 1} \right) \tag{4.9}$$

where

$\overline{p}_{x_k}$ = Cumulative probability of state $x_k$ of arc $k$

In later applications, (4.9) is used for probability calculation.

## 4.3 Scenario Analysis

In this approach, prospective generation locations in the system are pre-selected by an expert. These candidate locations create various possible generation combinations, each of which yields different system reliability and cost. The generation combinations with acceptable costs are analyzed and the selection for the best location is based on system reliability, system loss of load probability in this case, with additional generation.

In this analysis, all prospective generation units and tie lines are included in the state space prior to the decomposition. The decomposition process applied to this augmented state space is then called *global decomposition* process. The process of decomposition is the same as described in the previous section. Reliability indices of any

generation and transmission line combination can be extracted from the *global state space* by assigning zero probability to the omitted states.

The concept of global decomposition is based on the fact that decomposition depends only on the state capacities and not the state probabilities. In this application, the problem is to select the best generation combination in the system that will yield the maximum reliability. The state space contains maximum possible number of additional generators in each area. The sets obtained from this state space are valid for all scenarios. Probability of each scenario can then be evaluated by allowing zero probability for some omitted states because of the non-inclusion of certain generators.

Scenario analysis examines all possible generation combinations with global decomposition as a reliability evaluation tool. The advantage of this tool is that a reliability index of any combination can be calculated after a single decomposition. A comparison is made to determine the best generation location. Instead of making a comparison after the global decomposition is complete, this research proposes a comparison algorithm that works interactively with each step of decomposition to gain computational efficiency. Two comparison algorithms are proposed for generation and transmission lines and presented in the following.

### 4.3.1 Comparison Algorithm for Generation Planning

Recall that at every step of decomposition, one *A* set, N *L* sets and N *U* sets are generated from one *U* set. The *A* sets will be deleted to minimize memory usage since the goal of this evaluation is to extract all *L* sets for system loss of load probability

computation. The *U* sets have to be kept and partitioned further into *A*, *U* and *L* sets. After global decomposition is performed, the state space will be completely partitioned into various *L* sets. Probability of each set is calculated from (4.9). System loss of load probability of each combination can be computed from the summation of probability over all *L* sets by assigning zero probability to the omitted states because of the absence of generators in the combination under consideration.

A straightforward approach for comparison is to compute system loss of load probability of each combination after complete global decomposition and then make comparison. This study proposes an algorithm that compares and cuts off some low performance generation combinations at each stage of decomposition. The proposed algorithm computes probability of *A* sets, and *L* sets of all possible combinations at each stage of decomposition. If the probability of *A* sets of combination *i* is greater than combination *j*, then, the following comparison is made.

$$\left(1 - P_A^i\right) < P_L^j \tag{4.10}$$

where

$P_A^i$ = Probability of *A* sets from combination *i*

$P_L^j$ = Probability of *L* sets from combination *j*

Equation (4.10) implies that maximum system loss of load probability of combination *i* is smaller than current (partial) system loss of load probability of combination *j*. This means that even if the resulting *U* sets of combination *i* were all loss of load sets, system loss of load probability from combination *i* will still be smaller than that from combination *j*. At each stage of decomposition, a comparison will be made and

low performance combination will be deleted from the possible solution list. The procedure may not require complete global decomposition process. It can be stopped when the possible solution list has only one combination or for all possible solutions, probability of unclassified sets is less than an epsilon. The steps of the algorithm are outlined below.

Step 0. Initialization

- System state space is the first *U* set.
- Possible solution list ← every combination *i*.

Step 1. Decomposition and Evaluation

- Partition *U* sets into *A* and *L* sets
- Compute and update $P_A^i$ and $P_L^i$ for every combination *i.*
- Find $P_A^{\max} = \max_{\forall i} P_A^i$

Step 2. Comparison

- If $P_L^i > \left(1 - P_A^{\max}\right)$, delete combination *i* from possible solution list.

Step 3. Stopping criterion

- Stop if number of combination is 1 or for all *i* $P_U^i = 1 - P_A^i - P_L^i < \varepsilon$
- Otherwise, create *U* sets and go to step 1.

This method improves computational efficiency and reduces memory usage for storing *U* sets and *L* sets. At each stage of decomposition, *A* and *L* sets will be deleted after probability evaluation. Probability of all possible scenarios is evaluated and a comparison in (4.10) is made to delete some solutions. When some low performance

solution is cut off, number of possible solutions that need to be evaluated will be smaller at each iteration.

### 4.3.2 Comparison Algorithm for Transmission Line Planning

Generally, reliability improvement is more marked with additional generators than the transmission lines. In this section, the previous algorithm is modified to make it easier to differentiate bad solutions from the good ones. At each stage, there will be some low probability *U* sets discarded during the decomposition process for better computational efficiency. The cumulative probability of the discarded *U* sets can be relatively significant in comparison process and should be taken into account in (4.10). Therefore, comparison equation is modified as follows.

$$\left(\left(1-P_{\overline{U}}^{i}\right)-P_{A}^{i}\right)<P_{L}^{j} \tag{4.11}$$

where

$P_{\overline{U}}^{i}$ = Probability of discarded *U* sets from combination *i*

Probability of discarded U sets can be computed from (4.12).

$$P_{\overline{U}}^{i}=1-\left(P_{A}^{i}+P_{U}^{i}+P_{L}^{i}\right) \tag{4.12}$$

where

$P_{U}^{i}$ = Probability of retained *U* sets from combination *i*

Then, the comparison equation becomes,

$$P_{U}^{i}+P_{L}^{i}<P_{L}^{j} \tag{4.13}$$

The process of selecting the best combination may not require completing global decomposition. It can be stopped when the possible solution list has only one

combination or for all possible solutions, probability of unclassified sets is less than an epsilon. The steps of the algorithm are outlined below.

Step 0 Initialization

- System state space is the first *U* set.
- Possible solution list ← every combination *i*.

Step 1 Decomposition and Evaluation

- Partition *U* sets into *A* and *L* sets
- Compute and update $P_A^i$, $P_U^i$ and $P_L^i$ for every combination *i*.
- Find $P^{\min} = \min_{\forall i}\left(P_U^i + P_L^i\right)$

Step 2 Comparison

- If $P_L^j > P^{\min}$, delete combination *j* from possible solution list.

Step 3 Stopping criterion

- Stop if number of combination is 1 or for all *i*, $P_U^i < \varepsilon$
- Otherwise, create *U* sets and go to step 1.

This method improves computational efficiency and reduces memory usage for storing *U* sets and *L* sets. The *A* and *L* sets will be deleted after evaluating their probabilities at each stage of decomposition. Probability of all possible scenarios is evaluated and a comparison in (4.13) is made to delete some solutions. When some low performance solutions are deleted, number of possible solutions that need to be evaluated will be smaller at each iteration.

## 4.4 Computational Results

The test system used in Chapter III is modified to mask the obvious solution by combining area 8 to area 12. The resulting system has only twelve area and its parameters are given in Appendix A. Generating unit failure and repair rate data are from IEEE Reliability Test System 1996.

### 4.4.1 Generation Planning

It is assumed that the budget is $150 million and the additional generators have capacity of 50 MW each. Table 4.1 shows area generation and loads as well as availability and cost per generator in prospective areas which are areas 1 to 5, and 9 to 12. Maximum number of unit additions allowed in each area is three units, which are included in the state space before performing global decomposition. Total number of scenarios is 165, i. e., 165 combinations of generators are to be analyzed. Probability distribution table for generation and tie-lines are developed with a capacity increment of 50 MW. System probability of loss of load before additional generation is 0.02639.

Table 4.1 Generation and Load Parameters

| Area *j* | Load (MW) | Generation (MW) | FOR of additional units | Cost per unit ($m) |
|---|---|---|---|---|
| 1 | 1400 | 2550 | 0.05 | 50 |
| 2 | 8000 | 23600 | 0.05 | 50 |
| 3 | 4800 | 15100 | 0.05 | 50 |
| 4 | 1200 | 3100 | 0.05 | 50 |
| 5 | 300 | 100 | 0.05 | 50 |
| 6 | 0 | 550 | - | - |
| 7 | 0 | 3500 | - | - |
| 8 | 0 | 400 | - | - |
| 9 | 1000 | 2100 | 0.05 | 50 |
| 10 | 1200 | 3100 | 0.05 | 50 |
| 11 | 1550 | 4150 | 0.05 | 50 |
| 12 | 1300 | 900 | 0.05 | 50 |

The optimal solution provided by the algorithm is to locate all three generators in area 12. Loss of load probability after additional generation is 0.00762. Table 4.2 shows number of possible scenarios to be evaluated and number of omitted scenarios at each stage of decomposition. The algorithm starts cutting off some scenarios at decomposition stage 15. These possible scenarios are deleted after a comparison in equation (8) is made. The number of possible scenarios (combinations of area generators) that need to be evaluated is smaller. This improves computational efficiency since number of *L* sets created in later decomposition is often large.

Table 4.2 Number of Possible and Omitted Scenarios at Each Decomposition Stage for Generation Planning

| Decomposition Stage | Number of possible scenarios | Number of omitted scenarios |
|---|---|---|
| 1-14 | 165 | 0 |
| 15 | 165 | 36 |
| 16 | 129 | 84 |
| 18 | 45 | 36 |
| 19 | 9 | 8 |

Since the goal of this study is to select the best generation location, there is no need to perform complete decomposition. If a comparison is made after performing global decomposition, more stages of decomposition need to be conducted. The proposed algorithm terminates after 19 stages of decomposition, which helps in reducing computational time and memory usage for storing *U* and *L* sets

### 4.4.2 Transmission Line Planning

It is assumed that the additional transmission lines have capacity of 100 MW each with a mean repair time of 8 hours and a failure rate of 10 per year. It is assumed that the ISO wishes to increase transfer capabilities between areas that is now less than 300 MW. Table 4.3 shows transfer capability between areas and the prospective locations for this study. The number of prospective locations is 13. Maximum number of unit additions is included in the state space before performing global decomposition. Total number of scenarios is 91, i e, 91 combinations of transmission lines are to be analyzed. Probability distribution tables for generation and tie-lines are developed with a

capacity increment of 50 MW. System probability of loss of load before additional capacities is 0.0042.

Table 4.3 Transfer Capability and Additional Capacity

| From Area | To Area | Transfer Capability (MW) | Possible Additional Capability (MW) |
|---|---|---|---|
| 1 | 2 | 4550 | - |
| 1 | 3 | 300 | - |
| 1 | 6 | 100 | 200 |
| 1 | 10 | 150 | 200 |
| 2 | 3 | 1050 | - |
| 2 | 8 | 150 | 200 |
| 2 | 9 | 900 | - |
| 2 | 10 | 450 | - |
| 3 | 7 | 400 | - |
| 3 | 10 | 200 | 200 |
| 3 | 11 | 50 | 200 |
| 4 | 5 | 50 | 200 |
| 4 | 7 | 300 | - |
| 4 | 10 | 200 | 200 |
| 4 | 11 | 150 | 200 |
| 5 | 6 | 400 | - |
| 5 | 10 | 50 | 200 |
| 5 | 11 | 650 | - |
| 7 | 11 | 350 | - |
| 7 | 12 | 950 | - |
| 9 | 10 | 150 | 200 |
| 9 | 11 | 150 | 200 |
| 10 | 11 | 150 | 200 |
| 10 | 12 | 100 | 200 |

Table 4.4 shows number of omitted scenarios at each stage of decomposition. The optimal solution found is to locate both transmission lines between area 2 and area 8 which improves system loss of load probability to 0.0007. The proposed method requires

45 stages of decomposition while complete global decomposition requires 126 stages of decomposition.

Table 4.4 Number of Possible and Omitted Scenarios at Each Decomposition Stage for Transmission Line Planning

| Decomposition Stage | Number of omitted scenarios |
|---|---|
| 1-41 | 0 |
| 43 | 78 |
| 44 | 0 |
| 45 | 12 |

## 4.5 Discussion and Conclusions

The algorithms for long term generation adequacy planning and transmission line planning are described utilizing global decomposition as a reliability evaluation tool. Scenario analysis is applied for the selection of the best solution. The direct approach is to perform single global decomposition, calculate system loss of load probability of all possible combinations, and then make a comparison for the best solution. However, the direct comparison after global decomposition requires high memory usage for all $L$ sets.

The algorithms select the best scenario by comparing reliability index which is loss of load probability in this case. The proposed approaches require less number of stages of global decomposition than a straightforward approach when system loss of load probability of all scenarios is compared after complete decomposition. The algorithms converge when there is only one solution left in the possible solution lists. The methods require less memory usage since all $L$ sets from each stage of

decomposition can be deleted after evaluation. The comparisons in (4.10) and (4.13) also help reduce number of possible solutions at each stage of decomposition. Therefore, the number of evaluations and comparisons is smaller at a given stage of decomposition. Global decomposition need not be completed once the solution is found. The algorithm can also be extended to compute other reliability indices of interest from global decomposition such as frequency of loss of load.

# CHAPTER V

# MULTI-AREA POWER SYSTEM ADEQUACY PLANNING USING GLOBAL DECOMPOSITION WITH DYNAMIC PROGRAMMING*

## 5.1 Introduction

This study proposes dynamic programming to determine the location of generators in multi-area power systems with global decomposition as a reliability evaluation tool. Original generation probability distribution in each area is modified to incorporate additional generators. An equation relating the number of additional units in each area to generation probability distribution is developed in this paper. After global decomposition, an equation for reliability is derived and approximated. The problem structure is transformed and solved by dynamic programming.

There are two ways to formulate the problem. One is to minimize the cost subject to loss of load probability constraint and the other is minimizing the loss of load probability subject to cost constraint. Either objective can be achieved by the method described in this paper. The basic formulation is based on minimizing the loss of load probability with budget as a constraint but the same formulation can be used for the

---

* Reprinted with permission from
"A Method for Generation Adequacy Planning in Multi-Area Power Systems Using Dynamic Programming" by P. Jirutitijaroen and C. Singh, *Proceedings of the 2006 IEEE Power Engineering Society General Meeting*, Montreal, Canada, June 2006. © 2006 IEEE
"Reliability and Cost Trade-Off in Multi-Area Power System Generation Expansion Using Dynamic Programming and Global Decomposition" by P. Jirutitijaroen and C. Singh, *IEEE Transactions on Power Systems,* vol.21, no. 3, pp. 1432-1441, August 2006. © 2006 IEEE
"A Hybrid Method for Multi-Area Generation Expansion Using Tabu-search and Dynamic Programming" by P. Jirutitijaroen and C. Singh, *Proceedings of the 2006 International Conference on Power System Technology*, Chongqing, China, October 2006. © 2006 IEEE

alternate objective. If the minimized loss of load probability is not acceptable, the budget can be changed and reliability re-optimized. Through such an iterative procedure, a suitable solution that minimizes the cost subject to a reliability constraint can be found. Since decomposition needs to be performed only once in the proposed method, such an iterative procedure is quite efficient.

Global decomposition is an efficient reliability evaluation technique for this type of analysis. With global decomposition, the additional generators in prospective areas are included in the system. This global state space is valid for all generation combinations. The concept is based on the fact that decomposition depends on state capacities and not state probabilities. The unavailability (forced outage rate) of additional generators is also considered in the formulation. The major advantage of this technique is that decomposition is performed only once. Reliability indices of each combination can be evaluated by allowing zero probability to the omitted states. One of the contributions of this study is to derive the relationship of reliability index to the additional generation in each area.

This chapter is organized as follows. The problem is formulated in section 5.2. Section 5.3 presents reliability equation and approximation after global decomposition. Dynamic programming application to this problem is given in section 5.4. The proposed method is illustrated by a three-area power system in section 5.5 and implemented to a twelve-area power system in section 5.6. Discussions and conclusions are given in the last section.

## 5.2 Problem Formulation

A multi-area power system is modeled as given in Chapter III Section 3.2. The problem is formulated as a network flow problem as given in Chapter IV Section 4.2.1. The capacity of every arc in the network is a random variable because generation, tie line and load capacity are random with discrete probability distributions. For computational efficiency, all arc capacities are rounded off to a fixed increment so that only the minimum capacity state and number of states in each arc need to be known. States with very small probability are ignored.

The decision variables of network flow problem are integer as the number of additional generators is an integer value. This network flow problem is called stochastic integer programming problem due to randomness in capacity arcs, reliability constraints, and integer decision variable. The standard formulation is derived in the following with the objective of minimizing loss of load probability subject to cost and network capacity constraints.

Index set

I = Network nodes *{s, t, 1, 2,…, n}*

Assumption

The additional generators have capacity of $C^G$ MW each and additional tie lines have capacity of $C^T$ MW each.

Parameters

$\overline{G_i}$ = Capacity of existing generation arc *i* (MW)

$a_i^G$ = Cost of an additional generation unit at node *i* ($/MW)

$C^G$ = Capacity of an additional generator (MW)

$N^G$ = Total number of addition generators

$\overline{L}_i$ = Capacity of load arc *i* (MW)

$\overline{T}_{ij}$ = Capacity of tie line arc *i* (MW)

$a_{ij}^T$ = Cost of a tie line between line *i* and *j* ($/MW)

$C^T$ = Capacity of an additional tie line (MW)

$N^T$ = Total number of addition tie line

$R$ = Total available budget ($)

$s$ = Source node

$t$ = Sink node

Decision variables

$X_{ij}$ = Flow from node *i* to *j*

$X_i^G$ = Number of addition generators at node *i*, integer

$X_{ij}^T$ = Number of addition tie line between node *i* and *j* where *(i,j) = (j,i)*, integer

The objective function to minimize loss of load probability is given below.

$$\text{Min}\Pr\left\{X_{1t}, X_{2t}, ..., X_{nt} : X_{1t} < \overline{L}_1 \cup X_{2t} < \overline{L}_2 ... \cup X_{nt} < \overline{L}_n\right\} \quad (5.1)$$

The problem has the following constraints.

Capacity constraints

– Flow in generation arc

$$X_{si} \le \overline{G}_i + C^G X_i^G \qquad \forall i \in I \tag{5.2}$$

– Flow in tie line

$$\left| X_{ji} - X_{ij} \right| \le \overline{T}_{ij} + C^T X_{ij}^T \qquad \forall i, j \in I, i \ne j \tag{5.3}$$

– Flow in load arc

$$X_{it} \le \overline{L}_i \qquad \forall i \in I \tag{5.4}$$

Conservation of flow at node *i* in the network

$$X_{si} + \sum_{\substack{j \in I \\ j \ne i}} X_{ji} = \sum_{\substack{j \in I \\ j \ne i}} X_{ij} + X_{it} \qquad \forall i \in I \tag{5.5}$$

Maximum number of additional generators

$$\sum_{i \in I} X_i^G = N^G \tag{5.6}$$

Maximum number of additional transmission line

$$\sum_{\substack{i \in I \\ i \ne j}} \sum_{j \in J} X_{ij}^T = N^T \tag{5.7}$$

Budget constraint

$$\sum_{i \in I} a_i^G X_i^G + \sum_{\substack{i \in I \\ i \ne j}} \sum_{j \in J} a_{ij}^T X_{ij}^T \le R \tag{5.8}$$

Non negativity

$$X_{ij}, X_i^G, X_{ij}^T \ge 0 \qquad \forall i, j \in I \tag{5.9}$$

The expression within the parenthesis in equation 1 represents the system loss of load event. The problem is thus formulated so as to minimize the loss of load probability index subject to cost constraint. If the optimal system reliability obtained through this

process does not satisfy the requirements, the cost constraint can be relaxed to allow more additional generators in the system and the LOLP can be re-optimized

All possible additional generation units are included in each prospective area of the system before performing global decomposition. In the global decomposition process, constraints (2) to (7) and (9) have already been included. The problem has only one additional constraint which is the budget constraint (8). However, the objective function has no available explicit formulation in terms of the decision variables. In order to express the objective function in terms of number of additional generators in each area, generation probability distribution is modified to incorporate additional units as described in the next section.

### 5.2.1 Generation Probability Distribution Equation Incorporating Identical Additional Units

The generation probability distribution of each area is modified as additional units are added to the area. The expression for the modified probability distribution is developed as a function of the number of additional units. For the sake of simplicity, this expression (5.11) is presented assuming that the capacity of additional units in a given area is the same. This, however, is not an inherent limitation of the method but if the units are non-identical then (5.11) becomes more complex. The equation in the case of non-identical units is given in the next section.

The capacity, $C_j$, of an additional unit $j$ is assumed as multiple, $\mu_j$, of the fixed increment, $\eta$, used in the discrete probability distribution, i.e.

$$\mu_j = \frac{C_j}{\eta} \tag{5.10}$$

The following equation describes generation probability incorporating the additional units, $y_j$ in area $j$.

$$P_{G_i^j}^{y_j} = \sum_{k=0}^{y_j} P_{G_{i-\mu_j k}^j}^{0} \binom{y_j}{k} (\text{FOR}_j)^{y_j - k} (1 - \text{FOR}_j)^k \tag{5.11}$$

where

$P_{G_{i-\mu_j k}^j}^{0}$ = Probability of original generation at level $i$- $\mu_j k$ before additional units in area $j$, 0 if $i \le \mu_j k$

$\text{FOR}_j$ = Forced outage rate of additional units in area $j$

Equation (5.11) describes the probability of a given generation level in each area in terms of number of additional units in this area.

### 5.2.2 Generation Probability Distribution Equation Incorporating Non-Identical Additional Units

Let the additional units in area $j$ have the capacities, $C_j^1, C_j^2, \ldots, C_j^m$ and corresponding number of additional units in area $j$ is $y_j^1, y_j^2, \ldots, y_j^m$ respectively. Each additional unit has the capacity as multiple, $\mu_j^t$, $t = 1,2,\ldots,m$ of the fixed increment, $\eta$, used in the discrete probability distribution. The following equation describes generation probability incorporating the additional units, $y_j^t$, in area $j$.

$$P_{G_i^j}^{y_j^t} = \sum_{k=0}^{y_j^t} P_{G^j_{i-\mu_j^t k}}^{t-1} \binom{y_j^t}{k} \left(\text{FOR}_j^t\right)^{y_j^t - k} \left(1 - \text{FOR}_j^t\right)^k, t = 1, \ldots, m \tag{5.12}$$

where

$$P_{G_i^j}^{t} = \sum_{k=0}^{y_j^{t,\max}} P_{G^j_{i-\mu_j^t k}}^{t-1} \binom{y_j^{t,\max}}{k} \left(\text{FOR}_j^t\right)^{y_j^{t,\max} - k} \left(1 - \text{FOR}_j^t\right)^k, t = 1, \ldots, m \tag{5.13}$$

and

$P_{G^j_{i-\mu_j^t k}}^{t-1}$ = Probability of generation at level $i - \mu_j^t k$ with additional units, $y_j^1, y_j^2, \ldots, y_j^{t-1}$ in area *j*, 0 if $i \le \mu_j^t k$

$\text{FOR}_j^t$ = Forced outage rate of additional unit *t* in area *j*

$y_j^{t,\max}$ = Maximum number of additional units of capacity $C_j^t$

### 5.2.3 Reliability Equation and Approximation after Global Decomposition

The system state space consists of generation states in each area and inter-area tie line states. It is defined as (5.14).

$$\Omega = \begin{bmatrix} M_1 & M_2 & \ldots & M_N \\ m_1 & m_2 & \ldots & m_N \end{bmatrix} \tag{5.14}$$

where

$M_k$ = Maximum state of arc *k*

$m_k$ = Minimum state of arc *k*

$N$ = Number of arcs in the network

A system state, $x$, can assume any value between its minimum and maximum state as shown in (5.15).

$$x = \begin{bmatrix} x_1 & x_2 & \dots & x_N \end{bmatrix} \tag{5.15}$$

where $m_k \le x_k \le M_k$

$x_k$ = State of arc $k$

The maximum possible number of additional generators in each area is included in the state space before performing global decomposition. The additional generation capacity in each area is rounded off to the closest integral multiple of the fixed increment, $\eta$, used when constructing its distribution.

Let the budget constraint be of the following form,

$$a_1 y_1 + a_2 y_2 + \ldots + a_N y_N \le R \tag{5.16}$$

where

$a_j$ = Cost per additional generator to area $j$

$R$ = Total budget available

The maximum number of additional generation levels in area $j$ is calculated from (5.17).

$$\gamma_j^{\max} = \mu_j \left\lfloor \frac{R}{a_j} \right\rfloor \tag{5.17}$$

where

$\gamma_j^{\max}$ = Maximum number of additional generation levels in area $j$

$\mu_j$ = Maximum number of additional generation levels in area $j$

The sets obtained from this state space are valid for all scenarios of distribution of additional generators. Probability of each scenario can then be evaluated by allowing zero probability for the excluded states because of the omission of corresponding additional generators included in the original decomposition.

After global decomposition is performed, the state space is completely partitioned into a number of $L$ sets. Probability of a set is calculated from (5.18).

$$\Pr(\omega) = \prod_{k=1}^{N} \sum_{m_k^{\omega} \le x_k \le M_k^{\omega}} p_{x_k} \tag{5.18}$$

where

$\omega$ = A given set

$x_k$ = State of arc $k$

$p_{x_k}$ = Probability of state $x_k$ of arc $k$

$M_k^{\omega}$ = Maximum state of arc $k$ in set $\omega$

$m_k^{\omega}$ = Minimum state of arc $k$ in set $\omega$

Now area generation probability can be written as a function of additional units in the area as given in (5.11) or (5.12) for identical and non-identical units correspondingly. Therefore, equation (5.18) can be written in terms of number of additional units in each area as in (5.19).

$$\Pr(\omega) = \prod_{j=1}^{N} h_j(y_j) \tag{5.19}$$

and

$$h_j(y_j) = \sum_{k=0}^{y_j} \left[ \left( \sum_{i=m_j^{\omega}}^{M_j^{\omega}} P^0_{G^j_{i-\mu_j k}} \right) \binom{y_j}{k} (\mathrm{FOR}_j)^{y_j-k} (1-\mathrm{FOR}_j)^k \right]$$

$$= \sum_{k=0}^{y_j} \left[ \left( \overline{P}^0_{G^j_{M_j^{\omega}-\mu_j k}} - \overline{P}^0_{G^j_{m_j^{\omega}-\mu_j k-1}} \right) \binom{y_j}{k} (\mathrm{FOR}_j)^{y_j-k} (1-\mathrm{FOR}_j)^k \right] \quad (5.20)$$

where

$y_j$ = Number of additional units in area $j$

$\overline{P}^0_{G^j_{i-\mu_j k}}$ = Cumulative probability of original generation at level $i$- $\mu_j k$ before additional units in area $j$

Equation (5.20) is rewritten in the case of non-identical units as the following.

$$h_j(y_j^t) = \sum_{k=0}^{y_j^t} \left[ \left( \sum_{i=m_j^{\omega}}^{M_j^{\omega}} P^{t-1}_{G^j_{i-\mu_j^t k}} \right) \binom{y_j^t}{k} (\mathrm{FOR}^t_j)^{y_j^t-k} (1-\mathrm{FOR}^t_j)^k \right]$$

$$= \sum_{k=0}^{y_j^t} \left[ \left( \overline{P}^{t-1}_{G^j_{M_j^{\omega}-\mu_j^t k}} - \overline{P}^{t-1}_{G^j_{m_j^{\omega}-\mu_j^t k-1}} \right) \binom{y_j^t}{k} (\mathrm{FOR}^t_j)^{y_j^t-k} (1-\mathrm{FOR}^t_j)^k \right], t = 1, \ldots, m \quad (5.21)$$

where

$y_j^t$ = Number of additional units of capacity $C_j^t$ in area $j$

$\overline{P}^{t-1}_{G^j_{i-\mu_j k}}$ = Cumulative probability of generation at level $i - \mu_j^t k$ with additional units, $y_j^1, y_j^2, \ldots, y_j^{t-1}$ in area $j$, 0 if $i \le \mu_j^t k$

Probability of an $A$ set and $U$ set can also be expressed in terms of number of additional units in all areas as (5.19). Loss of load probability is calculated from summation of probability of loss of load sets. The objective function for the optimization problem can be expressed as (5.22).

$$LOLP = \sum_{i=1}^{n_d} \sum_{k=1}^{d_i} \Pr\left(L_k^i\right) \tag{5.22}$$

where

$n_d$ = Total number of decompositions

$d_i$ = Number of $L$ sets generated at $i^{th}$ decomposition

The problem is transformed into a single cost constraint (5.8) with an objective function to minimize loss of load probability (5.22). In order to apply dynamic programming, separable functions in both objective function and constraints are favorable structures. However, equation (5.22) is a very complex function with no specific pattern and has a nonlinear relationship between the decision variables which are the number of additional generators in each area. Because of the restriction of the function structure, it is more efficient to do the optimization with only 1 set from the global decomposition process or with $L$ sets only from the first stage of global decomposition process.

#### 5.2.3.1 The First *A* Set Equation

Instead of minimizing system loss of load probability from $L$ sets produced by global decomposition, this study proposes to maximize system availability computed from the first $A$ set of global decomposition. The first $A$ set contains unbiased information since it is extracted from the overall state space. Its probability equation is the same as in (5.19), which is a multiplication of one variable functions. The separable function structure of the first $A$ set probability equation is a desirable one; however, the

first *A* set generated from global decomposition is not likely to produce high probability. Most of the time, the first *L* sets generates higher probability than all other *L* sets generated in the decomposition process. In the following, the structure of the first *L* sets probability function is presented.

#### 5.2.3.2 The First *L* Set Equation

`After the first decomposition, loss of load sets can be found from reducing capacity in generation arc for each area until the loss of load state is found. The *L* sets generated from reducing generation arc in area 1 have the following structures.

$$L_1 = \begin{bmatrix} v_1 - 1 & M_2 & \cdots & M_n \\ 1 & 1 & 1 & 1 \end{bmatrix} \tag{5.23}$$

where

$M_i$ = Maximum capacity for the generation arc of area *i*

$v_1$ = Minimum capacity of generation in area 1 that the system remains in success state

In order to produce disjointed sets, the second *L* set obtained from reducing generation arc in area 2 is found below.

$$L_2 = \begin{bmatrix} M_1 & v_2 - 1 & \cdots & M_n \\ v_1 & 1 & 1 & 1 \end{bmatrix} \tag{5.24}$$

where

$v_2$ = Minimum capacity of generation in area 2 that the system remains in success state

Then, the first decomposition will create *n L* sets as a result of *n* generation area,

$$L_i = \begin{bmatrix} M_1 & M_2 & \cdots & v_i - 1 & \cdots & M_n \\ v_1 & v_2 & \cdots & 1 & 1 & 1 \end{bmatrix} \tag{5.25}$$

where

$v_i$ = Minimum capacity of generation in area *i* that the system remains in success state

Loss of load probability equation from the first *L* sets can be written as (5.26) and (5.27) in case of identical units and (5.82) in the case of non-identical units.

$$\Pr(L) = \sum_{i=1}^{N} \Pr(L_i) = \sum_{i=1}^{N} \prod_{j=1}^{N} g_j^i(y_j) \tag{5.26}$$

and

$$g_j^i(y_j) = \sum_{k=0}^{y_j} \left[ \left( \overline{P}^0_{G^j_{v_i - \mu_j k-1}} \right) \binom{y_j}{k} (\mathrm{FOR}_j)^{y_j - k} (1 - \mathrm{FOR}_j)^k \right] \tag{5.27}$$

$$g_j^i(y_j^t) = \sum_{k=0}^{y_j^t} \left[ \left( \overline{P}^{t-1}_{G^j_{v_i - \mu_j^t k-1}} \right) \binom{y_j^t}{k} (\mathrm{FOR}_j^t)^{y_j^t - k} (1 - \mathrm{FOR}_j^t)^k \right], t = 1, \ldots, m \tag{5.28}$$

where

$\overline{P}^0_{G^j_{v_i - \mu_j k-1}}$ = Cumulative probability of capacity arc $v_i$-$\mu_j k$-1 generation area *j* before unit addition

From (5.23), a probability equation of this set is rewritten as (5.29).

$$\Pr(L_1) = \prod_{j=1}^{N} g_j^1(y_j) = g_1^1(y_1) g_2^1(y_2) \cdots g_N^1(y_N) \tag{5.29}$$

Due to the structure of the first $L$ sets described by (5.25), the states of component from 2 to $N$ in $L_1$ set take all possible value from 1 to their maximum states, i.e.,

$$g_i^1(y_i) = 1,\ i = 2,\ldots,N \tag{5.30}$$

Therefore, (5.29) can be written as (5.31)

$$\Pr(L_1) = g_1^1(y_1) \tag{5.31}$$

Consider probability equation of $L_2$, the same argument can applied to the states from 2 to $N$, the probability from $L_2$ is (5.32)

$$\Pr(L_2) = g_1^2(y_1)g_2^2(y_2) \tag{5.32}$$

Since the capacity arc of area 1 in both $L_1$ and $L_2$ takes all possible value from 1 to $M_1$. This gives (5.33).

$$g_1^1(y_1) + g_1^2(y_1) = 1 \tag{5.33}$$

From (5.33), (5.32) can be simplified as (5.34)

$$\Pr(L_2) = \left(1 - g_1^1(y_1)\right)g_2^2(y_2) \tag{5.34}$$

The same analysis is then applied to all $L$ sets, the probability equation of $L_i$ set is (5.35). Even though the order of the generation arc we pick will create different $L$ sets, it can be shown that the resulting probability equations are exactly the same.

$$\Pr(L_i) = \left(1 - g_1^1(y_1)\right)\left(1 - g_2^2(y_2)\right)\cdots\left(1 - g_{i-1}^{i-1}(y_{i-1})\right)g_i^i(y_i) \tag{5.35}$$

The probability of loss of load after the first decomposition is (5.36). This equation has a separable structure; this will be clear when dynamic programming is applied to solve this problem.

$$\begin{aligned}\Pr(L) &= \sum_{i=1}^{N} \Pr(L_i) \\ &= g_1^1(y_1) + \left(1 - g_1^1(y_1)\right) g_2^2(y_2) + \ldots + \\ &\quad \left(1 - g_1^1(y_1)\right)\left(1 - g_2^2(y_2)\right) \cdots \left(1 - g_{N-1}^{N-1}(y_{N-1})\right) g_N^N(y_N)\end{aligned} \tag{5.36}$$

It should be observed that if any arc has '$v$' value equal to one, the effect of unit addition in that area to system reliability cannot be calculated from (5.36). In the process of obtaining $L$ sets, '$v$' values can be expressed as the smallest capacity of an area generation before the system enters loss of load state. In other words, the capacity below the '$v$' values will result in system failure (or loss of load in any area). The '$v$' values obtained from the decomposition are very important variables since they are the preliminary indications of area generation deficiency. It can also be implied from the '$v$' value that the components with '$v$' value equal to one do not contribute as much to the system reliability. In other words, without the capacity in that area ('$v$' value equal to one), the system can still remain in success state. Therefore, in this application, the '$v$' value will indicate the prospective area for the optimization process.

## 5.3 Dynamic Programming Application to the Problem

Dynamic programming is an optimization procedure that can be applied to a problem with discrete decision variables which are the number of additional units in each area in this application. The problem has the following formulation.

$$\text{Min } \Pr(L) \text{ or Max } \Pr(A)$$

$$\text{s.t. } a_1 y_1 + a_2 y_2 + \ldots + a_N y_N \le R$$

The first step in solving a problem with dynamic programming is to define stages and states of the problem. In this application, stages represent area of interest and states are the available budget at each stage as shown in Fig. 5.1. At each stage, a decision is made on how much should be spent on each area generation.

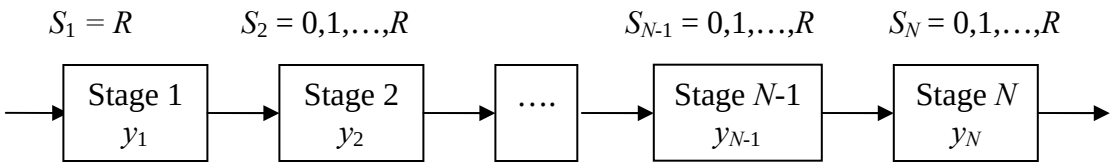


Fig. 5.1. State Diagram of the Problem

where

$S_j$ = Available budget at stage $j$

Dynamic programming initially solves the smallest sub problem, which contains the smallest number of variables. The optimal solution to the next sub problem (next stage) is calculated using the solution from the previously computed smaller sub problem (previous stage). A recursive function can be derived to describe this relationship. In this problem, the last stage is the smallest sub problem; therefore, the solution obtained from the last stage is the starting point of a recursive function.

If a solution from optimization does not satisfy system reliability criteria, a budget constraint can then be relaxed to incorporate more generation units. Global

decomposition is not required to be performed once again if the maximum number of additional units in each area remains the same. The problem can then be re-optimized until the reliability criterion is satisfied. The following analysis covers the recursive function derivation for the first *L* set and the first *A* set optimization. With this recursive function, solutions from each stage can be evaluated. The recursive function describes a relationship between (already computed) solutions from a previous stage to a current stage. The optimal solution can then be traced back when the solution to the first stage is found.

### 5.3.1 Recursive Function of the First *A* Set Optimization

Recall that the probability of the first *A* set is (5.19).

$$\Pr(A) = \prod_{j=1}^{N} h_j(y_j) \tag{5.19}$$

At the very last stage, there is only one area in the subproblem, which is (5.37).

$$\begin{aligned} &\max h_N(y_N) \\ &s.t. \quad a_N y_N \le S_N \\ &\qquad y_N \in I^+ \end{aligned} \tag{5.37}$$

where

$S_N$ = 0, 1, …, $R$

For the preceding stages, the numbers of variables considered are larger and the problem at any stages is (5.38).

$$\begin{aligned} &\max \prod_{k=j}^{N} h_k(y_k) \\ &s.t. \quad a_j y_j + a_{j+1} y_{j+1} + \ldots + a_N y_N \le S_j \\ &\qquad y_k \in I^+ \end{aligned} \tag{5.38}$$

Note that the first stage represents the overall problem since it considers all variables. Let $f_j(S_j)$ be the optimal objective function at stage *j* with available budget $S_j$

The optimal solution to the last stage is (5.39)

$$f_N(S_N) = h_N(y_N) \tag{5.39}$$

Since $0 \le y_N \le \left\lfloor \frac{S_N}{a_N} \right\rfloor$, (5.39) is rewritten as (5.40).

$$f_N(S_N) = h_N\left(\left\lfloor \frac{S_N}{a_N} \right\rfloor\right) \tag{5.40}$$

Recall that the problem at any stages is (5.38) and the optimal solution to any stage is (5.41)

$$f_j(S_j) = \max\left\{h_j(y_j) \cdot f_{j+1}(S_j - a_j y_j)\right\} \tag{5.41}$$

where $0 \le y_j \le \left\lfloor \frac{S_j}{a_j} \right\rfloor$

The recursive function is written as (5.41)

$$f_j(S_j) = \begin{cases} h_j\left(\left\lfloor \frac{S_j}{a_j} \right\rfloor\right) & , j = N \\ \max\limits_{0 \le y_j \le \left\lfloor \frac{S_j}{a_j} \right\rfloor} \left\{h_j(m_j) \cdot f_{j+1}(S_j - a_j y_j)\right\} & , j = 1, \ldots, N-1 \end{cases} \tag{5.41}$$

### 5.3.2 Recursive Function of the First *L* Set Optimization

Recall that the probability of the first *L* set is (5.36).

$$\begin{aligned}\Pr(L) &= \sum_{i=1}^{N} \Pr(L_i) \\ &= g_1^1(y_1) + \left(1 - g_1^1(y_1)\right) g_2^2(y_2) + \ldots + \\ &\quad \left(1 - g_1^1(y_1)\right)\left(1 - g_2^2(y_2)\right) \cdots \left(1 - g_{N-1}^{N-1}(y_{N-1})\right) g_N^N(y_N)\end{aligned} \tag{5.36}$$

At the very last stage, there is only one area in the subproblem, which is (5.42)

$$\begin{aligned}&\min g_N^N(y_N) \\ &s.t. \quad a_N y_N \le S_N \\ &\qquad y_N \in I^+\end{aligned} \tag{5.42}$$

where

$S_N$ = 0, 1, …, $R$

For the preceding stages, the numbers of variables considered are larger, the problem in any stages is (5.43)

$$\begin{aligned}&\min g_j^j(y_j) + \left(1 - g_j^j(y_j)\right)\left\{\cdots\left\{g_{N-1}^{N-1}(y_{N-1}) + \left(1 - g_{N-1}^{N-1}(y_{N-1})\right) g_N^N(y_N)\right\}\right\} \\ &s.t. \quad a_j y_j + a_{j+1} y_{j+1} + \ldots + a_N y_N \le S_j \\ &\qquad y_j \in I^+\end{aligned} \tag{5.43}$$

Let $f_j(S_j)$ be the optimal objective function at stage *j* with available budget $S_j$, the optimal solution to the last stage is (5.44)

$$f_N(S_N) = g_N^N(y_N) \tag{5.44}$$

Since $0 \le y_N \le \left\lfloor \frac{S_N}{a_N} \right\rfloor$, (5.44) is rewritten as (5.45).

$$f_N(S_N) = h_N\left(\left\lfloor \frac{S_N}{a_N} \right\rfloor\right) \tag{5.45}$$

The optimal solution to any stage is (5.46)

$$f_j(S_j) = \min\left\{g_j^j(y_j) + \left(1 - g_j^j(y_j)\right) f_{j+1}\left(S_j - a_j y_j\right)\right\} \tag{5.46}$$

where $0 \le y_j \le \left\lfloor \frac{S_j}{a_j} \right\rfloor$

The same function (5.46) is also applied to the first stage where $S_1 = R$ and the recursive function is (5.47)

$$f_j(S_j) = \begin{cases} g_j^j\left(\left\lfloor \frac{S_j}{a_j} \right\rfloor\right) & , j = N \\ \min\limits_{0 \le y_j \le \left\lfloor \frac{S_j}{a_j} \right\rfloor} \left\{g_j^j(y_j) + \left(1 - g_j^j(y_j)\right) f_{j+1}\left(S_j - a_j y_j\right)\right\} & , j = 1, \ldots, N-1 \end{cases} \tag{5.47}$$

## 5.4 Illustration on Three-Area Test System

The proposed approach is applied to a three-area power system with step-by-step calculation. The three-area test system parameters are given in Appendix C. The addition unit parameters of three area system are shown in Table 5.1. Assume that the budget is 10 million dollars, the problem is to locate the best generation combination in the three areas. Stage diagram of the problem is shown in Fig. 5.2.

Table 5.1 Three Area Addition Unit Parameters

| Area $j$ | $a_j$ (m$) | Load (MW) | FOR$_i$ |
|---|---|---|---|
| 1 | 3 | 500 | 0.15 |
| 2 | 5 | 600 | 0.05 |
| 3 | 4 | 500 | 0.10 |

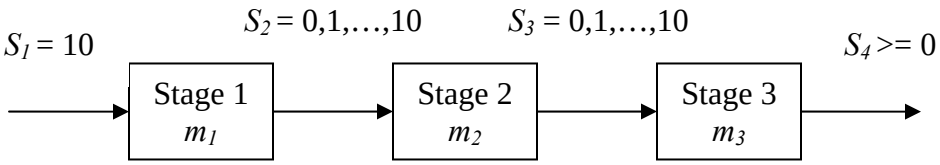


Fig. 5.2 Stage Diagram of Three Area System

From the budget constraint, the maximum numbers of unit addition in each area are 3 units in area 1, 2 units in area 2, and 2 units in area 3. These units will be included in the system before performing global decomposition. State of capacity arc will start from 1 to 9. The solution steps from the first $A$ set optimization and the first $L$ set optimization are presented in the following.

### 5.4.1 Illustration of the First *A* Set Optimization

After the first decomposition,

$$A = \begin{bmatrix} 9 & 9 & 8 & 2 & 2 & 2 \\ 6 & 7 & 6 & 1 & 1 & 1 \end{bmatrix}$$

The problem can be formulated as (5.48)

$$\begin{aligned} &\max \Pr(A) = h_1(y_1) \cdot h_2(y_2) \cdot h_3(y_3) \\ &s.t. \quad 3y_1 + 5y_2 + 4y_3 \le 10 \\ &\qquad y_j \in I^+ \end{aligned} \tag{5.48}$$

where

$$h_1(y_1) = \sum_{k=0}^{y_1} \left( \overline{P}^0_{G^1_{9-k}} - \overline{P}^0_{G^1_{5-k}} \right) \binom{y_1}{k} (0.15)^{y_1-k} (0.85)^k \tag{5.49}$$

$$h_2(y_2) = \sum_{k=0}^{y_2} \left( \overline{P}^0_{G^2_{9-k}} - \overline{P}^0_{G^2_{6-k}} \right) \binom{y_2}{k} (0.05)^{y_2-k} (0.95)^k \tag{5.50}$$

$$h_3(y_3) = \sum_{k=0}^{y_3} \left( \overline{P}^0_{G^3_{8-k}} - \overline{P}^0_{G^3_{5-k}} \right) \binom{y_3}{k} (0.1)^{y_3-k} (0.9)^k \tag{5.51}$$

The table relating available budget $S_j$ (from 0 to 10) with the probability of each $y_j$, $h_j(y_j)$ are developed with the following calculations. Possible values of $y_1$ are 0, 1, 2 and 3. The calculation is shown below.

$$h_1(0) = \overline{P}^0_{G^1_9} - \overline{P}^0_{G^1_5} = 0.3277 \tag{5.52}$$

$$h_1(1) = \left( \overline{P}^0_{G^1_9} - \overline{P}^0_{G^1_5} \right)(0.15) + \left( \overline{P}^0_{G^1_8} - \overline{P}^0_{G^1_4} \right)(0.85) = 0.6758 \tag{5.53}$$

$$h_1(2) = \sum_{k=0}^{2} \left( \overline{P}^0_{G^1_{9-k}} - \overline{P}^0_{G^1_{5-k}} \right) \binom{2}{k} (0.15)^{2-k} (0.85)^k = 0.8760 \tag{5.54}$$

$$h_1(3) = \sum_{k=0}^{3} \left( \overline{P}^0_{G^1_{9-k}} - \overline{P}^0_{G^1_{5-k}} \right) \binom{3}{k} (0.15)^{3-k} (0.85)^k = 0.9597 \tag{5.55}$$

Possible values of $y_2$ are 0, 1 and 2. The calculation is shown below.

$$h_2(0) = \overline{P}^0_{G^2_9} - \overline{P}^0_{G^2_6} = 0.2621 \tag{5.56}$$

$$h_2(1) = \left( \overline{P}^0_{G^2_9} - \overline{P}^0_{G^2_6} \right)(0.05) + \left( \overline{P}^0_{G^2_8} - \overline{P}^0_{G^2_5} \right)(0.95) = 0.6357 \tag{5.57}$$

$$h_2(2) = \sum_{k=0}^{2} \left( \overline{P}^0_{G^2_{9-k}} - \overline{P}^0_{G^2_{6-k}} \right) \binom{2}{k} (0.05)^{2-k} (0.95)^k = 0.8762 \tag{5.58}$$

Possible values of $y_3$ are 0, 1 and 2. The calculation is shown below.

$$h_3(0) = \overline{P}^0_{G^3_8} - \overline{P}^0_{G^3_5} = 0.3277 \tag{5.59}$$

$$h_3(1) = \left( \overline{P}^0_{G^3_8} - \overline{P}^0_{G^3_5} \right)(0.1) + \left( \overline{P}^0_{G^3_7} - \overline{P}^0_{G^3_4} \right)(0.9) = 0.6963 \tag{5.60}$$

$$h_3(2) = \sum_{k=0}^{2} \left( \overline{P}^0_{G^3_{8-k}} - \overline{P}^0_{G^3_{5-k}} \right) \binom{2}{k} (0.1)^{2-k} (0.9)^k = 0.8991 \tag{5.61}$$

Table 5.2 shows a relationship between available budget ($S_j$ from 0 to 10) and the probability of each $y_j$, $h_j(y_j, S_j)$

Table 5.2 Available Budget and Modified Probability with Additional Units for the First *A* Set Optimization

| Budget of (m$) | Probability and number of unit addition in each area | | | | | |
|---|---|---|---|---|---|---|
| | $y_1$ | $h_1(y_1)$ | $y_2$ | $h_2(y_2)$ | $y_3$ | $h_3(y_3)$ |
| 0-2 | 0 | 0.3277 | 0 | 0.2621 | 0 | 0.3277 |
| 3 | 1 | 0.6758 | 0 | 0.2621 | 0 | 0.3277 |
| 4 | 1 | 0.6758 | 0 | 0.2621 | 1 | 0.6963 |
| 5 | 1 | 0.6758 | 1 | 0.6357 | 1 | 0.6963 |
| 6-7 | 2 | 0.8760 | 1 | 0.6357 | 1 | 0.6963 |
| 8 | 2 | 0.8760 | 1 | 0.6357 | 2 | 0.8991 |
| 9 | 3 | 0.9597 | 1 | 0.6357 | 2 | 0.8991 |
| 10 | 3 | 0.9597 | 2 | 0.8762 | 2 | 0.8991 |

The decision of the budget that will be spent in each area is made at each stage. At stage 3 from (5.62), the optimal decision at each budget level and its corresponding objective function value are shown in Table 5.3.

$$f_3(S_3) = h_3\left(\left\lfloor \frac{S_3}{4} \right\rfloor\right) \tag{5.62}$$

Table 5.3 Optimal Decision at Stage 3 for the First *A* Set Optimization

| $S_3$ | $y_3$ | $f_3(S_3)$ |
|---|---|---|
| 0-3 | 0 | 0.3277 |
| 4-7 | 1 | 0.6963 |
| 8-10 | 2 | 0.8991 |

At stage 2, we have

$$f_2(S_2) = \max\{h_2(y_2, S_2) \cdot f_3(S_2 - 5y_2)\}. \tag{5.63}$$

where $0 \le y_2 \le \left\lfloor \frac{S_2}{5} \right\rfloor$

The optimal decision at stage 2 is shown in Table 5.4

Table 5.4 Optimal Decision at Stage 2 for the First *A* Set Optimization

| $S_2$ | $y_2$ | | | Opt. $y_2$ | $f_2(S_2)$ |
|---|---|---|---|---|---|
| | 0 | 1 | 2 | | |
| 0-3 | $0.2621 \cdot f_3(0-3)$ = 0.0859 | - | - | 0 | 0.0859 |
| 4 | $0.2621 \cdot f_3(4)$ = 0.1825 | - | - | 0 | 0.1825 |
| 5 | $0.2621 \cdot f_3(5)$ = 0.1825 | $0.6357 \cdot f_3(0)$ = 0.2083 | - | 1 | 0.2083 |
| 6 | $0.2621 \cdot f_3(6)$ = 0.1825 | $0.6357 \cdot f_3(1)$ = 0.2083 | - | 1 | 0.2083 |
| 7 | $0.2621 \cdot f_3(7)$ = 0.1825 | $0.6357 \cdot f_3(2)$ = 0.2083 | - | 1 | 0.2083 |
| 8 | $0.2621 \cdot f_3(8)$ = 0.2357 | $0.6357 \cdot f_3(3)$ = 0.2083 | - | 0 | 0.2357 |
| 9 | $0.2621 \cdot f_3(9)$ = 0.2357 | $0.6357 \cdot f_3(4)$ = 0.4427 | - | 1 | 0.4427 |
| 10 | $0.2621 \cdot f_3(10)$ = 0.2357 | $0.6357 \cdot f_3(5)$ = 0.4427 | $0.8762 \cdot f_3(0)$ = 0.2871 | 1 | 0.4427 |

At stage 1,

$$f_1(10) = \max\{h_1(y_1,10) \cdot f_2(10-3y_1)\} \tag{5.64}$$

where $0 \le y_1 \le \left\lfloor \frac{10}{3} \right\rfloor$

The optimal decision at stage 1 is shown in Table 5.5.

Table 5.5 Optimal Decision at Stage 1 for the First *A* Set Optimization

| $y_1$ | | | | Opt. $y_1$ | $f_1(10)$ |
|---|---|---|---|---|---|
| 0 | 1 | 2 | 3 | | |
| $0.3277 \cdot f_2(10)$ = 0.1450 | $0.6759 \cdot f_2(7)$ = 0.1408 | $0.8760 \cdot f_2(4)$ = 0.1598 | $0.9597 \cdot f_2(1)$ = 0.0824 | 2 | 0.1598 |

The solution is to locate 2 generation at area 1, 0 generation at area 2, and 1 generation at area 3. The total cost is 10 m$. This combination will yield the maximum probability of the first *A* set which is 0.1598.

### 5.4.2 Illustration of the First *L* Set Optimization

After the first decomposition, the first *L* sets are as follows.

$$L_1 = \begin{bmatrix} 3 & 9 & 8 & 2 & 2 & 2 \\ 1 & 1 & 1 & 1 & 1 & 1 \end{bmatrix} \quad L_2 = \begin{bmatrix} 9 & 4 & 8 & 2 & 2 & 2 \\ 4 & 1 & 1 & 1 & 1 & 1 \end{bmatrix} \quad L_3 = \begin{bmatrix} 9 & 9 & 3 & 2 & 2 & 2 \\ 4 & 5 & 1 & 1 & 1 & 1 \end{bmatrix}$$

The problem can be formulated as (5.65)

$$\begin{aligned} &\min \Pr(L) = g_1^1(y_1) + \left(1 - g_1^1(y_1)\right)\left[g_2^2(y_2) + \left(1 - g_2^2(y_2)\right)g_3^3(y_3)\right] \\ &s.t. \quad 3y_1 + 5y_2 + 4y_3 \le 10 \\ &\qquad y_j \in I^+ \end{aligned} \tag{5.65}$$

where

$$g_1^1(y_1) = \sum_{k=0}^{y_1}\left[\overline{P}^0_{G^1_{3-k}}\binom{y_1}{k}(0.15)^{y_1-k}(0.85)^k\right] \tag{5.66}$$

$$g_2^2(y_2) = \sum_{k=0}^{y_2}\left[\overline{P}^0_{G^2_{4-k}}\binom{y_2}{k}(0.05)^{y_2-k}(0.95)^k\right] \tag{5.67}$$

$$g_3^3(y_3) = \sum_{k=0}^{y_3} \left[ \overline{P}^0_{G^3_{3-k}} \binom{y_3}{k} (0.1)^{y_3-k} (0.9)^k \right] \tag{5.68}$$

The table relating available budget $S_j$ (from 0 to 10) with the probability of each $y_j$, $g_j^j(y_j)$ are developed with the following calculations.

Possible values of $y_1$ are 0, 1, 2 and 3. The calculation is shown below.

$$g_1^1(0) = \overline{P}^0_{G_3^1} = 0.0579 \tag{5.69}$$

$$g_1^1(1) = \overline{P}^0_{G_3^1} \binom{1}{1} (0.15) + \overline{P}^0_{G_2^1} \binom{1}{0} (0.85) = 0.0144 \tag{5.70}$$

$$g_1^1(2) = \overline{P}^0_{G_3^1} \binom{2}{2} (0.15)^2 + \overline{P}^0_{G_2^1} \binom{2}{1} (0.15)(0.85) + \overline{P}^0_{G_1^1} \binom{2}{0} (0.85)^2 = 0.0033 \tag{5.71}$$

$$g_1^1(3) = \overline{P}^0_{G_3^1} \binom{3}{3} (0.15)^3 + \overline{P}^0_{G_2^1} \binom{3}{2} (0.15)^2 (0.85) + \overline{P}^0_{G_1^1} \binom{3}{1} (0.15)(0.85)^2 = 0.0007 \tag{5.72}$$

Possible values of $y_2$ are 0, 1 and 2. The calculation is shown below.

$$g_2^2(0) = \overline{P}^0_{G_4^2} = 0.0989 \tag{5.73}$$

$$g_2^2(1) = \overline{P}^0_{G_4^2} \binom{1}{1} (0.05) + \overline{P}^0_{G_3^2} \binom{1}{0} (0.95) = 0.0211 \tag{5.74}$$

$$g_2^2(2) = \overline{P}^0_{G_4^2} \binom{2}{2} (0.05)^2 + \overline{P}^0_{G_3^2} \binom{2}{1} (0.05)(0.95) + \overline{P}^0_{G_2^2} \binom{2}{0} (0.95)^2 = 0.0033 \tag{5.75}$$

Possible values of $y_3$ are 0, 1 and 2. The calculation is shown below.

$$g_3^3(0) = \overline{P}^0_{G_3^3} = 0.0578 \tag{5.76}$$

$$g_3^3(1) = \overline{P}_{G_3^3}^0 \binom{1}{1}(0.1) + \overline{P}_{G_2^3}^0 \binom{1}{0}(0.9) = 0.0118 \tag{5.77}$$

$$g_3^3(2) = \overline{P}_{G_3^3}^0 \binom{2}{2}(0.1)^2 + \overline{P}_{G_2^3}^0 \binom{2}{1}(0.1)(0.9) + \overline{P}_{G_1^3}^0 \binom{2}{0}(0.9)^2 = 0.0020 \tag{5.78}$$

Table 5.6 shows a relationship between available budget ($S_j$ from 0 to 10) and the probability of each $y_j$, $g_j^j(y_j, S_j)$.

Table 5.6 Available Budget and Modified Probability with Additional Units for the First $L$ Set Optimization

| Budget of (m$) | Probability and number of unit addition in each area | | | | | |
|---|---|---|---|---|---|---|
| | $y_1$ | $g_1^1(y_1)$ | $y_2$ | $g_2^2(y_2)$ | $y_3$ | $g_3^3(y_3)$ |
| 0-2 | 0 | 0.0579 | 0 | 0.0989 | 0 | 0.0579 |
| 3 | 1 | 0.0144 | 0 | 0.0989 | 0 | 0.0579 |
| 4 | 1 | 0.0144 | 0 | 0.0989 | 1 | 0.0118 |
| 5 | 1 | 0.0144 | 1 | 0.0211 | 1 | 0.0118 |
| 6-7 | 2 | 0.0033 | 1 | 0.0211 | 1 | 0.0118 |
| 8 | 2 | 0.0033 | 1 | 0.0211 | 2 | 0.0020 |
| 9 | 3 | 0.0007 | 1 | 0.0211 | 2 | 0.0020 |
| 10 | 3 | 0.0007 | 2 | 0.0033 | 2 | 0.0020 |

The decision of the budget that will be spent in each area is made at each stage. At stage 3,

$$f_3(S_3) = g_3\left(\left\lfloor \frac{S_3}{4} \right\rfloor\right) \tag{5.79}$$

The optimal decision at each budget level and its corresponding objective function value are shown in Table 5.7.

Table 5.7 Optimal Decision at Stage 3 for the First *L* Set Optimization

| $S_3$ | $y_3$ | $f_3(S_3)$ |
|---|---|---|
| 0-3 | 0 | 0.0579 |
| 4-7 | 1 | 0.0118 |
| 8-10 | 2 | 0.0020 |

At stage 2, we have

$$f_2(S_2) = \min\left\{g_2^2(y_2) + \left(1 - g_2^2(y_2)\right) f_3(S_2 - 5y_2)\right\} \tag{5.80}$$

where $0 \le y_2 \le \left\lfloor \frac{S_2}{5} \right\rfloor$

The optimal decision at stage 2 is shown in Table 5.8.

Table 5.8 Optimal Decision at Stage 2 for the First $L$ Set Optimization

| $S_2$ | $y_2$ | | | Opt. $y_2$ | $f_2(S_2)$ |
|---|---|---|---|---|---|
| | 0 | 1 | 2 | | |
| 0-3 | 0.0989 + (1-0.0989)$\cdot f_3(0)$ = 0.1511 | - | - | 0 | 0.1511 |
| 4 | 0.0989 + (1-0.0989)$\cdot f_3(4)$ = 0.1095 | - | - | 0 | 0.1095 |
| 5 | 0.0989 + (1-0.0989)$\cdot f_3(5)$ = 0.1095 | 0.0211 + (1-0.0211)$\cdot f_3(0)$ = 0.0778 | - | 1 | 0.0778 |
| 6 | 0.0989 + (1-0.0989)$\cdot f_3(6)$ = 0.1095 | 0.0211+ (1-0.0211)$\cdot f_3(1)$ = 0.0778 | - | 1 | 0.0778 |
| 7 | 0.0989+ (1-0.0989)$\cdot f_3(7)$ = 0.1095 | 0.0211 + (1-0.0211)$\cdot f_3(2)$ = 0.0778 | - | 1 | 0.0778 |
| 8 | 0.0989 + (1-0.0989)$\cdot f_3(8)$ = 0.1007 | 0.0211+ (1-0.0211)$\cdot f_3(3)$ = 0.0778 | - | 1 | 0.0778 |
| 9 | 0.0989+ (1-0.0989)$\cdot f_3(9)$ = 0.1007 | 0.0211+ (1-0.0211)$\cdot f_3(4)$ = 0.0326 | - | 1 | 0.0326 |
| 10 | 0.0989 + (1-0.0989)$\cdot f_3(10)$ = 0.1007 | 0.0211 + (1-0.0211)$\cdot f_3(5)$ = 0.0326 | 0.0033 + (1-0.0033)$\cdot f_3(0)$ = 0.0610 | 1 | 0.0326 |

At stage 1,

$$f_1(10) = \min\left\{g_1^1(y_1) + \left(1 - g_1^1(y_1)\right) f_2(10 - 3y_1)\right\} \tag{5.81}$$

where $0 \le y_1 \le \left\lfloor \frac{10}{3} \right\rfloor$

The optimal decision at stage 1 is shown in Table 5.9.

Table 5.9 Optimal Decision at Stage 1 for the First $L$ Set Optimization

| $y_1$ | | | | Opt. $y_1$ | $f_1(10)$ |
|---|---|---|---|---|---|
| 0 | 1 | 2 | 3 | | |
| 0.0579 + {(1-0.0579) $\cdot f_2(10)$} = 0.0887 | 0.0144 + {(1-0.0144) $\cdot f_2(7)$} = 0.0910 | 0.0033 + {(1-0.0033) $\cdot f_2(4)$} = 0.1124 | 0.0007 + {(1-0.0007) $\cdot f_2(1)$} = 0.1517 | 0 | 0.0887 |

The optimal solution is to locate 0 generation at area 1, 1 generation at area 2, and 1 generation at area 3. The total cost is 9 million dollars. This combination yields the minimum loss of load probability of the first $L$ sets which is 0.0887. The solutions from the first $L$ sets optimization are compared with the optimal from enumeration as shown in Table 5.10.

Table 5.10 Comparison between Solutions from the First $L$ Set Optimization and Enumerations

| Possible combination | | | Cost | LOLP of the first $L$ set obtained from global decomposition | Actual LOLP |
|---|---|---|---|---|---|
| $y_1$ | $y_2$ | $y_3$ | | | |
| 0 | 0 | 2 | 8 | 0.1528 | 0.7101 |
| 0 | 1 | 1 | 9 | 0.0887 | 0.6850 |
| 0 | 2 | 0 | 10 | 0.1154 | 0.6883 |
| 1 | 0 | 1 | 7 | 0.1224 | 0.7060 |
| 1 | 1 | 0 | 8 | 0.0910 | 0.6950 |
| **2** | **0** | **1** | **10** | **0.1124** | **0.5280** |
| 3 | 0 | 0 | 9 | 0.1517 | 0.5959 |

Table 5.10 shows that the optimal solution is to locate 2 generation units in area 1, and 1 generation units in area 3. The solution obtained from dynamic programming application to the first *L* set is not optimal; however, it is close to the optimal solution. Recall that the solution from the first *A* set optimization is the optimal one. In the following, area load is reduced to observe the effectiveness of the approach. Table 5.11 shows the result with system load of 400, 500, and 400 in area 1, 2 and 3. Table 5.12 shows the result with system load of 300, 400, and 300 in area 1, 2 and 3.

Table 5.11 Comparison between Solutions from the First *L* Set Optimization and Enumerations with System Load of 400, 500, and 400 in Areas 1, 2 and 3

| Possible combination | | | Cost | LOLP of the first *L* set obtained from global decomposition | LOLP |
|---|---|---|---|---|---|
| $y_1$ | $y_2$ | $y_3$ | | | |
| 0 | 0 | 2 | 8 | 0.0237 | 0.1485 |
| 0 | 1 | 1 | 9 | 0.0100 | 0.1157 |
| 0 | 2 | 0 | 10 | 0.0136 | 0.1247 |
| 1 | 0 | 1 | 7 | 0.0192 | 0.1354 |
| 1 | 1 | 0 | 8 | 0.0103 | 0.1219 |
| **2** | **0** | **1** | **10** | **0.0181** | **0.0837** |
| 3 | 0 | 0 | 9 | 0.0236 | 0.1174 |

Table 5.12 Comparison between Solutions from the First $L$ Set Optimization and Enumerations with System Load of 300, 400, and 300 in Areas 1, 2 and 3

| Possible combination | | | Cost | LOLP of the first $L$ set obtained from global decomposition | LOLP |
|---|---|---|---|---|---|
| $y_1$ | $y_2$ | $y_3$ | | | |
| 0 | 0 | 2 | 8 | 0.0019 | 0.0115 |
| **0** | **1** | **1** | **9** | **0.0005** | **0.0057** |
| 0 | 2 | 0 | 10 | 0.0006 | 0.0074 |
| 1 | 0 | 1 | 7 | 0.0017 | 0.0092 |
| 1 | 1 | 0 | 8 | 0.0005 | 0.0061 |
| 2 | 0 | 1 | 10 | 0.0016 | 0.0070 |
| 3 | 0 | 0 | 9 | 0.0019 | 0.0105 |

It can be seen that even though the solution is not optimal, it requires less cost than an optimal one and therefore should be acceptable as a near optimal one. It appears that the proposed approach works better for systems with smaller loss of load probabilities.

## 5.5 Implementation on Twelve-Area Test System

A 12-area power system is shown in Appendix A. The test system is a multi-area representation of an actual power system [73] that has 137 generation units and 169 tie line connections between areas. Generating unit failure and repair rate data are from IEEE Reliability Test System 1996. Transfer capabilities between areas are given in Appendix A. Table 5.13 shows area generations and loads as well as availability and cost per generator in prospective areas which are areas 1 to 5, and 9 to 12. It is assumed that the additional generators have capacity of 200 MW each. Probability distribution tables for generation and tie-lines are developed with a capacity increment of 50 MW.

System loss of load probability before unit additions is 0.0041 for original load and 0.0153 for 10% increased load. Reliability indices presented in the analysis are calculated from complete decomposition approach.

Table 5.13 Generation and Load Parameters of a Twelve Area Test System

| Area *j* | Load (MW) | 10 % increased Load (MW) | Generation (MW) | FOR of additional units | Cost ($m) |
|---|---|---|---|---|---|
| 1 | 1750 | 1900 | 2550 | 0.025 | 250 |
| 2 | 16650 | 18300 | 23600 | 0.025 | 250 |
| 3 | 9300 | 10250 | 15100 | 0.025 | 250 |
| 4 | 2000 | 2200 | 3100 | 0.025 | 250 |
| 5 | 550 | 600 | 900 | 0.025 | 250 |
| 6 | 0 | 0 | 550 | - | - |
| 7 | 0 | 0 | 3500 | - | - |
| 8 | 0 | 0 | 400 | - | - |
| 9 | 1100 | 1200 | 2100 | 0.025 | 250 |
| 10 | 2200 | 2400 | 3100 | 0.025 | 250 |
| 11 | 2600 | 2850 | 4150 | 0.025 | 250 |
| 12 | 750 | 850 | 900 | 0.025 | 250 |

The analysis is implemented with two load scenarios; original and 10% increased, and repeated with two budgets; $0.5 and $1 billion. Maximum number of additional units allowed in each area is two units for $0.5 billion budget and four units for $1 billion budget, which gives 45 and 495 possible generator combinations respectively. The purpose of having two different budgets is to test the correctness of the proposed method. The proposed method is applied to smaller budget first and then to

larger budget. To verify the correctness of the solution from this procedure, an optimal solution for each scenario is also obtained by enumeration.

The additional units are included in the state space before performing global decomposition according to the budget. Once global decomposition is performed, candidate areas are determined by the '*v*' value and the optimal solution from the first *L* set optimization is computed. Table 5.14 shows the solution for the system with original load and $0.5 billion budget. Table 5.15 shows the solution with 10% increased load and $0.5 billion budget. Table 5.16 shows the solution with original load and $1 billion budget. Table 5.17 shows the solution with 10% increased load and $1 billion budget. Table 5.18 shows the comparison between the optimal solution from proposed method and that from enumeration.

Table 5.14 Solution with $0.5 Billion Budget

| Area | 1 | 2 | 3 | 4 | 5 | 9 | 10 | 11 | 12 |
|---|---|---|---|---|---|---|---|---|---|
| '*v*' value | 1 | 248 | 147 | 27 | 1 | 1 | 16 | 23 | 1 |
| Solution from DP | - | 0 | 0 | 2 | - | - | 0 | 0 | - |
| Optimal Solution | 0 | 0 | 0 | 2 | 0 | 0 | 0 | 0 | 0 |

Table 5.15 Solution with $0.5 Billion Budget and 10% Increased Load

| Area | 1 | 2 | 3 | 4 | 5 | 9 | 10 | 11 | 12 |
|---|---|---|---|---|---|---|---|---|---|
| '*v*' value | 1 | 284 | 166 | 31 | 1 | 1 | 20 | 28 | 1 |
| Solution from DP | - | 0 | 0 | 2 | - | - | 0 | 0 | - |
| Optimal Solution | 0 | 0 | 0 | 2 | 0 | 0 | 0 | 0 | 0 |

Table 5.16 Solution with $1 Billion Budget

| Area | 1 | 2 | 3 | 4 | 5 | 9 | 10 | 11 | 12 |
|---|---|---|---|---|---|---|---|---|---|
| '*v*' value | 1 | 240 | 147 | 27 | 1 | 1 | 16 | 23 | 1 |
| Solution from DP | - | 0 | 0 | 3 | - | - | 1 | 0 | - |
| Optimal Solution | 0 | 1 | 0 | 3 | 0 | 0 | 0 | 0 | 0 |

Table 5.17 Solution with $1 Billion Budget and 10% Increased Load

| Area | 1 | 2 | 3 | 4 | 5 | 9 | 10 | 11 | 12 |
|---|---|---|---|---|---|---|---|---|---|
| '*v*' value | 1 | 276 | 166 | 31 | 1 | 1 | 20 | 28 | 1 |
| Solution from DP | - | 0 | 1 | 3 | - | - | 0 | 0 | - |
| Optimal Solution | 0 | 2 | 0 | 2 | 0 | 0 | 0 | 0 | 0 |

Table 5.18 Comparison between the Solutions from the Proposed Method and the Optimal Solution

| Scenarios | LOLP of optimal solution from proposed method | LOLP of optimal solution from enumeration | % Difference |
|---|---|---|---|
| Original Load, $0.5 B | 0.001640 | 0.001640 | 0 |
| Increased Load, $0.5 B | 0.010182 | 0.010182 | 0 |
| Original Load, $1 B | 0.001320 | 0.001284 | 2.80 |
| Increased Load, $1 B | 0.008975 | 0.007834 | 14.56 |

Results show that when the maximum number of additional units in each area is small, the proposed method accurately provides optimal solution. However, when the maximum number of additional units in each area is higher, the proposed method provides a solution with LOLP close to the one obtained from the optimal solution. This

is due to the fact that all possible additional units are included in the state space before performing global decomposition. Since all the states are assumed to exist in the system, the first $L$ sets from global decomposition can underestimate capacity deficiency, and thus, LOLP. Even though the proposed method may not necessarily provide the optimal solution, it still gives a solution close to optimal one that can be adjusted with some other sensitivity techniques to obtain the optimal solution.

Results also show that when system loss of load probability is small, the proposed method produces optimal or close to optimal solution. System with small loss of load probability tends to have much more generation than load. When the system loses its generation in any single area, the surrounding areas can provide assistance allowed by transfer capabilities from its neighborhood areas. This means that there is smaller probability that the system will lose its generations in two areas or more to produce loss of load state.

The first $L$ sets from global decomposition are partitioned from the overall state space by lowering generation in one area while keeping generation in other areas at their maximum until the system reaches loss of load state. They provide information about the effect of additional generation in any area to partial system loss of load probability which is produced from loss of generation in a single area i.e. $L_i$ is produced from loss of generation in area $i$. The combined effects of loss of area generation in two (or three or more) areas are evaluated at the second (or third and so on) stage of decomposition.

However, when there are small probabilities that loss of two or more area generators creates loss of load states, the effects of additional generation on loss of load

probability are mainly dominated by loss of generation in one area and transfer capability of its surrounding areas, or equivalently, the first *L* set from global decomposition

## 5.6 Improvements Using Heuristic Search

Tabu search is one of many heuristic techniques applied to generation expansion problem. It has been recognized as an efficient method for combinatorial optimization problems. The algorithm is powerful due to the flexible forms of memory in the search space. The search performance, however, depends on a good starting solution. This dissertation combines Tabu search with the solution from the first L set optimization to obtain optimal solution. The comparison between using randomly generated starting solutions and solution from the first L set optimization is made.

Tabu search is an intelligent search procedure that has been widely applied to combinatorial optimization problems. The procedure starts with an initial solution. Neighborhood solutions are then created by some pre-specified neighborhood function. Objective function value of these neighborhood solutions is evaluated. The decision on moving from current solution to the next solution is made based on adaptive memory in Tabu list and current aspiration level. This list is vital since it prevents cycling in the search procedure.

In this application, neighborhood function is simply a random sampling of location to add and drop one generator. Objective function is calculated from global decomposition technique. From computational experiment, it is efficient to sample 8

neighborhood solutions and keep 3 moves in Tabu list. The algorithm is presented in the following.

Step 0. Initialization, $k = 0$

- Initial feasible solution, $\vec{x}^0 = \begin{bmatrix} x_1^0 & x_2^0 & \dots & x_n^0 \end{bmatrix}$
- Initialize Tabu list, $T^0$, and aspiration level, $A^0 = f\left(x^0\right)$
- Initialize best solution, $\vec{x}^* \leftarrow \vec{x}^0$

where

$x_i^k$ = Number of additional units in area *i* at iteration *k*

$\vec{x}^k$ = Current solution vector at iteration *k*

$T^k$ = Tabu list

$A^k$ = Aspiration level at iteration *k* which is the reliability Index in this application

$f(\cdot)$ = Objective function value of solution vector

While iteration $k <$ maximum iterations do the following,

Step 1. Generate neighborhood solutions, $\left\{\vec{x}^{nbhd}\right\} \subset N\left(\vec{x}^{k-1}\right)$

where

$\left\{\vec{x}^{nbhd}\right\}$ = Set of neighborhood solutions

$N(\cdot)$ = Neighborhood function generation

Step 2. Compute objective function values, $\left\{f\left(\vec{x}^{nbhd}\right)\right\}$ and find the best neighborhood solution, $\vec{x}^{nbhd,best}$

where $\vec{x}^{nbhd,best} = \arg\min\left\{f\left(\vec{x}^{nbhd}\right)\right\}$

Step 3. Check move with $T^{k-1}$

- If not in $T^{k-1}$,
  - $\vec{x}^{k} \leftarrow \vec{x}^{nbhd,best}$, $A^{k} \leftarrow f\left(\vec{x}^{nbhd,best}\right)$, and update $T^{k}$
  - If $f\left(\vec{x}^{nbhd,best}\right) < f\left(\vec{x}^{*}\right)$ then update best solution, $\vec{x}^{*} \leftarrow \vec{x}^{nbhd,best}$
  - Advance $k \leftarrow k+1$ and go to step 1.
- If in $T^{k-1}$,
  - Check aspiration criteria, if $f\left(\vec{x}^{nbhd,best}\right) < A^{k-1}$, then $\vec{x}^{k} \leftarrow \vec{x}^{nbhd,best}$, $\vec{x}^{*} \leftarrow \vec{x}^{nbhd,best}$, $A^{k} \leftarrow f\left(\vec{x}^{nbhd,best}\right)$, and update $T^{k}$
  - Otherwise, advance $k \leftarrow k+1$ and go to step 1.

Note that in this application, a move is stored as number of the area that a unit is added in the solution vector. A move is checked by comparing the area that a unit is dropped in the solution vector with number of areas in the Tabu list. This criterion prevents cycling since it checks whether the area that a generator is dropped has a generator added in the previous iteration or not. If a generator has been added to this area in previous iteration, we rather not drop it out in current iteration

The solution found from section 5.5 when a budget is 1 billion dollars and load is increased by 10 is chosen to be a starting solution in this study. Solutions from random sampling are sampled for comparison. These solutions are used as starting solutions in Tabu search procedure as shown in Table 5.19.

Table 5.19 Solution from an Optimization Method and Random Sampling

| Area | 1 | 2 | 3 | 4 | 5 | 9 | 10 | 11 | 12 |
|---|---|---|---|---|---|---|---|---|---|
| Solution from the first L set optimization | 0 | 0 | 1 | 3 | 0 | 0 | 0 | 0 | 0 |
| Random Sampling 1 | 1 | 1 | 0 | 0 | 0 | 1 | 1 | 0 | 0 |
| Random Sampling 2 | 0 | 0 | 0 | 1 | 0 | 0 | 1 | 0 | 2 |
| Random Sampling 3 | 0 | 0 | 1 | 1 | 1 | 0 | 0 | 1 | 0 |

Each initial solution in Table 5.19 is used in Tabu search procedure. The algorithm iterates for 10 times. The comparison between results using initial solution obtained from dynamic programming and those from random sampling are made. Fig. 5.3 shows objective function values at each iteration resulting from different starting solutions.

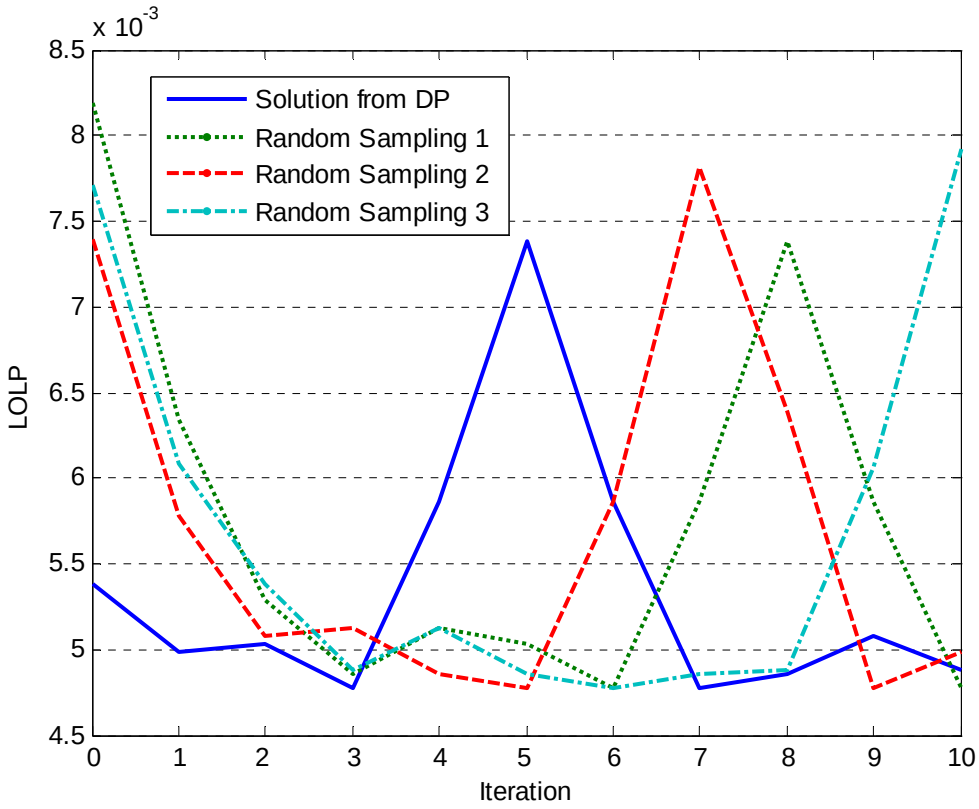


Fig. 5.3 Comparison of Algorithm Efficiency Produced by Different Initial Solutions

The optimal solution found from enumeration is to locate 2 generators in area 2 and 2 generators in area 4. Random sampling 1, 2, and 3 reach optimal solution at the $6^{th}$, $5^{th}$, and $6^{th}$ iteration. Initial solution from optimization reaches optimal solution at the $3^{rd}$ iteration. Even though the difference in number of iterations is small, initial solution from optimization provide better assurance of getting good solution than those from random sampling. In actual application, optimal solution is not known; therefore, there will be no guarantee at which iteration it will be reached. Initial solution from

optimization at least offers a solution that is close to optimal and likely to achieve it in timely manner.

## 5.7 Discussion and Conclusions

After the decomposition is performed, the best generation location can be found from scenario analysis as presented in Chapter IV. However, if the optimal solution is required, exhaustive search has to be performed. Instead of exhaustive search, dynamic programming provides a solution to the problem in a more systematic approach and a flexible choice of cost constraints.

Dynamic programming reduces number of computations made during the search for best solution. Number of multiplication depends on available budget, *R* as seen in the three area test system. Number of possible combination is shown in (5.82). In the worst case, multiplication will be performed to all components in the table of the size $R \times (m_j + 1)$ at each stage (except the last stage). The operation used in exhaustive search and dynamic programming are compared in the Table 5.20. The computation will be significantly improved for large system with dynamic programming.

$$\text{Number of possible combinations} = \prod_{j=1}^{N} (y_j + 1) \tag{5.82}$$

where

$N$ = Number of area in the system

$y_j$ = Maximum number of unit additions in each area

$R$ = Budget

Table 5.20 Comparison of Number of Computations between Exhaustive Search and Dynamic Programming

| Operation | Exhaustive Search | Dynamic Programming |
|---|---|---|
| Multiplication | $(N-1)\times\prod_{j=1}^{N}(y_j+1)$ | At most $(N-1)\times\sum_{j=1}^{N}(R\times(y_j+1))$ |
| Comparison | $\prod_{j=1}^{N}(y_j+1)-1$ | At most $(N-1)\times\sum_{j=1}^{N}(R\times y_j)$ |

Dynamic programming can also be applied to a problem with different cost constraints, as long as the constraint is in separable form. For example, a summation of one variable function as in (5.83), the same analysis can be applied.

$$\sum_{j=1}^{N} h_j(y_j) \tag{5.83}$$

As an example, the constraint can also be of the quadratic form as in (5.84). It is also possible to consider problems with multiple constraints; however, the algorithm may not be as efficient.

$$\sum_{j=1}^{N} \alpha_j y_j^2 + \beta_j y_j + \varphi_j \tag{5.84}$$

Another advantage of the approach is that the proposed technique can be extended to incorporate transfer capability adequacy analysis between areas. Global decomposition allows us to include additional state capacities of any arc in the network which can either be additional generation or additional tie lines. Thus, the same analysis

can be applied so that generation and tie line expansion can be analyzed together by the proposed method.

However, the structure of the optimization problem does not allow simple analysis when considering $L$ sets from more than one stage of decomposition. The problem is then simplified by considering sets from the first stage of decomposition only; the first $L$ sets optimization. This introduces an approximation to the problem given that the objective of the problem is to maximize reliability of the overall system. This approximation is reasonable since the first $L$ sets provide preliminary information on the generation deficiency in each area from the overall state space which represents the system characteristic. The optimization process depends significantly on these sets.

With the first $A$ set method, the optimization process depends significantly on the set characteristic. For example, consider three area test system in section 5.4 with 600, 700, and 600 MW load in area 1, 2, and 3 correspondingly, then the first $A$ set will become (5.85)

$$A = \begin{bmatrix} 9 & 9 & 8 & 2 & 2 & 2 \\ 7 & 8 & 7 & 1 & 1 & 1 \end{bmatrix} \tag{5.85}$$

The generation state in the first $A$ set contains only artificial states (7, 8, and 9). With the total budget of 10 m$, it is impossible to locate new generation in every area (3+5+4 = 12 m$). Clearly, this $A$ set can never have probability more than 0. Therefore, if the first $A$ set only consists of artificial states and the available budget is not enough to spend on new generation in every area, then the optimal available probability is zero. This simply means that the information from the first $A$ set is not enough for

optimization process. Thus, it is important that the set from decomposition phase give substantial information to the optimization phase.

As described in section 5.2.3.2 that '*v*' values are the critical variables in determining the prospective generation locations before performing optimization process. It is possible that the selection of the location from '*v*' values cuts off the optimal solution. Moreover, the system with plenty of generation and highly connected tie line with large capacity is likely to have all '*v*' value equals to one in the first decomposition to which the proposed method can not be applied.

An optimization procedure is proposed to find an optimal or near optimal generation location in multi area power systems. The term near optimal is used to indicate that the LOLP of the proposed solution is equal or close to that of the optimal solution. The problem has reliability constraint that does not have an explicit expression and therefore complicates the optimization process. Global decomposition is introduced to effectively evaluate reliability index of different generation combinations. Even though reliability equation can be derived, it is a very complex function. This reliability equation is then approximated by considering only *L* sets from the first decomposition since they possess separable structure which can be solved by dynamic programming.

The problem is formulated with minimization of LOLP index as an objective function subject to cost constraint. If a solution obtained from the optimization provides unsatisfactory system reliability, budget constraint can be relaxed to include more additional units in each area. The problem can be re-optimized without performing global decomposition again if the maximum number of additional units in each area

remains unchanged. This iterative procedure between cost constraint and reliability optimization can be used to get a satisfactory solution. The procedure is quite efficient as decomposition needs to be performed only once.

Generation expansion problem including reliability constraint is a very challenging and complex optimization problem. Due to the problem complexity, certain assumptions and approximations have been made. The study proposes a method to explicitly incorporate reliability into consideration. The main contribution is to propose an approximation to LOLP equation. The proposed approach simplifies the problem by optimizing over a smaller set of state space and thus the solution cannot guarantee global optimality. However, the solution from this approach is likely to be near optimal, if not optimal, and can provide a starting point to which sensitivity analysis can be applied to locate the optimal solution.

Meta-heuristic techniques, which require good starting solution for efficiency, can be applied along with the proposed method to ensure an optimal solution. The proposed approach is efficient and ensures a better optimal solution when initial solution from optimization is used. The comparison between randomly selected initial solutions and initial solution from the first $L$ set optimization is made. The algorithm reaches optimal solution faster with initial solution from optimization procedure than with random initial solutions. Other meta-heuristic techniques such as Particle Swamp Optimization (PSO) or Simulated Annealing (SA) can also be applied along with classical optimization procedure.

# CHAPTER VI

# MULTI-AREA POWER SYSTEM ADEQUACY PLANNING USING STOCHASTIC PROGRAMMING*

## 6.1 Introduction

In Chapter V, reliability calculation is not based on complete information about the state space and thus the solution obtained can be considered near optimal only. In this Chapter, the problem is formulated as two-stage recourse model. The first stage decision variables are the additional capacity units and the second stage decision variables are network flows. Reliability aspect is included in the second stage objective function as an expected cost of load loss. This formulation does not require generation to meet demand at all time, it rather maximizes reliability within available resource, i.e. minimize expected loss of load cost subject to available expansion budget. It should be noted that this reliability index is also a stochastic variable and minimizing this index makes the problem more challenging than incorporating random uncertainties in system capacities and load. The overall objective is to minimize expansion cost in the first stage and at the same time to minimize expected loss of load cost in the second stage.

---

This chapter is organized as follows. Section 6.2 presents problem formulation. Solution procedures are proposed in section 6.3. Section 6.4 shows computational results. Unit availability consideration is given in section 6.5. Discussion and conclusions are given in the last section.

## 6.2 Problem Formulation

A multi-area power system is modeled as given in Section 3.2. The problem is formulated as a network flow problem as given in Section 4.2.1. The formulation presented here is similar to that in Section 5.2.

Indices

$I$ = *{1,2,...,n}* Set of network nodes

$s$ = Source node

$t$ = Sink node

$i,j$ = Network nodes

$\omega$ = System state (scenario), $\omega \in \Omega$

$\Omega$ = State space (all possible scenarios)

Parameters

$N^g$ = Maximum number of additional generation units

$N^t$ = Maximum number of additional transmission lines

$c_i^g$ = Cost of an additional generation unit at area *i* ($)

$c_{ij}^t$ = Cost of an additional transmission lines between area *i* and area *j* ($)

$c_i^l(\omega)$ = Cost of load loss in area *i* in state $\omega$ ($/MW)

$c_i^o(\omega)$ = Operation cost of generators in area *i* in state $\omega$ ($/MW)

$M_i^g$ = Additional generation capacity in area *i* (MW)

$M_{ij}^t$ = Additional transmission lines capacity between area *i* and area *j* (MW)

$g_i(\omega)$ = Capacity of generation in area *i* in state $\omega$ (MW)

$t_{ij}(\omega)$ = Tie line capacity between area *i* and *j* in state $\omega$ (MW)

$l_i(\omega)$ = Load in area *i* in state $\omega$ (MW)

Decision variables

$x_i^g$ = Number of additional generators in area *i*, integer

$x_{ij}^t$ = Number of additional transmission lines between area *i* and area *j*, integer

$y_{ij}(\omega)$ = Flow from arc *i* to *j* for system state $\omega$

Using system expected cost of load loss as a reliability index, the problem is formulated as two-stage recourse model. The first stage decision variables are number of generators to be invested in each area that are determined before the realization of randomness in the problem. The second stage decision variables are the actual flows in the network. The failure probability of additional generators can be taken into account by using their effective capacities [89]. The formulation is given in the following.

$$\text{Min} \quad z = \sum_{i \in I} c_i^g x_i^g + \sum_{\substack{i \in I \\ i \neq j}} \sum_{j \in I} c_{ij}^t x_{ij}^t + E_{\tilde{\omega}}\left[f(x, \tilde{\omega})\right] \tag{6.1}$$

$$\text{s.t.} \quad \sum_{i \in I} x_i^g = N^g \tag{6.2}$$

$$\sum_{\substack{i \in I \\ i \neq j}} \sum_{j \in I} x_{ij}^t = N^t \tag{6.3}$$

$$x_i^g, x_{ij}^t \geq 0, \text{integer} \tag{6.4}$$

where constraints (6.2) and (6.3) in the first stage are restrictions on maximum number of additional generators and transmission lines in the system. Constraint (6.4) is an integer requirement for the number of additional generators. The function in (6.1) is the second stage objective value of minimizing operation cost and loss of load cost under a realization $\omega$ of $\Omega$ and is given as follows.

$$f(x, \omega) = \text{Min} \sum_{i \in I} \left[ c_i^l(\omega)(l_i(\omega) - y_{it}(\omega)) + c_i^o(\omega) y_{si}(\omega) \right] \tag{6.5}$$

$$\text{s.t.} \quad y_{si}(\omega) \leq g_i(\omega) + M_i^g x_i^g; \quad \forall i \in I \tag{6.6}$$

$$\left| y_{ji}(\omega) - y_{ij}(\omega) \right| \leq t_{ij}(\omega) + M_{ij}^t x_{ij}^t; \quad \forall i, j \in I, i \neq j \tag{6.7}$$

$$y_{it}(\omega) \leq l_i(\omega); \quad \forall i \in I \tag{6.8}$$

$$y_{si}(\omega) + \sum_{\substack{j \in I \\ j \neq i}} y_{ji}(\omega) = \sum_{\substack{j \in I \\ j \neq i}} y_{ij}(\omega) + y_{it}(\omega); \quad \forall i \in I \tag{6.9}$$

$$y_{ij}(\omega), y_{si}(\omega), y_{it}(\omega) \geq 0; \quad \forall i, j \in I \tag{6.10}$$

where, constraints (6.6), (6.7), and (6.8) are maximum capacity flow in the network under uncertainty in generation, tie line, and load arc respectively. Constraint (6.9) constitutes conservation of flow in network. Constraint (6.10) is non-negativity requirement for actual flow in the network.

To simplify the problem, operation cost in the second stage objective function is neglected and only generation expansion is considered in this study. It should be noted that the cost of load loss coefficient depends on system states. The calculation of this coefficient is performed separately and is shown in the following.

Loss of load cost depends on interruption duration as well as type of interrupted load. The most common approach to represent power interruption cost is through customer damage function (CDF) [22]. This function relates different types of load and interruption duration to cost per MW. In order to accurately calculate system expected LOLC, LOLC coefficient needs to be evaluated according to the mean duration time of each state ($\omega$).

Mean duration of each stage can be assessed by taking a reciprocal of equivalent transition rate from that state to others. State mean duration is presented in (6.11). Equivalent transition rate of all components can be calculated using the recursive formula in [43] when constructing probability distribution function.

$$D_{\omega} = \frac{24}{\sum_{i \in I} \lambda_{g_i}^{\omega+} + \sum_{i \in I} \lambda_{g_i}^{\omega-} + \sum_{\substack{i,j \in I \\ i \neq j}} \lambda_{t_{ij}}^{\omega+} + \sum_{\substack{i,j \in I \\ i \neq j}} \lambda_{t_{ij}}^{\omega-} + \sum_{k=1}^{m_l} \lambda_{l_k}^{\omega}} \tag{6.11}$$

where

$D_{\omega}$ = Mean duration of state $\omega$ (hours)

$\lambda_{g_i}^{\omega+}$ = Equivalent transition rate of generation in area $i$ from a capacity of state $\omega$ to higher capacity (per day)

$\lambda_{g_i}^{\omega-}$ = Equivalent transition rate of generation in area $i$ from a capacity of state

$\omega$ to lower capacity (per day)

$\lambda_{t_{ij}}^{\omega+}$ = Equivalent transition rate of transmission line from area *i* to area *j* from a capacity of state $\omega$ to higher capacity (per day)

$\lambda_{t_{ij}}^{\omega-}$ = Equivalent transition rate of transmission line from area *i* to area *j* from a capacity of state $\omega$ to lower capacity (per day)

$\lambda_{l_k}^{\omega}$ = Equivalent transition rate of area load from state $\omega$ to other load states (per day)

$m_l$ = Total number of area load states

Customer damage function used in this paper is taken from [22]. The function was estimated from electric utility cost survey in the US. For small-medium commercial and industrial loads, interruption cost in dollars per kW-h can be described, as a function of outage duration, by (6.12).

$$c^l\left(D_\omega\right) = e^{6.48005+0.38489D_\omega-0.02248D_\omega^2} \tag{6.12}$$

## 6.3 Solution Procedures

L-shaped algorithm [60] is the most common approach for stochastic programming procedure and is thus chosen for this study. At each iteration, the algorithm approximates the second stage objective function by generating piecewise linear function and appends it to the master problem. The linear function is generated from solving all the second stage problems, i. e. all realization in the second stage. For large systems, the number of system states grows exponentially and thus it is impractical

to enumerate and evaluate the entire state space. Direct application of L-shaped algorithm cannot be achieved in timely manner since the algorithm evaluates all system states (scenarios) in sub problems when generating cut for the master problem.

To overcome this problem of dimensionality, in the proposed method sampling technique is employed to reduce number of system states [9], [29]. There are two fundamental approaches to apply sampling techniques; interior [60], [62] and exterior [9], [29]. The key difference between the two is that interior sampling deals with sampling in the course of optimization algorithm while exterior sampling performs sampling *before* the optimization algorithm. The objective of the second stage, called sample-average approximation of the actual expected value, is defined by these samples. This approximation makes it possible to solve the problem with deterministic equivalent model.

This study proposes both direct implementation of the L-Shaped algorithm and the Sample Average Approximation (SAA) to solve the problem. Exterior sampling is chosen to overcome numerous number of system states. The number of system states is selected and the expected loss of load cost is approximated. Two sampling techniques are used and compared, Monte Carlo simulation and Latin Hypercube sampling to construct the sample-average function. Details of each method are given in the following.

### 6.3.1 L-Shaped Algorithm

The algorithm is implemented with Xpress-IVE student edition. Steps of L-shaped algorithm [29] for this problem are as follows.

Step 0. Initialization

- Find $x^0$ from solving master problem; discard the second stage objective function.

$$\begin{aligned} &\text{Min} \quad \sum_{i \in I} c_i^g x_i^g \\ &s.t. \quad \sum_{i \in I} x_i^g = N^g \\ &x_i^g \geq 0, \text{integer} \end{aligned} \tag{6.13}$$

- Set upper bound (UB) and lower bound (LB), i.e., $UB \leftarrow \infty$ and $LB \leftarrow -\infty$

Step 1. Solve sub problem at iteration $k$

- Reset the linear approximation function coefficients, $\beta_i^k \leftarrow 0; \forall i \in I$, its right-hand-side value $\alpha^k \leftarrow 0$, and the sub problem objective function value $f^k \leftarrow 0$.
- For all states $\omega$ = 1 to $|\Omega|$, solve sub problem $k$ where each scenario has probability, $p_\omega$

$$f_{\omega}^{k} = \text{Min} \sum_{i \in I} c_i^l(\omega)(l_i(\omega) - y_{it}(\omega)) \tag{6.14}$$

$$\begin{aligned} s.t. \quad & y_{si}(\omega) \le g_i(\omega) + M_i^g x_i^{g,k}; \quad \forall i \in I \\ & \left| y_{ji}(\omega) - y_{ij}(\omega) \right| \le t_{ij}(\omega); \quad \forall i, j \in I, i \ne j \\ & y_{it}(\omega) \le l_i(\omega); \quad \forall i \in I \\ & y_{si}(\omega) + \sum_{\substack{j \in I \\ j \ne i}} y_{ji}(\omega) = \sum_{\substack{j \in I \\ j \ne i}} y_{ij}(\omega) + y_{it}(\omega); \quad \forall i \in I \\ & y_{ij}(\omega), y_{isi}(\omega), y_{it}(\omega) \ge 0; \quad \forall i, j \in I \end{aligned}$$

– Obtain dual solution, $\vec{\pi}_{\omega}^{k} = \left(\pi_{\omega,i}^{g}, \pi_{\omega,ij}^{t}, \pi_{\omega,i}^{l}\right)$ associated with generation, transmission line capacities, and load constraints respectively.

– Update the generated cut from $\beta_i^k += p_{\omega} \pi_{\omega,i}^{g} M_i^g$, and

$$\alpha_k += p_{\omega} \left( \sum_{\forall i \in I} \pi_{\omega,i}^{g} g_i(\omega) + \sum_{\substack{\forall i,j \in I \\ i \ne j}} \pi_{\omega,ij}^{t} t_{ij}(\omega) + \sum_{\forall i \in I} \pi_{\omega,i}^{l} l_i(\omega) \right) \tag{6.15}$$

– Update sub problem objective value $f_k += p_{\omega} f_{\omega}^{k}$

– Update $UB = \min\left\{ UB, \sum_{\forall i \in I} c_i^g x_i^{g,k} + f^k \right\}$, if changed, update the incumbent solution, $x^{incumbent} \leftarrow x^k$

Step 2. Solve master problem

– Append the following cut, $\eta \ge \alpha^k + \sum_{\forall i \in I} \beta_i^k x_i^g$

– Obtain solution $x_i^{g,k+1}, \eta^{k+1}$ from the following master problem

$$\begin{aligned} \text{Min} \quad & \sum_{\forall i \in I} c_i^g x_i^g + \eta \\ s.t. \quad & \sum_{\forall i \in I} x_i^g = N^g \\ & \eta \geq \alpha^q + \sum_{\forall i \in I} \beta_i^q x_i^g ; q = 0, \ldots, k \\ & x_i^g \geq 0, \text{integer} \end{aligned} \tag{6.16}$$

– Update $LB = \max\left\{ LB, \sum_{\forall i \in I} c_i^g x_i^{g,k+1} + \eta^{k+1} \right\}$

Step 3. Check convergence

– Compute percent gap from $\%gap = \dfrac{(UB - LB)}{UB}$

– If $\%gap \leq \varepsilon$, stop and obtain optimal solution, $x^* \leftarrow x^{incumbent}$, and objective value from upper bound, else, $k \leftarrow k+1$, return to step 1.

### 6.3.2 Sampled Average Approximation

The expected cost of load loss can be approximated by means of sampling. Let $\omega_1, \omega_2, \ldots, \omega_N$ be $N$ realizations of random vector for all uncertainties in the model, the expected cost of load loss can be replaced by (6.17).

$$\hat{f}_N(x) = \frac{1}{N} \sum_{k=1}^{N} f(x, \omega_k). \tag{6.17}$$

This function is a SAA of the expected cost of load loss. The problem can then be transformed into deterministic equivalent model as follows.

$$\text{Min} \quad \hat{z}_N = \sum_{i \in I} c_i^g x_i^g + \frac{1}{N} \sum_{k=1}^{N} \left\{ \sum_{i \in I} c_i^l(\omega_k) \left( l_i(\omega_k) - y_{it}^j(\omega_k) \right) \right\} \tag{6.18}$$

$$\text{s.t.} \quad \sum_{i \in I} x_i^g = N^g \tag{6.19}$$

$$y_{si}^k(\omega_k) \le g_i(\omega_k) + M_i^g x_i^g; \quad \forall i \in I, k \in \{1,2,\ldots,N\} \tag{6.20}$$

$$\left| y_{ji}^k(\omega_k) - y_{ij}^k(\omega_k) \right| \le t_{ij}(\omega_k); \quad \forall i, j \in I, i \ne j, k \in \{1,2,\ldots,N\} \tag{6.21}$$

$$y_{it}^k(\omega_k) \le l_i(\omega_k); \quad \forall i \in I, k \in \{1,2,\ldots,N\} \tag{6.22}$$

$$y_{si}^k(\omega_k) + \sum_{\substack{j \in I \\ j \ne i}} y_{ji}^k(\omega_k) = \sum_{\substack{j \in I \\ j \ne i}} y_{ij}^k(\omega_k) + y_{it}^k(\omega_k); \quad \forall i \in I \tag{6.23}$$
$$k \in \{1,2,\ldots,N\}$$

$$y_{ij}^k(\omega_k), y_{si}^k(\omega_k), y_{it}^k(\omega_k) \ge 0; \quad \forall i, j \in I, k \in \{1,2,\ldots,N\} \tag{6.24}$$

$$x_i^g \ge 0, \text{integer}$$

Note that the solution obtained from this sample-based approach does not as such guarantee optimality in the original problem. The optimal sample-based solutions, when obtained with different sample sets, rather provide statistical inference of a confidence interval of the actual optimal solution.

Let $x_N^*$ be the optimal solution and $\hat{z}_N^*$ be the optimal objective value of an approximated problem. Generally, $x_N^*$ and $\hat{z}_N^*$ varies by the sample size *N*. If $x^*$ is the optimal solution and $z^*$ is the optimal objective value of the original problem, then, obviously,

$$z^* \le \hat{z}_N^*. \tag{6.25}$$

Therefore, $\hat{z}_N^*$ constitutes an upper bound of the optimal objective value. Since $\hat{z}_N^*$ is the optimal solution of the approximated problem, then the following is true,

$$\hat{z}_N^* = \hat{z}_N\left(x_N^*\right) \le \hat{z}_N\left(x^*\right). \tag{6.26}$$

Taking expectation on both sides, (6.26) becomes

$$E\left[\hat{z}_N^*\right] \le E\left[\hat{z}_N\left(x^*\right)\right]. \tag{6.27}$$

Since the SAA is an unbiased estimator of the population mean,

$$E\left[\hat{z}_N^*\right] \le E\left[\hat{z}_N\left(x^*\right)\right] = z^* \tag{6.28}$$

which constitutes a lower bound of the optimal objective value. In the following, details on obtaining lower bound and upper bound estimates are discussed. The derivation of lower and upper bound confidence interval was presented in [46] and has been applied in [9], [29].

#### 6.3.2.1 Lower Bound Estimates

The expected value of $\hat{z}_N^*$, $E\left[\hat{z}_N^*\right]$, can be estimated by generating $M_L$ independent batches, each of $N_L$ samples. For each sample set $s$, solve the SAA problem which gives $\hat{z}_{N_L}^{*,s}$ and the lower bound can be found from

$$L_{N_L,M_L} = \frac{1}{M_L}\sum_{s=1}^{M_L} \hat{z}_{N_L}^{*,s} . \tag{6.29}$$

By the central limit theorem, the distribution of a lower bound estimate converges to a normal distribution $N\left(\mu_L, \sigma_L^2\right)$ where $\mu_L = E\left[\hat{z}_{N_L}^*\right]$, which can be approximated by a sample mean $L_{N_L,M_L}$, and $\sigma_L^2 = \mathrm{Var}\left[\hat{z}_{N_L}^*\right]$, which can be approximated by a sample variance

$$s_L^2 = \frac{1}{M_L - 1}\sum_{s=1}^{M_L}\left(\hat{z}_{N_L}^{*,s} - L_{N_L,M_L}\right)^2 . \tag{6.30}$$

Thus, the two-sided 100(1-α)% confidence interval of the lower bound is

$$\left[L_{N_L,M_L} - \frac{z_{\alpha/2}s_L}{\sqrt{M_L}}, L_{N_L,M_L} + \frac{z_{\alpha/2}s_L}{\sqrt{M_L}}\right]. \tag{6.31}$$

where $z_{\alpha/2}$ satisfies $\Pr\{z_{\alpha/2} \le N(0,1) \le z_{\alpha/2}\} = 1-\alpha$

It should be noted that the lower bound confidence interval is computed by solving $M_L$ independent SAA problems of sample size $N_L$.

#### 6.3.2.2 Upper Bound Estimates

Given a sample-based solution $x_N^*$, the upper bound of the actual optimal objective can be estimated by generating $M_U$ independent batches, each of $N_U$ samples. Since the solution is set to $x_N^*$, (6.18) can be decomposed based on system state $\omega_k$ to $N_U$ independent linear programming (LP) problems. For each sample batch $s$, solving the LP problems gives $\hat{z}_{N_U}^s\left(x_N^*\right)$. Then, the upper bound is approximated from

$$U_{N_U,M_U}\left(x_N^*\right) = \frac{1}{M_U}\sum_{s=1}^{M_U}\hat{z}_{N_U}^s\left(x_N^*\right). \tag{6.32}$$

By central limit theorem, the distribution of an upper bound estimate converges to a normal distribution $N\left(\mu_U, \sigma_U^2\right)$ where $\mu_U = E\left[\hat{z}_{N_U}\left(x_N^*\right)\right]$, which can be approximated by a sample mean $U_{N_U,M_U}$, and $\sigma_U^2 = \mathrm{Var}\left[\hat{z}_{N_U}\left(x_N^*\right)\right]$, which can be approximated by a sample variance

$$s_U^2\left(x_N^*\right)=\frac{1}{M_U-1}\sum_{s=1}^{M_U}\left(\hat{z}_{N_U}^{*,s}\left(x_N^*\right)-U_{N_U,M_U}\left(x_N^*\right)\right)^2 . \tag{6.33}$$

Thus, the two-sided 100(1-α)% confidence interval of the lower bound is

$$\left[U_{N_U,M_U}\left(x_N^*\right)-\frac{z_{\alpha/2}s_U\left(x_N^*\right)}{\sqrt{M_U}},U_{N_U,M_U}\left(x_N^*\right)+\frac{z_{\alpha/2}s_U\left(x_N^*\right)}{\sqrt{M_U}}\right]. \tag{6.34}$$

where $z_{\alpha/2}$ satisfies $\Pr\{z_{\alpha/2}\le N(0,1)\le z_{\alpha/2}\}=1-\alpha$

In this study, a solution $x_N^*$ is found from each batch *s* of $M_L$ batches in lower bound SAA problems and used to compute the upper bound estimates. It should be noted that the upper bound confidence interval depends on the chosen approximate solution $x_N^*$ from SAA problems. Thus, $M_L$ upper bound intervals are computed.

#### 6.3.2.3 Optimal Solution Approximation

The optimal solution can be extracted when unique solution is obtained from solving several SAA problems with different samples of a given size, *N*. In theory, optimality should be attained with sufficiently large *N*. However, it may be possible that each sample yields different solutions for small sample size. If an identical solution is found from solving SAA problems with these samples, it may be concluded that optimality is verified.

### 6.3.3 Sampling Techniques

The sampling techniques used in this paper are Monte Carlo sampling (MC) and Latin Hypercube Sampling (LHS). Random variables in the model are sampled based on

their corresponding discrete probability distributions. Details of MC and LHS technique are discussed in the following.

#### 6.3.3.1 Monte Carlo Simulation

MC is a well known sampling technique in reliability analysis. For each component in the system, a number between 0 and 1 is randomly chosen and the component state is found by performing inverse transformation according to its cumulative probability distribution. A system state is found when all component states have been assigned.

#### 6.3.3.2 Latin Hypercube Sampling

LHS was initially proposed in reference [85]. The number of samples $N$ needs to be known in advance. For each component in the system, the interval (0,1) is equally divided into $N$ subintervals and a random number is drawn from each subinterval. This means that there are $N$ random numbers for each component. For each subinterval, a sample value is obtained by performing inverse transformation according to its cumulative probability distribution *in that subinterval*. This constitutes a sample vector of size $N$ of a component. The process is repeated for all components in the system. With this data, we can construct a matrix of size $N \times$ number of components. A system state is found by randomly picking a value from each column of this matrix *without replacement*. This gives $N$ samples of system states. It should be noted that LHS yields a

stratified sample of the data. Thus, the variance of a sample from this technique is considered smaller than that from MC.

## 6.4 Computational Results

This study implements both methods presented in the previous section. A three-area power system, shown in Appendix C, is chosen for L-shaped algorithm method. The twelve-area power system, shown in Appendix A, is chosen for Sample Average Approximation method. Equivalent transition rates of area load are given in Appendix A, Table A.4 for a twelve area test system and Appendix C, Table C.6 for a three area test system.

### 6.4.1 L-Shaped Algorithm

A three area test system is shown in Fig. C.1. There are 5, 6, and 5 generating units of 100 MW each in area 1, 2, and 3 respectively. Each generator has failure rate of 0.1 per day and mean repair time of 24 hours. The system has three transmission lines each with 100 MW capacity, failure rate of 10 per year, and mean repair time of 8 hours. Table C.1, Table C.2, and Table C.3 show area generation, transmission line, and load probability distributions. Load cluster data is taken from [17]. It is assumed that the maximum number of additional units is 2 and the additional generators have capacity of 100 MW each. The cost of additional unit of the three-area system is 100 million dollars for all areas

The optimization procedure yields a solution to locate one generator in area 1 and one generator in area 2 that gives expected loss of load cost of 1.48 million dollar and expansion cost of 200 million dollar. The algorithm converges in 6 iterations. Upper bound and lower bound at each iteration are shown in Fig. 6.1. It should be noted that the expected loss of load cost depends on the customer damage function used. The study presented here is only for illustration purposes. Xpress-IVE student edition is the software used for implementation.

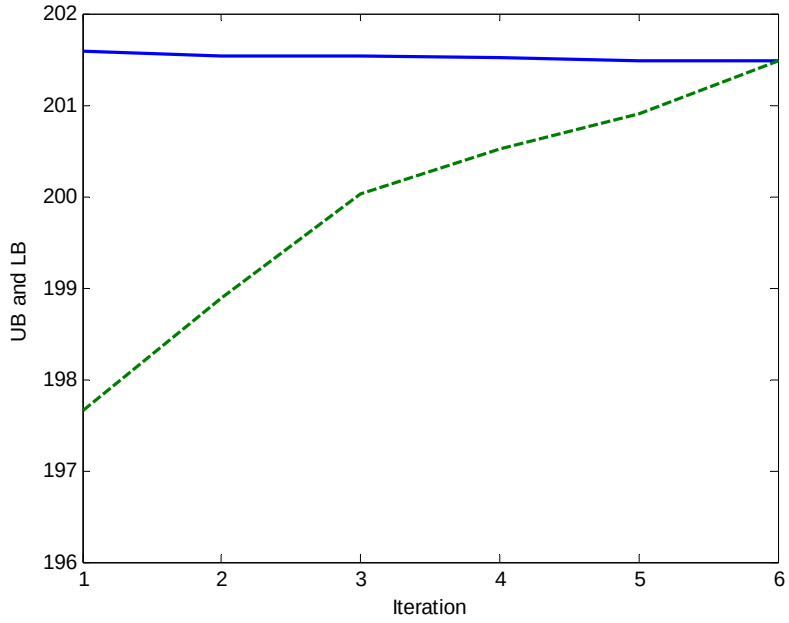


Fig. 6.1. Upper Bound and Lower Bound of Objective Function

### 6.4.2 Sampled Average Approximation

A 12-area power system is shown in Fig. A.1. The test system is a multi-area representation of an actual power system [17] that has 137 generation units and 169 tie

line connections between areas. System parameters can be found in Appendix A. This study uses original load as shown in Table 5.13. All the tie lines in the system are assumed to have a mean repair time of 8 hours and a failure rate of 10 per year. It is assumed that the additional generators have capacity of 200 MW each. In order to perform LHS, probability distribution table is constructed with an increment of 1 MW. Load cluster and its equivalent transition rate are shown in Appendix A. In this problem, it is assumed that number of additional generators is 4. Total number of system states ($|\Omega|$) of this problem is $1.62\times10^{49}$.

The study conducts three tests for lower bound estimate, upper bound estimate, and optimal solution approximation. To compare the effectiveness of the estimate, 5 different sample sizes are chosen for this study, which are 200, 500, 1000, 5000, and 10000. All three tests are implemented with two sampling techniques described in section V to compare the efficiency between MC and LHS. Lower bound estimate of each sample size is calculated by solving SAA problems with data generated by 5 different batches of sample. Therefore, $M_L$ is 5 and $N_L$ are 200, 500, 1000, 5000, and 10000. The 95 % confidence intervals of lower bound from different sample sizes are shown in Table 6.1 and Table 6.2 when using MC and LHS respectively.

Table 6.1 Lower Bound Estimate from Monte Carlo Sampling

| Sample size | Lower bound ( 95% confidence interval ) |
|---|---|
| 200 | 1868138 ± 164834 |
| 500 | 1721296 ± 134936 |
| 1000 | 1748388 ± 75527 |
| 5000 | 1731028 ± 29524 |
| 10000 | 1718414 ± 18765 |

Table 6.2 Lower Bound Estimate from Latin Hypercube Sampling

| Sample size | Lower Bound ( 95% confidence interval) |
|---|---|
| 200 | 1630427 ± 176359 |
| 500 | 1735213 ± 107946 |
| 1000 | 1706931 ± 54523 |
| 5000 | 1690686 ± 38665 |
| 10000 | 1682813 ± 7817 |

Note that, at this point, each sample size will produce five solutions, which may or may not be identical, from five batches of sample. These solutions are then used to calculate upper bound estimate.

Upper bound estimate of each sample size is obtained by substituting the solution obtained from that particular SAA problem. This will transform SAA problem into independent linear programming problem which makes it faster to solve than SAA problem. In this study, 10 batches of sample of size 10000 are used to estimate upper bound. Thus, $M_U$ is 10 and $N_U$ is 10000. The 95 % confidence intervals of upper bound from different batches of sample size ($N_L$) are shown in Table 6.3 and Table 6.4 when using MC and LHS respectively. In addition to upper bound estimate, the solution

obtained from different batches of sample size can be seen from Table 6.3 and Table 6.4. Note that the number of additional generators in all other area is zero.

Table 6.3 Upper Bound Estimate and Approximate Solutions from Monte Carlo Sampling

| Sample sizes | Batch | # of Add. Gen. in Area | | | Upper Bound ( 95% confidence interval ) |
|---|---|---|---|---|---|
| | | 2 | 9 | 10 | |
| 200 | 1 | 2 | 1 | 1 | 2185851 ± 167656 |
| | 2 | 1 | 1 | 2 | 2227225 ± 183308 |
| | 3 | 1 | 1 | 2 | 2200578 ± 215138 |
| | 4 | 3 | 0 | 1 | 1720037 ± 21728 |
| | 5 | 3 | 0 | 1 | 1712327 ± 18589 |
| 500 | 1 | 1 | 1 | 2 | 2210587 ± 154688 |
| | 2 | 2 | 1 | 1 | 2164757 ± 233365 |
| | 3 | 3 | 1 | 0 | 1730035 ± 15487 |
| | 4 | 1 | 2 | 1 | 2207378 ± 167284 |
| | 5 | 1 | 1 | 2 | 2128233 ± 300166 |
| 1000 | 1 | 2 | 1 | 1 | 1726760 ± 14041 |
| | 2 | 3 | 0 | 1 | 1728932 ± 20059 |
| | 3 | 3 | 1 | 0 | 1718296 ± 14514 |
| | 4 | 3 | 0 | 1 | 1726690 ± 14040 |
| | 5 | 2 | 1 | 1 | 1888449 ± 313452 |
| 5000 | 1 | 3 | 0 | 1 | 1717799 ± 14516 |
| | 2 | 3 | 0 | 1 | 1719699 ± 18318 |
| | 3 | 3 | 0 | 1 | 1726453 ± 20637 |
| | 4 | 3 | 0 | 1 | 1716471 ± 21303 |
| | 5 | 3 | 0 | 1 | 1723173 ± 24283 |
| 10000 | 1 | 3 | 0 | 1 | 1726690 ± 14040 |
| | 2 | 3 | 0 | 1 | 1728932 ± 20058 |
| | 3 | 3 | 0 | 1 | 1717799 ± 14516 |
| | 4 | 3 | 0 | 1 | 1719699 ± 18318 |
| | 5 | 3 | 0 | 1 | 1726453 ± 20637 |

Table 6.4 Upper Bound Estimate and Approximate Solutions from Latin Hypercube Sampling

| Sample sizes | Batch | # of Add. Gen. in Area | | | Upper Bound |
|---|---|---|---|---|---|
| | | 2 | 9 | 10 | ( 95% confidence interval ) |
| 200 | 1 | 1 | 2 | 1 | 1693587 ± 9270 |
| | 2 | 2 | 0 | 2 | 1674512 ± 9435 |
| | 3 | 2 | 1 | 1 | 1693948 ± 16963 |
| | 4 | 1 | 1 | 2 | 1679482 ± 10263 |
| | 5 | 2 | 1 | 1 | 1675370 ± 12153 |
| 500 | 1 | 2 | 1 | 1 | 1690918 ± 8868 |
| | 2 | 2 | 1 | 1 | 1679735 ± 11403 |
| | 3 | 2 | 0 | 2 | 1686659 ± 9646 |
| | 4 | 0 | 1 | 3 | 1693739 ± 10258 |
| | 5 | 2 | 0 | 2 | 1683681 ± 11471 |
| 1000 | 1 | 2 | 1 | 1 | 1679735 ± 11403 |
| | 2 | 2 | 0 | 2 | 1686659 ± 9646 |
| | 3 | 2 | 0 | 2 | 1691074 ± 10273 |
| | 4 | 1 | 1 | 2 | 1680107 ± 11382 |
| | 5 | 3 | 0 | 1 | 1686411 ± 9629 |
| 5000 | 1 | 2 | 0 | 2 | 1691074 ± 10273 |
| | 2 | 2 | 0 | 2 | 1683681 ± 11471 |
| | 3 | 3 | 0 | 1 | 1679388 ± 7809 |
| | 4 | 2 | 0 | 2 | 1691708 ± 9664 |
| | 5 | 3 | 0 | 1 | 1685699 ± 15859 |
| 10000 | 1 | 3 | 0 | 1 | 1679665 ± 11407 |
| | 2 | 2 | 0 | 2 | 1686659 ± 9646 |
| | 3 | 3 | 0 | 1 | 1690780 ± 10289 |
| | 4 | 3 | 0 | 1 | 1683386 ± 11464 |
| | 5 | 3 | 0 | 1 | 1679388 ± 7809 |

Next, optimal solution is approximated by solving SAA problems with increased sample sizes. In this study, the optimal solution is obtained when identical solutions are found within 5 consecutive batches of sample of the same size. It can be seen from Table 6.3 that in the case of MC sampling the solutions are identical when sample sizes are

5000 and 10000. Therefore, the optimal solution is to install 3 units in area 2 and 1 unit in area 10. However, in the case of LHS, the solutions shown in Table 6.4 are not identical even when the sample size is 10000. The converged solution is found, which is to install 3 units in area 2 and 1 unit in area 10, when sample size is increased to 12000.

With LHS, there are two possible candidate solutions which are 3 units in area 2, 1 in area 10, and 2 units in area 2, 2 units in area 10 when sample size is 5000 and 1000 as shown in Table 6.4. Note that the second solution does not appear when using MC sampling as seen in Table 6.3. In order to compare two sampling techniques, the total costs of the two solutions were found by performing reliability analysis. Expected cost of load loss is calculated by Monte Carlo simulation. The convergence criterion is 1% standard deviation. Table 6.5 shows the comparison between these two possible optimal solutions. It can be seen that these two solutions yield very close total costs with only 0.046% difference.

Table 6.5 Comparison between Possible Optimal Solutions

| Solution | # of Add. Gen. in Area | | | Expected total Cost, with 0.01 S.D. |
|---|---|---|---|---|
| | 2 | 9 | 10 | |
| 1 | 3 | 0 | 1 | 1687543 |
| 2 | 2 | 0 | 2 | 1687857 |

Even though it takes larger sample size to obtain converged solution in LHS, the candidate solutions found from LHS detect small changes in objective function value as shown in Table 6.5. It appears that with LHS the solution space is more thoroughly explored; therefore, the solutions with very close objective value are found. This may be helpful when alternative solutions are desirable for planning purposes.

Summary of lower bound and upper bound intervals of different sample sizes are shown in Fig. 6.2 and Fig. 6.3 using MC and LHS respectively. For each sample size, the best upper bound estimate is chosen based on its average value as well as the tightness of the interval. It can be seen that lower bound intervals are smaller as the sample size increases for both MC and LHS while upper bound estimates are tight in both sampling techniques. This is due to the fact that number of samplings ($N_U$) and number of batches ($M_U$) for upper bound estimates is sufficiently large enough for this problem. However, LHS gives tighter lower bound and upper bound estimates than MC. This is caused by the variance reduction property of LHS.

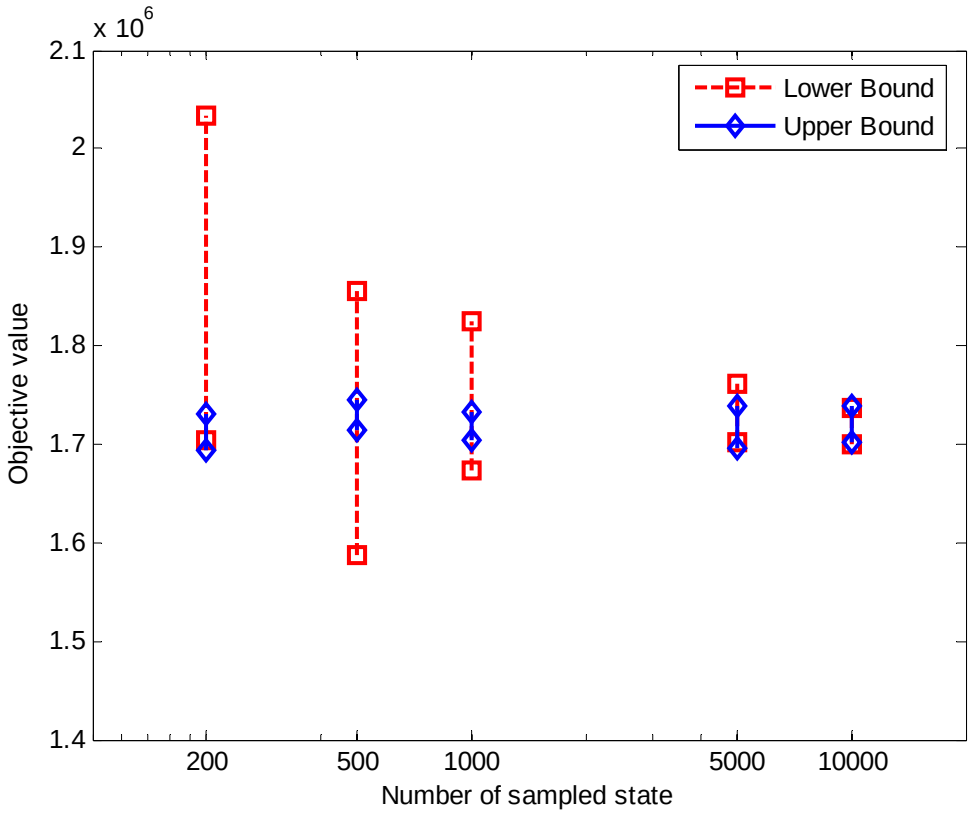


Fig. 6.2. Bounds of SAA Solution with Monte Carlo Sampling

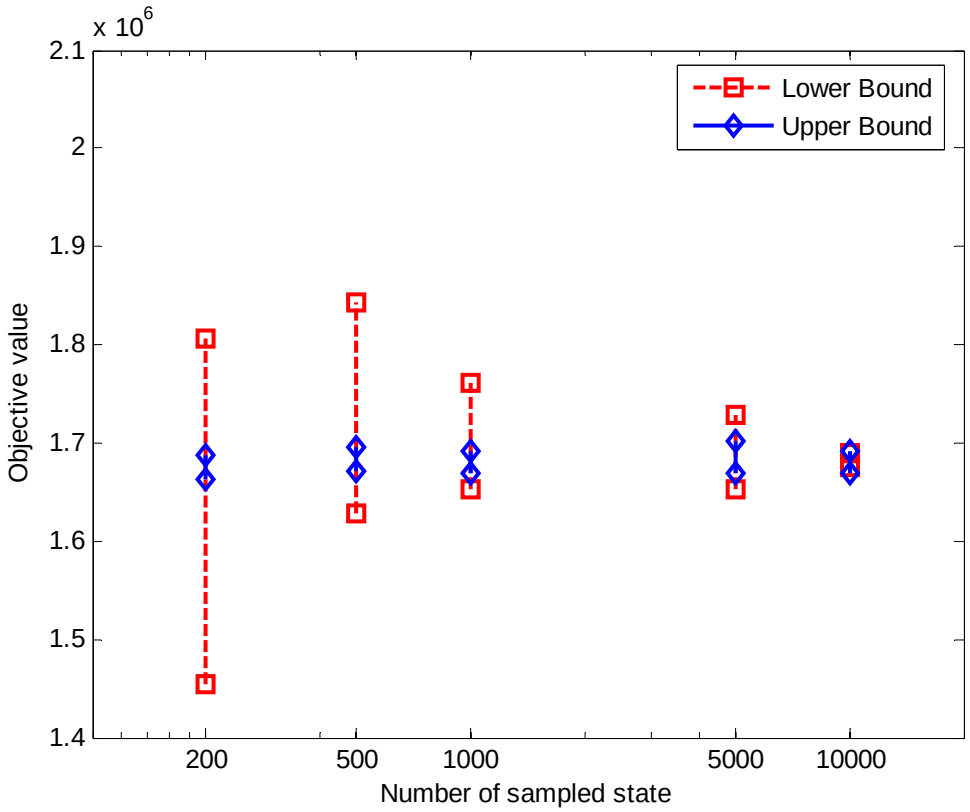


Fig. 6.3. Bounds of SAA Solution with Latin Hypercube Sampling

It is interesting to note that even though the original problem has very large number of system states ($1.62\times10^{49}$), SAA technique requires only small number of samples (10000) which provides sufficient information of the over all state space for optimization.

## 6.5 Unit Availability Consideration

Previously, the candidate generators are characterized by their effective

capacities with 100% availability instead of modeling their forced outage rates explicitly. This is due to the limitation of the available solution approaches of the stochastic programming framework that the state space of all random variables must remain the same with respect to decision variables. This restriction is violated when the additional units are modeled by integer decision variables, representing the number of additional units in each area, since the probability distribution function of their capacity changes with the number of additional units. The analysis is emphasized on generating units since the probability of failure of a generating unit is usually higher than that of a transmission line. The same analysis can also be applied to incorporate availability of a transmission line.

In this section, on the other hand, binary first stage variables are proposed to cope with the change of distribution because of the additional units. Binary first stage decision variables assume only two states, up or down with specified forced outage rates. This means that the additional capacity of all candidate units has two possible values, full capacity or none. Thus, the state space of all random variables, including the capacity of additional units remains unchanged throughout all decision variables. The problem formulation presented in section 6.2 is modified as follows.

The first stage variables are binary, individually representing decision of additional unit in each area. These variables are determined before the realization of random uncertainties.

Decision Variables

$$x_{i,k}^{g} = \begin{cases} 1 & \text{if generating unit } k \text{ is added in area } i \\ 0 & \text{otherwise} \end{cases}$$

The first stage constraint, modified from (6.2), contains only restriction on maximum number of additional units as follows.

$$\sum_{i \in I} \sum_{k \in K_i} x_{i,k}^{g} = N^{g} \tag{6.35}$$

The second stage constraints, modified from (6.6), describe a realization of the system. These constraints include generation capacity limit in each area in state $\omega$.

$$0 \le y_{si}(\omega) \le g_i(\omega) + \sum_{k \in K_i} M_{i,k}^{g}(\omega) x_{i,k}^{g}; \quad \forall i \in I \tag{6.36}$$

The randomness in additional generating units is represented by the additional capacity of that unit, $M_{i,k}^{g}(\omega)$. The probability distribution of additional capacities, $M_{i,k}^{g}(\omega)$, consists of two stages, fully available and zero capacity. However, if needed, the derated states of additional generating units can also be modeled by utilizing integer first stage variables as long as their distributions, $M_{i,k}^{g}(\omega)$, remain the same.

The overall objective is to minimize the expansion cost while also maximizing system reliability under uncertainty in area generation, load, and tie-lines. The first stage objective function, modified from (6.1), is shown below.

$$\text{Min} \quad z = \sum_{i \in I} \sum_{k \in K} c_{i,k}^{g} x_{i,k}^{g} + E_{\tilde{\omega}}\left[ f(x, \tilde{\omega}) \right] \tag{6.37}$$

Mean duration time calculation need to include the equivalent transition rate of additional generating units. Equation (6.11) is modified as follow.

$$D_{\omega} = \frac{24}{\lambda^{\omega}_{system} + \sum_{i \in I} \sum_{k \in K_i} \lambda^{\omega+}_{g_{i,k}} + \sum_{i \in I} \sum_{k \in K_i} \lambda^{\omega-}_{g_{i,k}}} \tag{6.37}$$

where

$$\lambda^{\omega}_{\text{system}} = \sum_{i \in I} \lambda^{\omega+}_{g_i} + \sum_{i \in I} \lambda^{\omega-}_{g_i} + \sum_{\substack{i,j \in I \\ i \neq j}} \lambda^{\omega+}_{t_{ij}} + \sum_{\substack{i,j \in I \\ i \neq j}} \lambda^{\omega-}_{t_{ij}} + \sum_{k=1}^{m_l} \lambda^{\omega}_{l_k} \tag{6.38}$$

$\lambda^{\omega+}_{g_{i,k}}$ = Equivalent transition rate of additional generating unit k in area i from a capacity of state $\omega$ to higher capacity (per day)

$\lambda^{\omega-}_{g_{i,k}}$ = Equivalent transition rate of additional generating unit k in area i from a capacity of state $\omega$ to lower capacity (per day)

Steps of L-shaped algorithm [60] for unit availability consideration are given as follows.

Step 0. Initialization

- Find $x^0$ from solving master problem; discard the second stage objective function.

$$\begin{aligned} &\text{Min} \quad \sum_{i \in I} \sum_{k \in K_i} c^g_{i,k} x^g_{i,k} \\ &s.t. \quad \sum_{i \in I} \sum_{k \in K_i} x^g_{i.k} = N^g \\ &x^g_{i,k} \text{ binary} \end{aligned} \tag{6.39}$$

- Set upper bound (UB) and lower bound (LB), i.e., $UB \leftarrow \infty$ and $LB \leftarrow -\infty$

Step 1. Solve subproblem at iteration $t$

– Reset the linear approximation function coefficients, $\beta_{i,k}^{t} \leftarrow 0; \forall i \in I, \forall k \in K_i$, its right-hand-side value $\alpha^{t} \leftarrow 0$, and the subproblem objective function value $f^{t} \leftarrow 0$.

– For all system states $\omega$ = 1 to $|\Omega|$, solve subproblem *t* where each scenario has probability, $p_{\omega}$

$$
\begin{aligned}
& f_{\omega}^{t} = \text{Min} \sum_{i \in I} c_i^{l}(\omega)\left(l_i(\omega) - y_{it}(\omega)\right) \qquad (6.40)\\
& s.t. \qquad y_{si}(\omega) \le g_i(\omega) + \sum_{k \in K_i} M_{i,k}^{g}(\omega) x_{i,k}^{g}; \quad \forall i \in I \\
& \qquad \left| y_{ji}(\omega) - y_{ij}(\omega) \right| \le t_{ij}(\omega); \quad \forall i, j \in I, i \ne j \\
& \qquad y_{it}(\omega) \le l_i(\omega); \quad \forall i \in I \\
& \qquad y_{si}(\omega) + \sum_{\substack{j \in I \\ j \ne i}} y_{ji}(\omega) = \sum_{\substack{j \in I \\ j \ne i}} y_{ij}(\omega) + y_{it}(\omega); \quad \forall i \in I \\
& \qquad y_{ij}(\omega), y_{isi}(\omega), y_{it}(\omega) \ge 0; \quad \forall i, j \in I
\end{aligned}
$$

– Obtain dual solution, $\vec{\pi}_{\omega}^{t} = \left(\pi_{\omega,i}^{g}, \pi_{\omega,ij}^{line}, \pi_{\omega,i}^{load}\right)$ associated with generation, transmission line capacities, and load constraints respectively.

– Update the generated cut from $\beta_{i,k}^{t} += p_{\omega} \pi_{\omega,i}^{g} M_{\omega,i,k}^{g}$, and

$$
\alpha^{t} += p_{\omega} \left( \sum_{\forall i \in I} \pi_{\omega,i}^{g} g_i(\omega) + \sum_{\substack{\forall i,j \in I \\ i \ne j}} \pi_{\omega,ij}^{line} t_{ij}(\omega) + \sum_{\forall i \in I} \pi_{\omega,i}^{load} l_i(\omega) \right) \qquad (6.41)
$$

– Update subproblem objective value $f^{t} += p_{\omega} f_{\omega}^{t}$

– Update $UB = \min\left\{ UB, \sum_{\forall i \in I} \sum_{\forall k \in K_i} c_{i,k}^{g} x_{i,k}^{g,t} + f^{t} \right\}$, if changed, update the incumbent solution, $x^{incumbent} \leftarrow x^{t}$

Step 2. Solve master problem

– Append the following cut, $\eta \geq \alpha^t + \sum_{\forall i \in I} \sum_{\forall k \in K_i} \beta_{i,k}^t x_{i,k}^g$

– Obtain solution $x_{i,k}^{g,t+1}, \eta^{t+1}$ from the following master problem

$$\begin{aligned} &\text{Min} \quad \sum_{\forall i \in I} \sum_{\forall k \in K_i} c_{i,k}^g x_{i,k}^g + \eta \\ &s.t. \quad \sum_{\forall i \in I} \sum_{\forall k \in K_i} x_{i,k}^g = N^g \\ &\eta \geq \alpha^q + \sum_{\forall i \in I} \sum_{\forall k \in K_i} \beta_i^q x_{i,k}^g ; q = 0, \ldots, t \\ &x_{i,k}^g \text{ binary} \end{aligned} \tag{6.42}$$

– Update $LB = \max\left\{ LB, \sum_{\forall i \in I} \sum_{\forall k \in K_i} c_{i,k}^g x_{i,k}^{g,t+1} + \eta^{t+1} \right\}$

Step 3. Check convergence

– Compute percent gap from $\%gap = \frac{(UB - LB)}{UB} \times 100$

– If $\%gap \leq \varepsilon$, stop and obtain optimal solution, $x^* \leftarrow x^{incumbent}$, and objective value from upper bound, else, $t \leftarrow t+1$, return to step 1

The algorithm is then implemented with the tree-area power system. The transmission lines are assumed to be fully available at all time. Load cluster data is taken from [17] and consists of 4 states in this study. Area generation, and load probability distributions are given in Appendix C. Equivalent transition rates of all components, calculated from the recursive formula in [43], are also shown in Appendix C. It is assumed that the maximum number of additional units is 2 and the additional generators have capacity of 100 MW each. The cost of an additional unit of the three-area system is

100 million dollars for all areas. Parameters of additional units in each area are given in Table 6.6.

Table 6.6 Three Area Additional Unit Parameters with Unit Availability Consideration

| Area | Unit cost ($m) | Failure rate (per day) | Mean repair time (hours) |
|---|---|---|---|
| 1 | 100 | 0.2 | 24 |
| 2 | 100 | 0.05 | 24 |
| 3 | 100 | 0.1 | 24 |

The optimal solution using the algorithm is to locate one generator in area 1 and one generator in area 2 which gives expected loss of load cost of 1.7 million dollars and expansion cost of 200 million dollars. The algorithm converges in 2 iterations. Upper bound and lower bound are shown in Table 6.7.

Table 6.7 Upper Bound and Lower Bound of Objective Function with Unit Availability Consideration

| Iteration | Lower Bound | Upper Bound | % Optimality Gap |
|---|---|---|---|
| 0 | 198.02 | 211.36 | 6.312 |
| 1 | 201.62 | 201.70 | 0.040 |
| 2 | 201.70 | 201.70 | 0.000 |

It should be noted that the study presented here is only for illustration purposes. The actual expected loss of load cost, however, may vary depending upon the system customer damage function given in the model. It can be seen from the results that the

number of iterations is very small. This may be due to the fact that the formulation individually represents decision variable of a generating unit and not as number of units in each area as in [4]. Therefore, it allows a candidate solution to move faster than that presented in [4], which converged in the $6^{th}$ iteration. However, the drawback of this formulation is that system states expand with the inclusion of additional units and the computation time per iteration increases as the state space grows. For a large system, sampling techniques [60] can be applied to reduce the number of system states to be evaluated for each subproblem. Truncation of state space can also be used when choosing a state for subproblem calculations.

## 6.6 Discussion and Conclusions

The problem is formulated as a two-stage recourse model with the objective to minimize expansion cost and maximize reliability subject to total budget. L-shaped algorithm is implemented and applied to solve the problem. Due to numerous system states in large systems, straightforward implementation of L-shaped method seems impractical for larger systems. To overcome this, exterior sampling method is proposed. Reliability function of the problem is approximated by the sample-average using two sampling techniques which are MC and LHS. The binary decision variables of additional generating units also allow explicit availability consideration of the additional units.

Results show that even though the problem itself has huge number of system states the proposed method can effectively estimate the optimal solution with a small number of samples. In addition, LHS seems to provide better solution with tighter

bounds than MC due to its variance reduction property.

Other reliability indices can also be used; for example, expected loss of load or loss of load probability. Expected loss of load can also be used as a reliability index in the second stage objective function since it may be difficult to assess the loss of load cost coefficient for various systems. However, some weighting coefficients need to be used in order to make this reliability index compatible with other costs in the objective function. To calculate loss of load probability, number of loss of load states has to be obtained. Therefore, minimizing loss of load probability is the same as minimizing number of loss of load states with the following second stage objective function in (6.43). The analysis should be made to verify that this function is convex on decision variables.

$$f(x,\omega) = \underset{i \in I}{\text{Max}}\left(l_i(\omega) - y_{it}(\omega), 0\right) \tag{6.43}$$

Instead of requiring maximum number of additional units, a budget constraint can be used to allow flexibility. Sensitivity analysis on the weight of load loss in each area can be conducted to provide the quantified information (expected loss of load reduction) of the next best generation location that improves system reliability subject to budget constraint. The problem can be formulated to minimize cost with subject to reliability constraint where reliability index can be obtained from different budget values. If reliability index (expected loss of load) is above the limit, budget can be increased. The algorithm has to be repeated until system reliability is below the limit.

Although the analysis is focused on the multi-area formulation, there does not appear to be any inherent limitation in extending this approach to more detailed

transmission networks used in composite system reliability formulations. It is possible to apply this approach with different problem formulation such as using DC flow model instead of network flow model. The problem formulation and solution technique are capable of including transmission line expansions although the studies reported are for generation.

# CHAPTER VII

# TRANSFORMER MAINTENANCE OPTIMIZATION: A PROBABILISTIC MODEL*

## 7.1 Introduction

Transformers are one of the most common equipment in power systems. There is relatively little literature on quantifying the effect of transformer maintenance on reliability. Transformer deterioration failures cause system interruption as well as high cost of lost load. Preventive maintenance can prevent this failure type and extend transformer lifetime. However, too little or too much maintenance may lead to poor reliability or high maintenance cost. In order to achieve cost effective maintenance, system reliability and cost should be balanced. This study proposes a probabilistic model for transformer maintenance optimization.

Model parameters in the proposed model are assumed to be known from historical data collected. The parameters include inspection rate of each stage, mean time in each stage, failure cost, maintenance cost, and inspection cost. This study also investigates the effect of model parameters on reliability and maintenance cost. An equivalent mathematical model is introduced for simpler analysis. The analysis covers Mean Time to the First Failure, maintenance and failure cost, and inspection cost. Simulation results of the proposed model are corroborated by mathematical equations of

---

the equivalent model using first passage time and steady state probability calculations [86]. The objective of this study is to give an insight into the effect of the model parameters on reliability and all associated cost.

This chapter is organized as follows. Basic background material for model building, namely, deterioration process of transformer, maintenance process, and transformer inspection tests are given in the following. Section 7.2 proposes a probabilistic maintenance model. Sensitivity analysis is given in section 7.3. Equivalent models for mathematical analysis are presented in section 7.4. Discussions and conclusions are given in the last section.

### 7.1.1 Deterioration Process of a Transformer

The two main components of an oil-immersed transformer are its windings and oil. The deterioration processes of these two components are described below.

#### 7.1.1.1 Deterioration Process of the Winding

The insulating paper in the winding is a cellulose material, which consists of a long chain Hydrocarbon glucose molecule. The condition of the paper is determined by the degree of polymerization (DP). The higher the DP is, the longer is the chain and better is the paper condition [37]. As paper ages, the chain breaks down and generates CO, $CO_2$, $H_2O$, Furfural or FFA, and fiber.

#### 7.1.1.2 Deterioration Process of the Oil

The oxidation of oil produces acids, moisture and sludge, which impair cooling property, resistivity and dielectric strength of the oil.

These two processes happen concurrently and dependently. Water produced in the deterioration process of the paper increases the ageing rate of the oil and vice versa. Both processes are accelerated by high temperature, moisture and oxygen. Deterioration failure is a long-term accumulated fault, which happens as a result of deterioration process. It can happen either in winding or oil; for example, loss of too much moisture of paper insulation in winding, dielectric breakdown, or partial discharge [47].

### 7.1.2 Maintenance Process of a Transformer

There are numbers of maintenance processes for a transformer. This study presents some of the processes below.

#### 7.1.2.1 Oil Filtering

Most of the moisture comes from the degradation process of paper, which is used in the winding for wrapping around conductors and spacers; therefore, maintenance action would require a complete dismantling of this device. Moreover, the cost of this action represents a replacement by new transformer. During the deterioration process of insulating paper, water and fiber are produced in the oil; thus, the effective action would be drying and filtering the oil. At high temperature, water content in oil is relatively high compared to water content in paper. The drying method consists of filtering oil at high

temperature. This on-line maintenance action will not only reduce moisture but also remove fiber and dirt particles, which are possible sources for partial discharge or electrical breakdown in the oil.

#### 7.1.2.2 Oil Replacement

This maintenance action will be done off-line when properties of oil; i.e., dielectric breakdown voltage, sludge, resistivity, etc. are in a more adverse condition.

### 7.1.3 Transformer Inspection Tests

There are a number of inspection tests for a transformer. This study presents some of the tests below.

- In routine sampling test, a sample is taken from oil and run through the following analysis; dielectric strength, resistivity, acidity, fiber count: small (<2 mm), medium (2-5 mm) and large (>5 mm) [52], and moisture content. Serviced-aged oils are classified into four conditions as follows [82]. Table 7.1 suggests test limits for group 1, Table 7.2 suggests test limit for group 2 and 3
    1. Group 1: satisfactory
    2. Group 2: requires reconditioning for further use
    3. Group 3: poor, should be reclaimed or disposed
    4. Group 4: adverse condition, dispose only

Table 7.1 IEEE Std. C57.100-1986 Suggested Limits for In-Service Oil Group 1 by Voltage Class

| Property | Limit | | |
|---|---|---|---|
| Voltage Class | 69 kV and below | 69– 288 kV | 345 kV and above |
| Dielectric breakdown voltage 60 Hz, 0.100 gap 1 min, kV, min | 26 | 26 | 26 |
| Dielectric breakdown voltage 0.040 gap, kV, min | 23 | 26 | 26 |
| Dielectric breakdown voltage 0.080 gap, kV, min | 34 | 45 | 45 |
| Neutralization number max, mg KOH/g | 0.2 | 0.2 | 0.1 |
| Interfacial tension, min, mN/m | 24 | 26 | 30 |
| Water max, ppm* | 35 | 25 | 20 |
| *Does not pertain to free breathing transformer or compartment | | | |

Table 7.2 IEEE Std. C57.100-1986 Suggested Limits for Oil to Be Reconditioned or Reclaimed

| Property | Group 2 | Group 3 |
|---|---|---|
| Neutralization number max, mg KOH/g | 0.2 | 0.5 |
| Interfacial tension, min, mN/m | 24 | 16 |

– Dissolved Gas Analysis measures gases that are produced by the ageing process ($H_2$, $C_2H_2$, $C_2H_4$, $CH_4$, CO). Levels of condition of dissolved gas in oil, and total dissolved combustible gas (TDCG) are listed in the following [77]. Table 7.3 lists the concentrations corresponding to each level. A suggested action based on TDCG, which impacts both maintenance action and inspection rate, is given in Table 7.4.

1. Condition 1: Satisfactory
2. Condition 2: Prompt additional investigation
3. Condition 3: Indicates high level of decomposition. Prompt additional investigation
4. Condition 4: Excessive decomposition

Table 7.3 IEEE Std. C57.104-1991 Dissolved Gas Concentrations

| Dissolved Gas | Concentration Limits (ppm) | | | |
|---|---|---|---|---|
| | C1 | C2 | C3 | C4 |
| $H_2$ | 100 | 101-700 | 701-1800 | >1800 |
| $CH_4$ | 120 | 121-400 | 401-1000 | >1000 |
| $C_2H_2$ | 35 | 36-50 | 51-80 | >80 |
| $C_2H_4$ | 50 | 51-100 | 101-200 | >200 |
| $C_2H_6$ | 65 | 66-100 | 101-150 | >150 |
| CO | 350 | 351-570 | 571-1400 | >1400 |
| $CO_2$ | 2500 | 2500-4000 | 4001-10000 | >10000 |
| TDCG | 720 | 721-1920 | 1921-4630 | >4630 |

Table 7.4 IEEE Std. C57.104-1991 Action Based on TDCG Analysis

| | TDCG Levels (ppm) | TDCG Rates (ppm/day) | Sampling Intervals and Operating Procedures for Gas Generation Rates | |
|---|---|---|---|---|
| | | | Sampling Interval | Operation Procedures |
| C4 | >4630 | >30 | Daily | Consider removal from service. Advise manufacturer. |
| | | 10-30 | Daily | |
| | | <10 | Weekly | Exercise extreme caution. Analyze for individual gases. Pan outage. Advise manufacturer. |
| C3 | 1921-4630 | >30 | Weekly | Exercise extreme caution. Analyze for individual gases. Pan outage. Advise manufacturer. |
| | | 10-30 | Weekly | |
| | | <10 | Monthly | |
| C2 | 721-1920 | >30 | Monthly | Exercise caution. Analyze for individual gases. Determine load dependence. |
| | | 10-30 | Monthly | |
| | | <10 | Quarterly | |
| C1 | <721 | >30 | Monthly | Exercise caution. Analyze for individual gases. Determine load dependence. |
| | | 10-30 | Quarterly | Continue normal operation. |
| | | <10 | Annual | |

– Furfural Analysis measures FFA which can determine the age of the paper insulation.

– Partial Discharge Monitoring helps to predict and prevent breakdown of transformer [40]. Many types of equipment have been developed for this test, for example, radio interference and acoustic emission. The cost varies according to accuracy of results and sophistication of tools used. The analysis of PD from acoustic emissions should be made according to the size of the transformer. Large transformers are considered for further investigation if any internal partial

discharges are detected. Smaller transformers, on the other hand, use PD count rate to examine the condition of transformer [40].

- Temperature Measurement provides information on ageing of oil and paper since high temperature has a major impact on this process.

## 7.2 Transformer Maintenance Model

A general probabilistic model of the effect of maintenance on reliability of a device is proposed in [50] [53]. The model represents the deterioration process of the device by discrete stages [86]. A proposed probabilistic model utilizes this general model shown in Fig. 7.1. In the proposed models, three stages of deterioration process are introduced; D1, D2, and D3.

At each stage, inspection test is implemented to determine oil condition in the investigation process. After inspection, oil condition is determined by the criteria indicated in the previous section. The criteria categorizes oil condition into 4 groups ranging from normal (C1) to adverse condition (C4). To simplify the problem, we

classify only two levels of maintenance which are oil filtering and oil replacement. Three types of inspection tests are introduced in the model since they are relatively common in the industry; Routine Test, Dissolved Gas Analysis, and Partial Discharge.

Maintenance action is assigned corresponding to the oil condition. It is assumed that after oil filtering, the probability of going back to the previous stage is relatively high and after oil replacement, system stage is set back to the beginning (D1). If oil condition is C1, nothing is done. If oil condition is C2, C3, or C4, two options are available and are assigned with different probabilities, oil filtering or oil replacement. For example, if the present stage is D2 with oil condition C2, the probability of oil filtering will be higher than oil replacement. On the other hand, if the present stage is D2 with oil condition C3 or C4, the probability of oil replacement will be higher. After maintenance, the device will have 3 options, going to stage D1, D2, or D3. The probability of transferring to other stages depends on the present stage and maintenance practice.

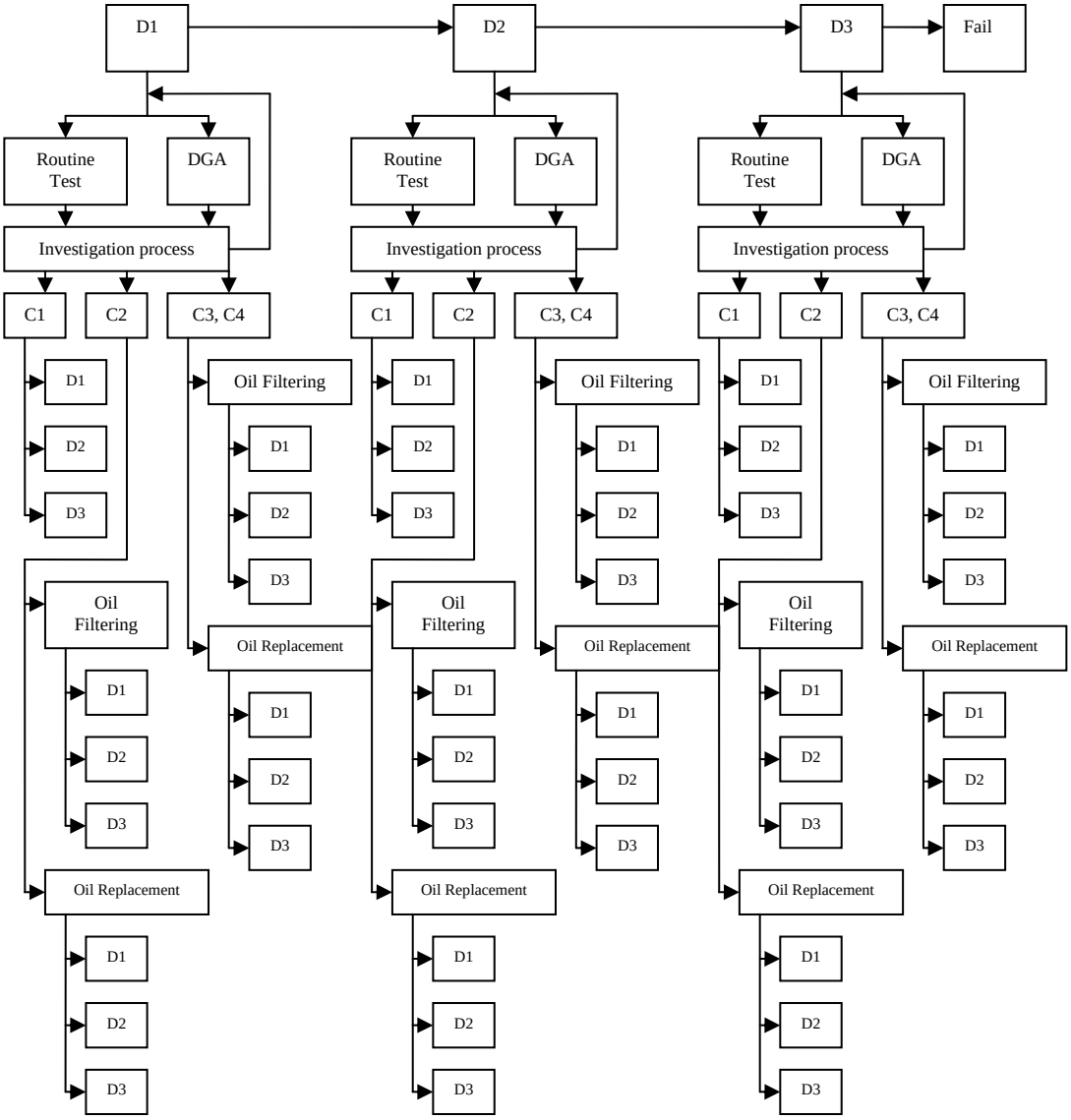


Fig. 7.1 Transformer Maintenance Model

Parameters in the model are listed below.

- Mean time in each stage determines the transition rate of each stage in the deterioration process.
- Inspection rate of each stage can be treated as maintenance rate of each stage under the assumption that inspection, test and maintenance actions are implemented sequentially.
- Probabilities of transition from one stage to others are the probabilities of oil condition after the inspection process, probabilities of transferring from any oil condition to a given stage, probabilities of filtering or replacing the oil, and probabilities of transferring to each stage after maintenance. These probabilities can be treated as equivalent transition rates from one stage to others. The equivalent model is introduced to clarify this point later.

Notice that mean time in each stage and transition probabilities can be approximated from historical data of oil condition of a physical transformer; thus, these parameters are assumed to be given. However, inspection rate of each stage can be varied to achieve high reliability with minimum cost. Therefore, this parameter is of the most concern in the analysis.

In the following section, sensitivity analysis of inspection rate of each stage is implemented on the model in Fig. 7.1. Model parameters are listed in Appendix D. The analysis covers two aspects, namely, mean time to the first failure, and all associated costs (failure cost, maintenance cost, and inspection cost).

## 7.3 Sensitivity Analysis

Mean time to the first failure (MTTFF) is the expected operating time before failure of the transformer starting from initial stage. This analysis will provide information of how the transformer operating time changes when the inspection rate of each stage changes. Let

$i_1$ = Inspection rate of D1 (per year)

$i_2$ = Inspection rate of D2 (per year)

$i_3$ = Inspection rate of D3 (per year)

The simulation results of the relationship of each inspection rate and MTTFF are shown in Fig. 7.2, Fig. 7.3, and Fig. 7.4.

The following observations can be drawn from these simulation results.

- In Fig. 7.2, MTTFF decreases with $i_1$. This is caused by the assumption of exponential distribution of time spent in each stage. The exponential distribution implies constant failure rate. This is of particular significance in stage D1. This means that the inspections, which lead back to D1, will not improve the time to failure in D1; however, those leading to D2 and D3 will result in degradation. Thus, the effect of inspection will always be degradation. In other words, if we assume an exponential distribution for stage 1, then maintenance is of minimal use.
- In Fig. 7.3, MTTFF increases at a decreasing rate with $i_2$ and stays at some value.
- In Fig. 7.4, MTTFF has a positive and linear relationship with $i_3$.

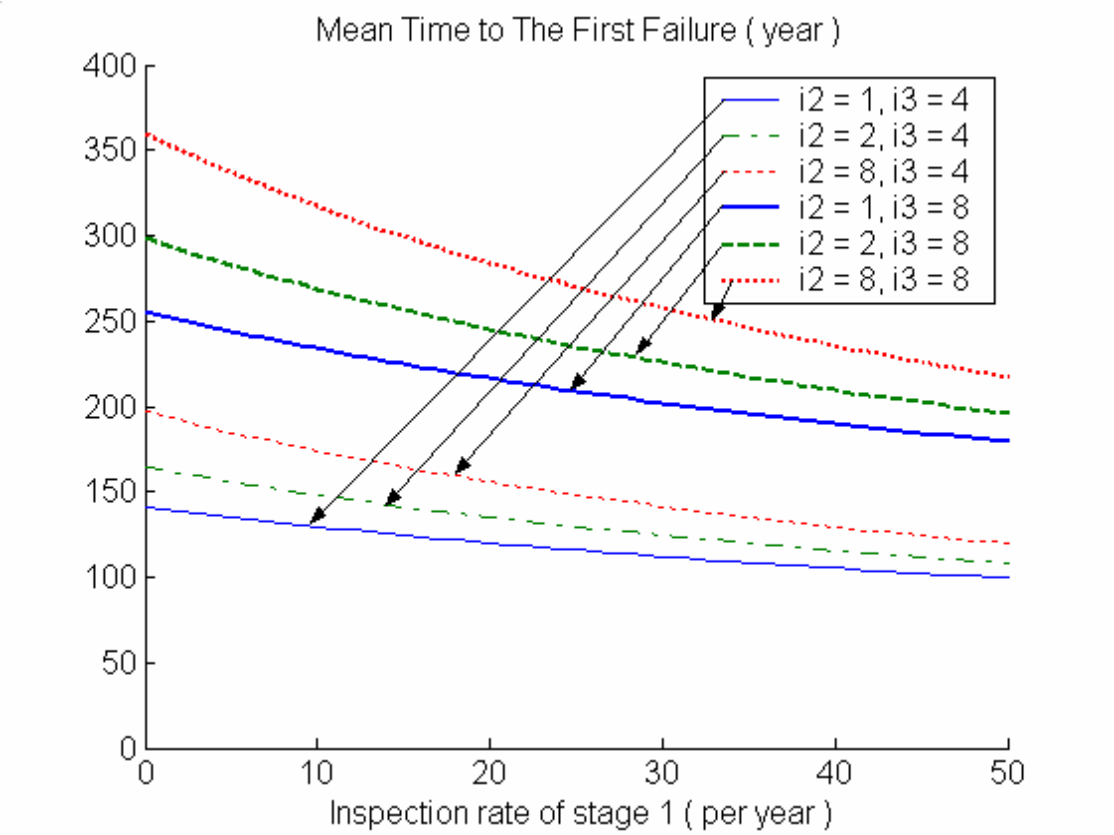


Fig. 7.2 Relationship between MTTFF and Inspection Rate of Stage 1

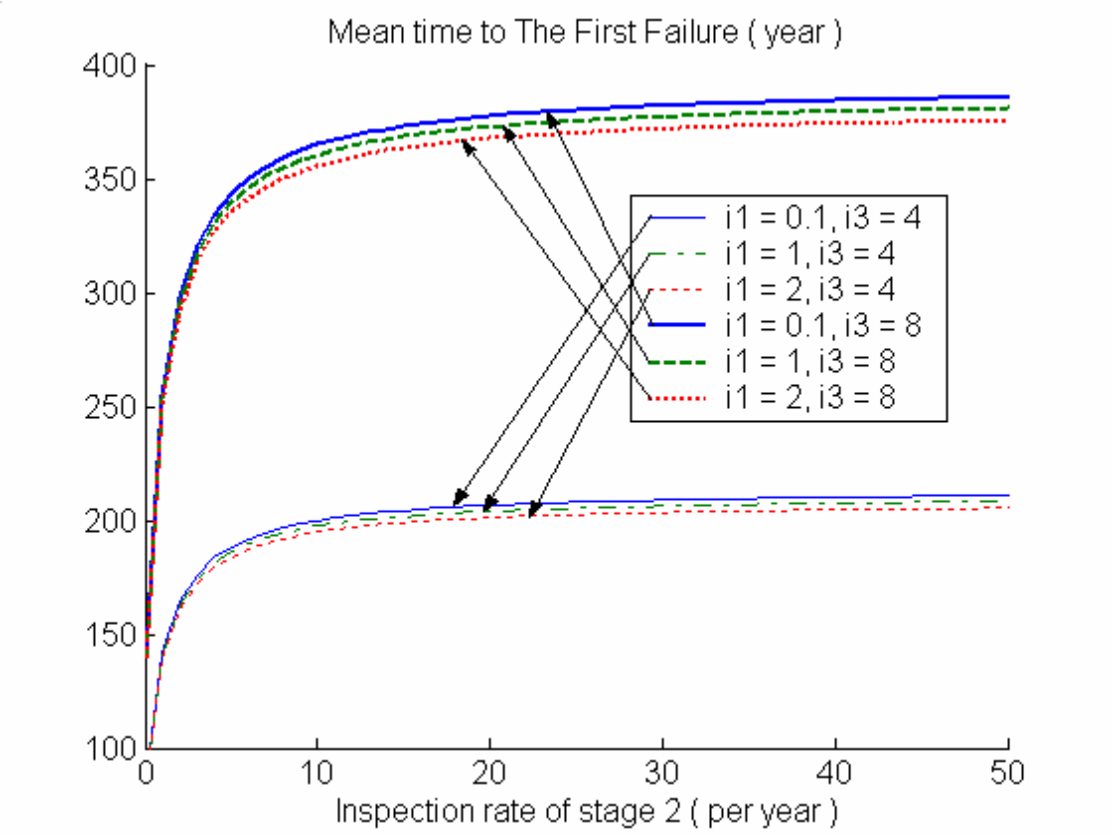


Fig. 7.3 Relationship between MTTFF and Inspection Rate of Stage 2

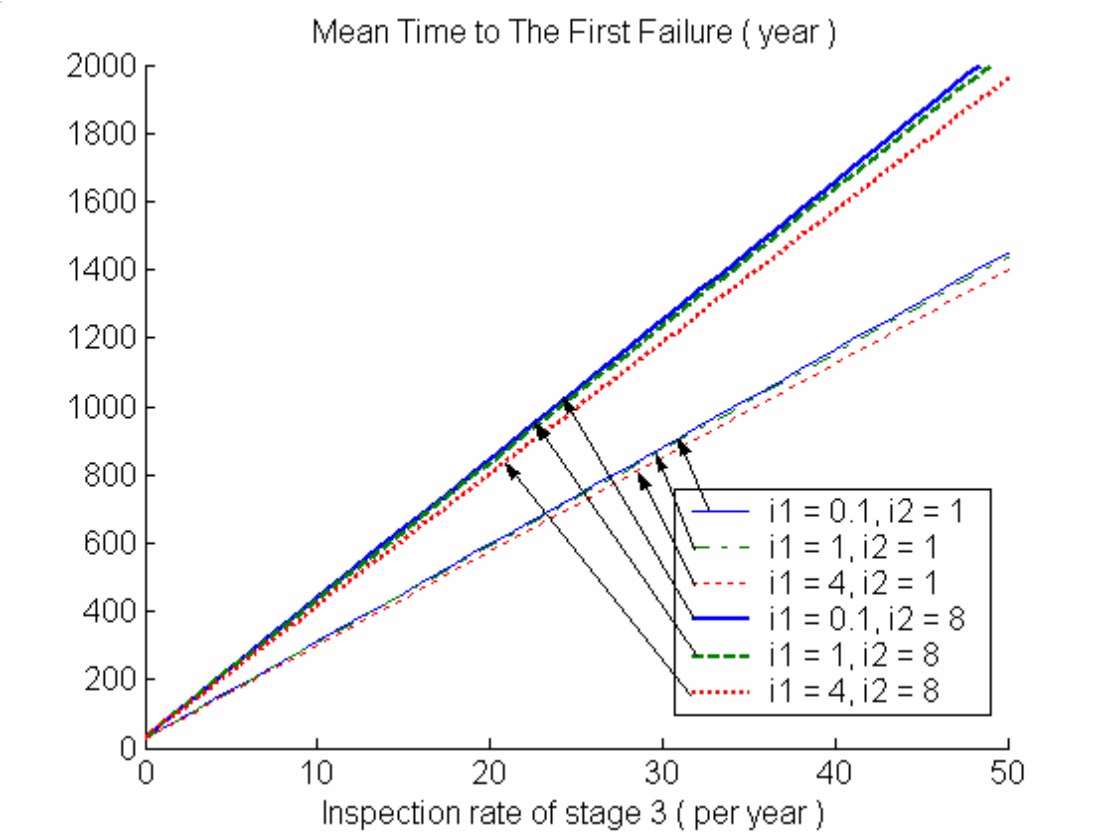


Fig. 7.4 Relationship between MTTFF and Inspection Rate of Stage 3

In order to relax the assumption of exponential distribution, the proposed model in Fig.7.1 is modified by representing stage D1 by three sub-stages. Although each sub-stage is exponentially distributed, the overall D1 will have deterioration. The simulation results of relationship of each inspection rate and MTTFF are shown in Fig. 7.5, Fig. 7.6, and Fig. 7.7.

In Fig. 7.5, MTTFF increases rapidly when increasing $i_1$ and then slightly decreases at high $i_1$. The simulation results in Fig. 7.6 and Fig. 7.7 give the same observations as in Fig. 7.3 and Fig. 7.4.

The simulation results on MTTFF suggest that inspection rate of D1 helps extending MTTFF; however, having too high inspection rate of D1 might reduce MTTFF. In addition, inspection rate of D2, when higher than a certain value, has a minimal impact on reliability. Fig. 7.7 indicates that transformer lifetime is longer with increased inspection rate of D3. Next, the analysis on inspection cost, maintenance cost, and failure cost are made. This analysis provides information about the effect of inspection rate on all associated cost. It can be seen from Fig. 7.1 that the cost from maintenance practices are oil filtering and oil replacement cost. We assume cost parameters from Appendix D.

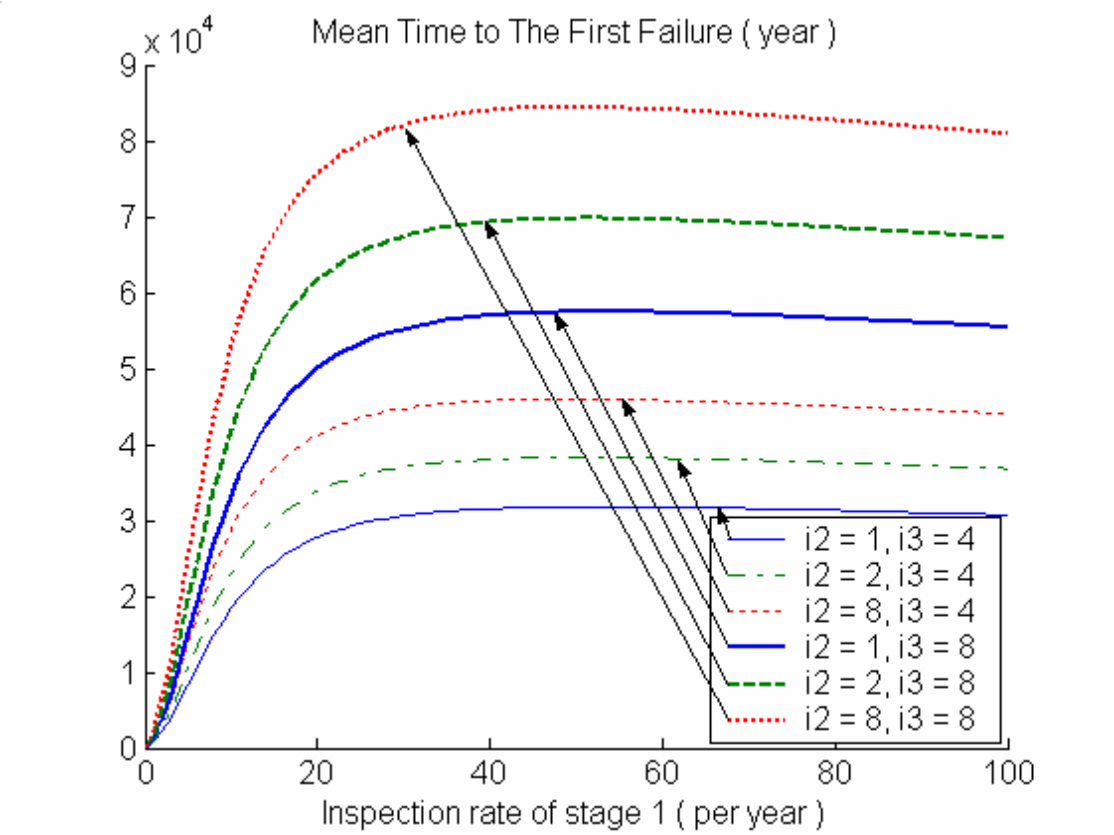


Fig. 7.5 Relationship between MTTFF and Inspection Rate of Stage 1 with Three Sub-Stages in Stage 1

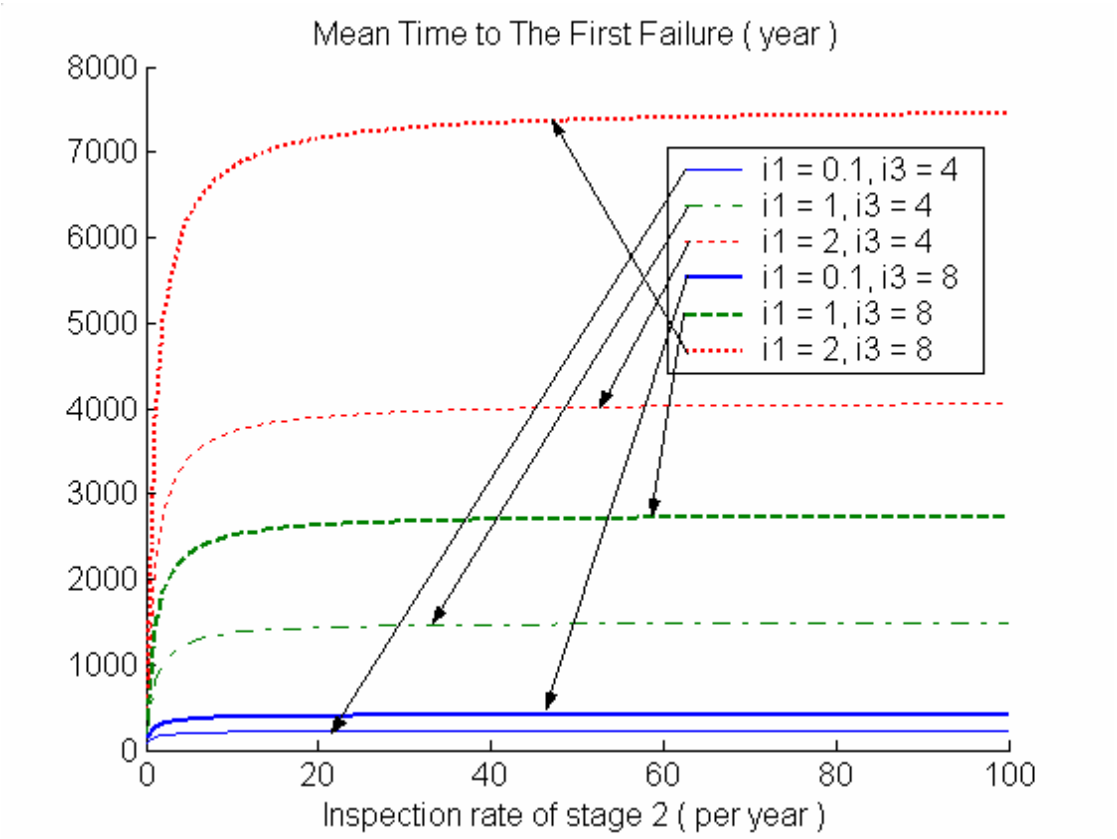


Fig. 7.6 Relationship between MTTFF and Inspection Rate of Stage 2 with Three Sub-Stages in Stage 1

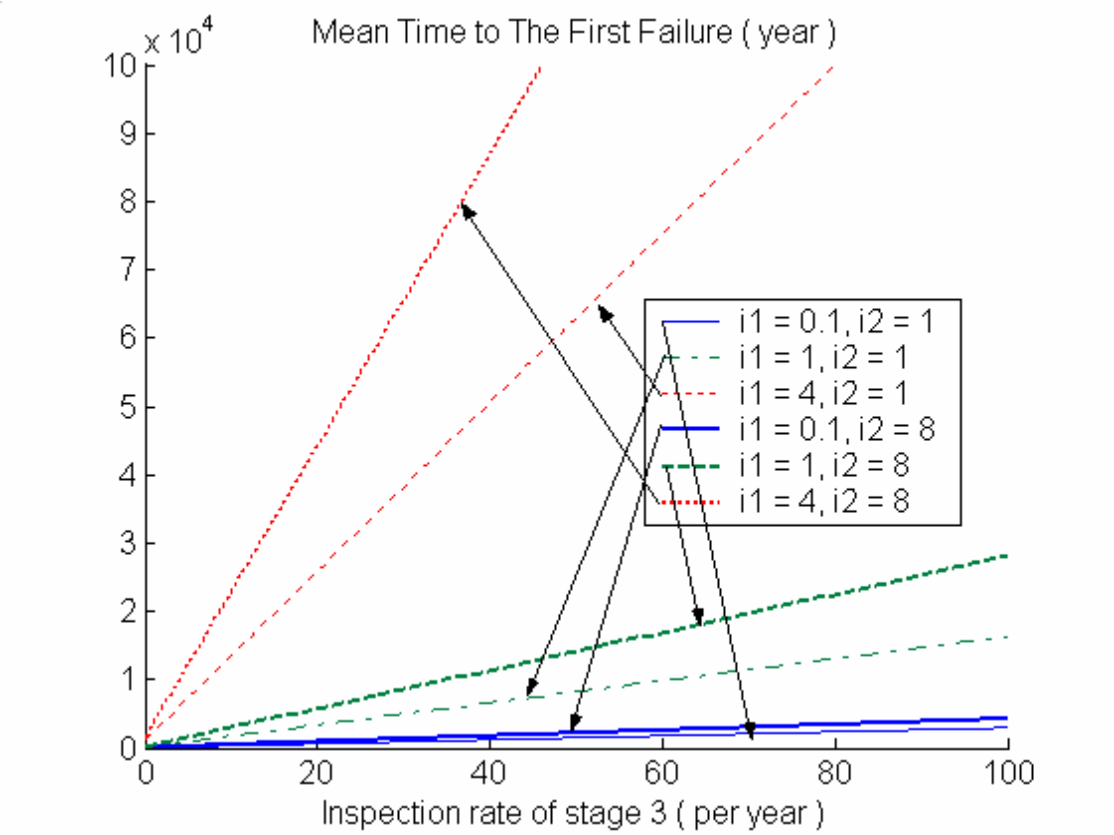


Fig. 7.7 Relationship between MTTFF and Inspection Rate of Stage 3 with Three Sub-Stages in Stage 1

The simulation results of relationship between inspection rate and all associated costs are shown in Fig. 7.8-7.19. The following observations can be made from the simulation results.

- In Fig. 7.8, 7.12 and 7.16, failure cost decreases exponentially as inspection rate of D1, D2 and D3 increases.
- In Fig. 7.9, maintenance cost first decreases as inspection rate of D1 increases and then increase with inspection rate of D1. The optimal region of inspection rate of D1 that minimizes maintenance cost is 0.5 to 1 per year.
- In Fig. 7.13 and 7.17, maintenance cost increases with inspection rate of D2 and D3 and stays at constant value at higher inspection rate of D2 and D3.
- In Fig. 7.10, inspection cost increases linearly with inspection rate of D1.
- In Fig. 7.14 and 7.18, inspection cost increases as inspection rate of D2 and D3 increases and remains constant at high inspection rate of D2 and D3.
- In Fig. 7.11, the optimum region of inspection rate of D1 that minimizes total cost depends on inspection rate of D2 and D3. If the inspection rate of D2 and D3 are higher, the optimal value of inspection rate of D1 will be smaller. Failure cost dominates total cost at small inspection rate of D1 while maintenance cost dominates total cost at high inspection rate of D1.
- In Fig. 7.15 and 7.19, the total cost is minimal at very high inspection rate of D2 and D3. Failure cost dominates the total cost at small inspection rate of D2 and D3 while maintenance cost dominates total cost at high inspection rate of D2 and D3.

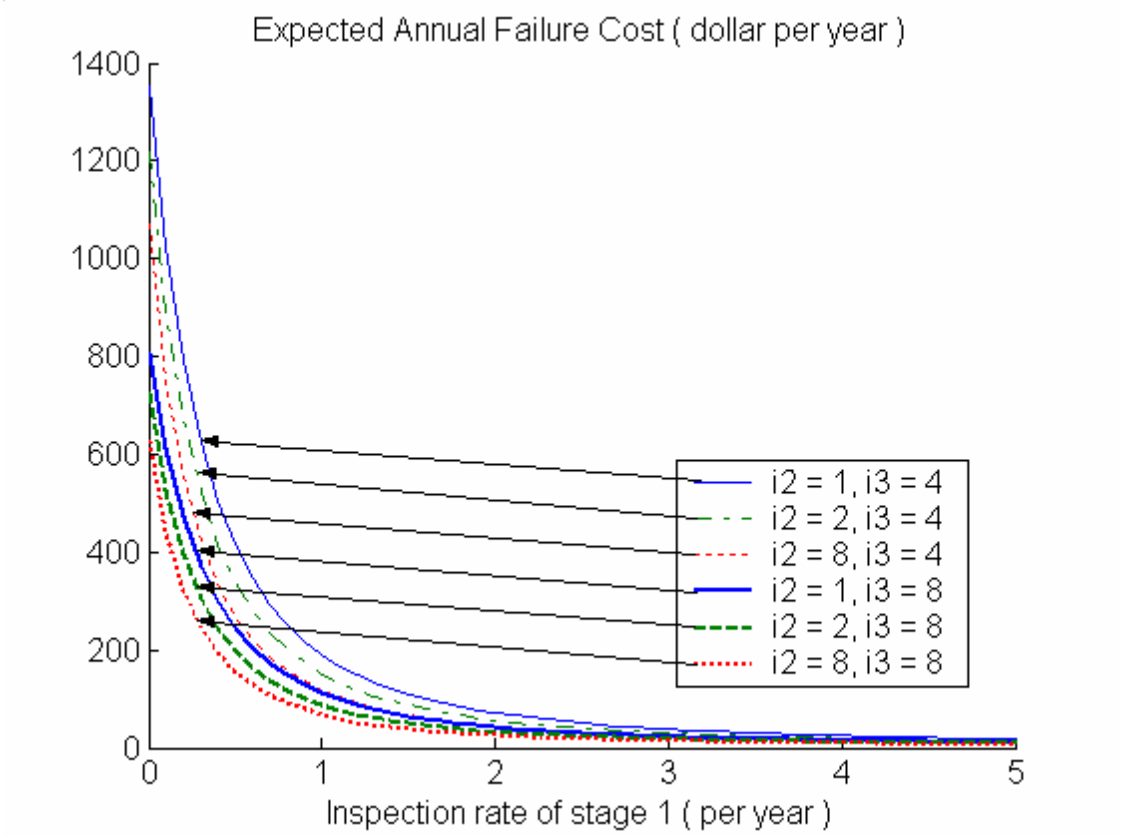


Fig. 7.8 Relationship between Expected Annual Failure Cost and Inspection Rate of Stage 1

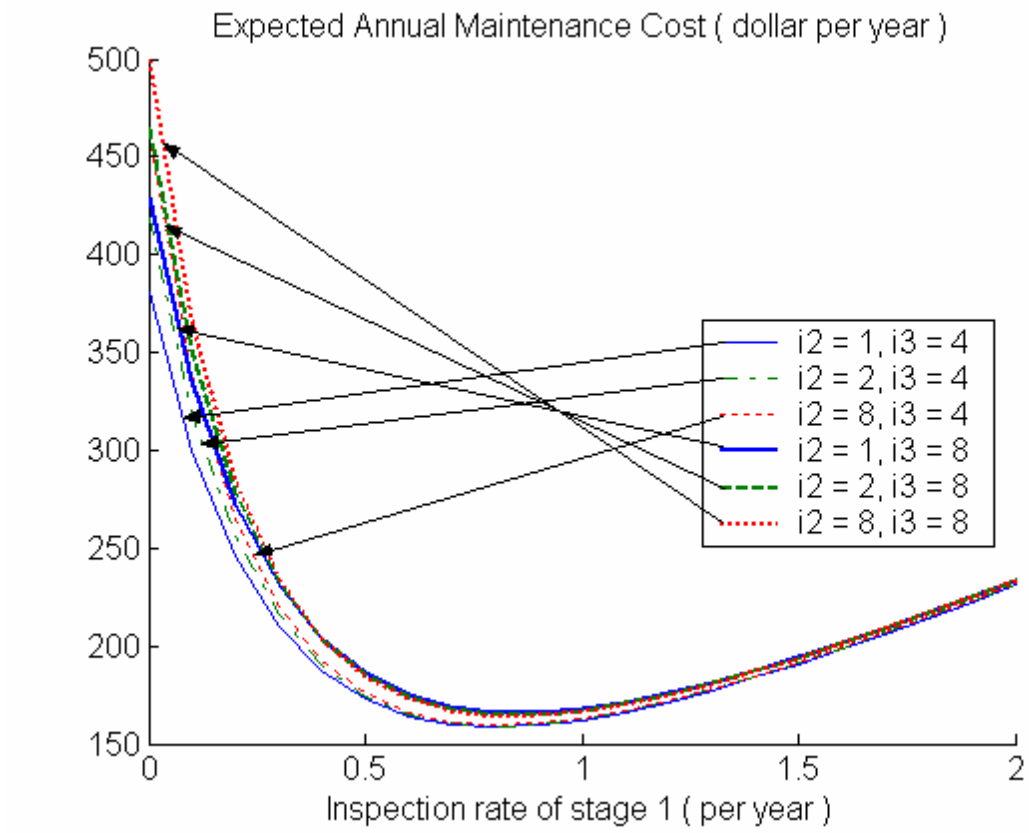


Fig. 7.9 Relationship between Expected Annual Maintenance Cost and Inspection Rate of Stage 1

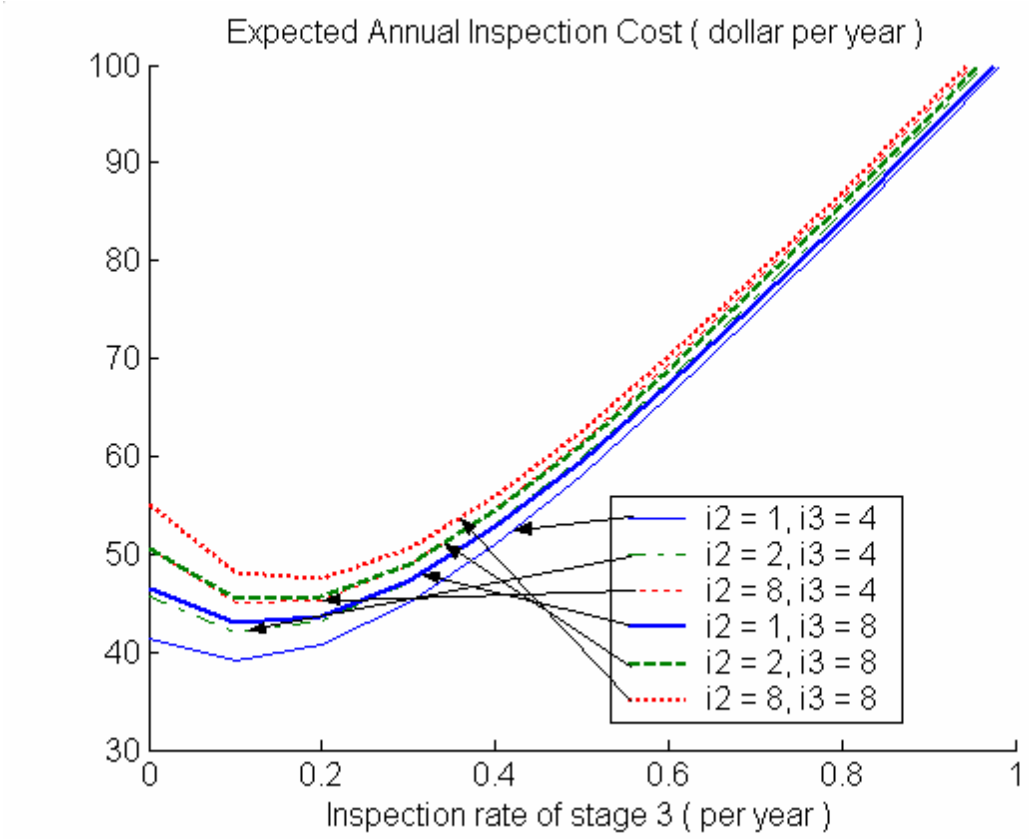


Fig. 7.10 Relationship between Expected Annual Inspection Cost and Inspection Rate of Stage 1

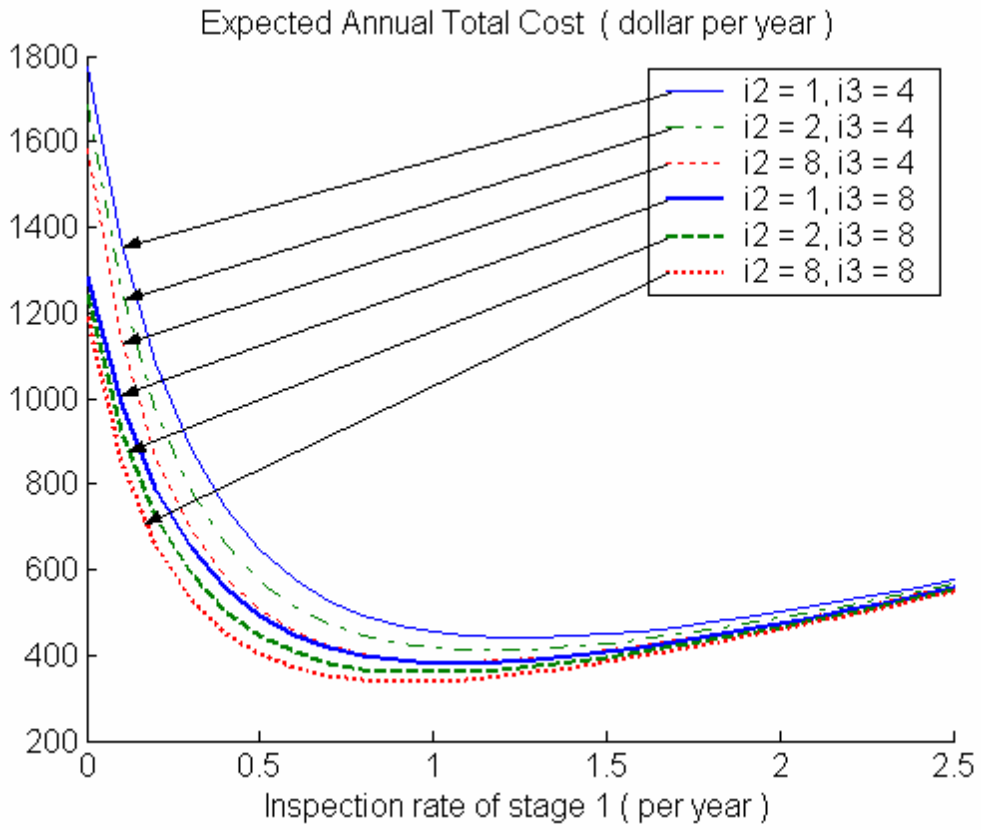


Fig. 7.11 Relationship between Expected Annual Total Cost and Inspection Rate of Stage 1

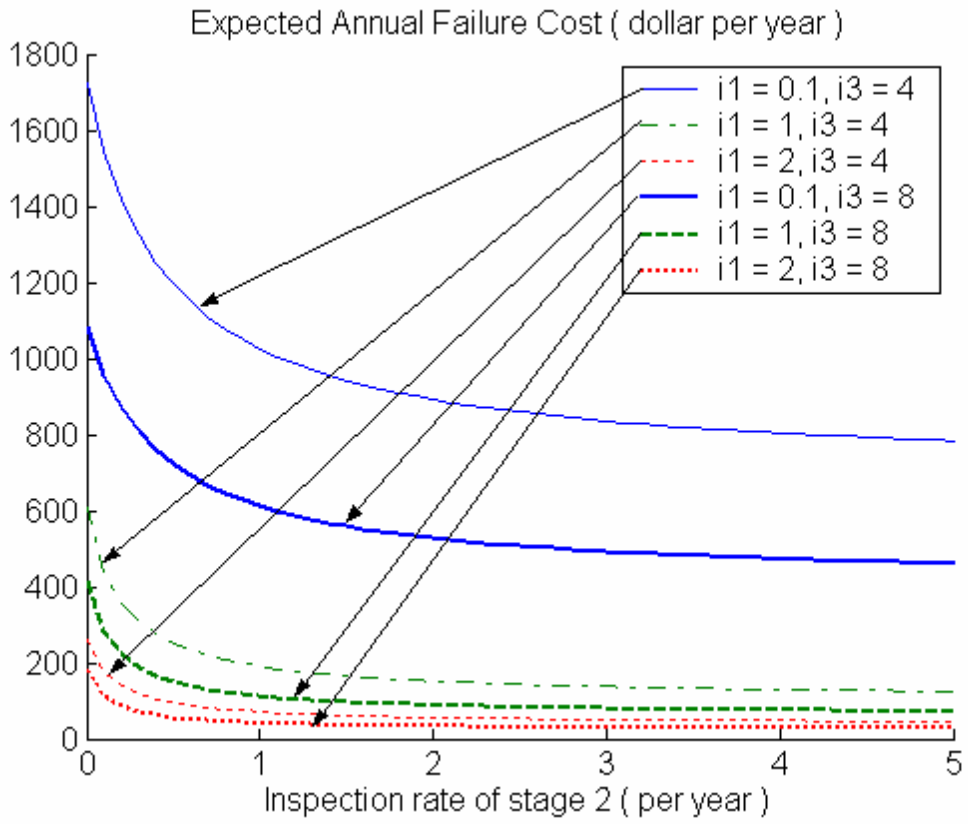


Fig. 7.12 Relationship between Expected Annual Failure Cost and Inspection Rate of Stage 2

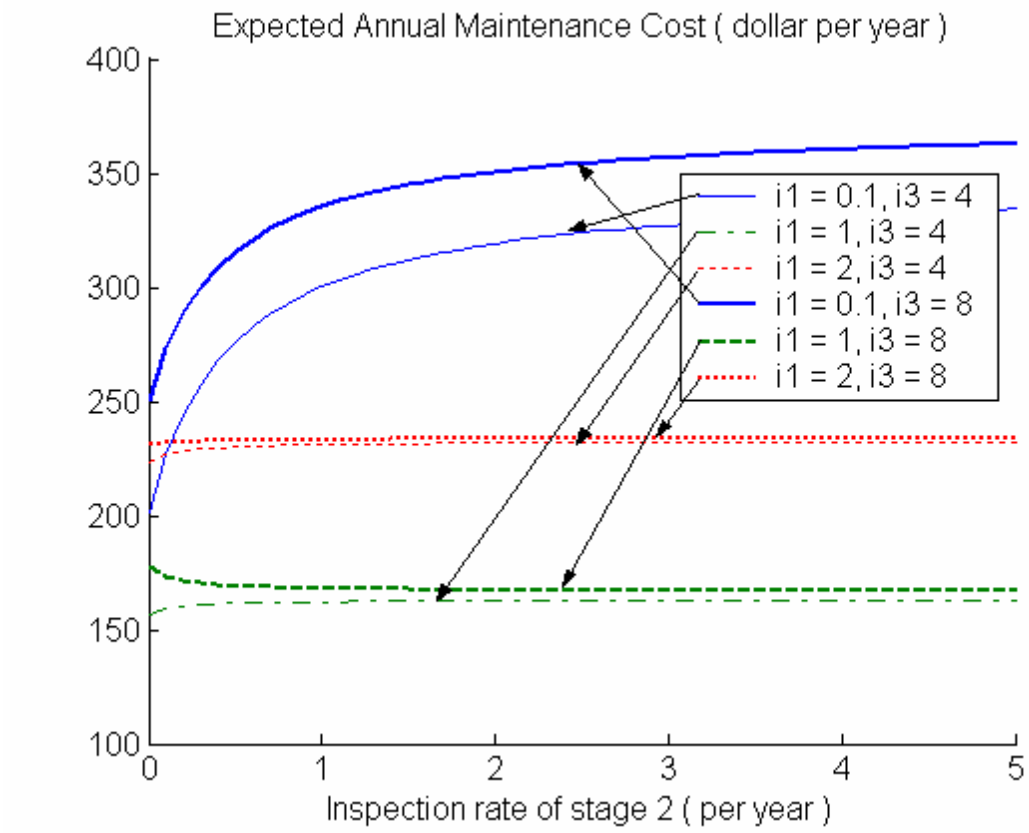


Fig. 7.13 Relationship between Expected Annual Maintenance Cost and Inspection Rate of Stage 2

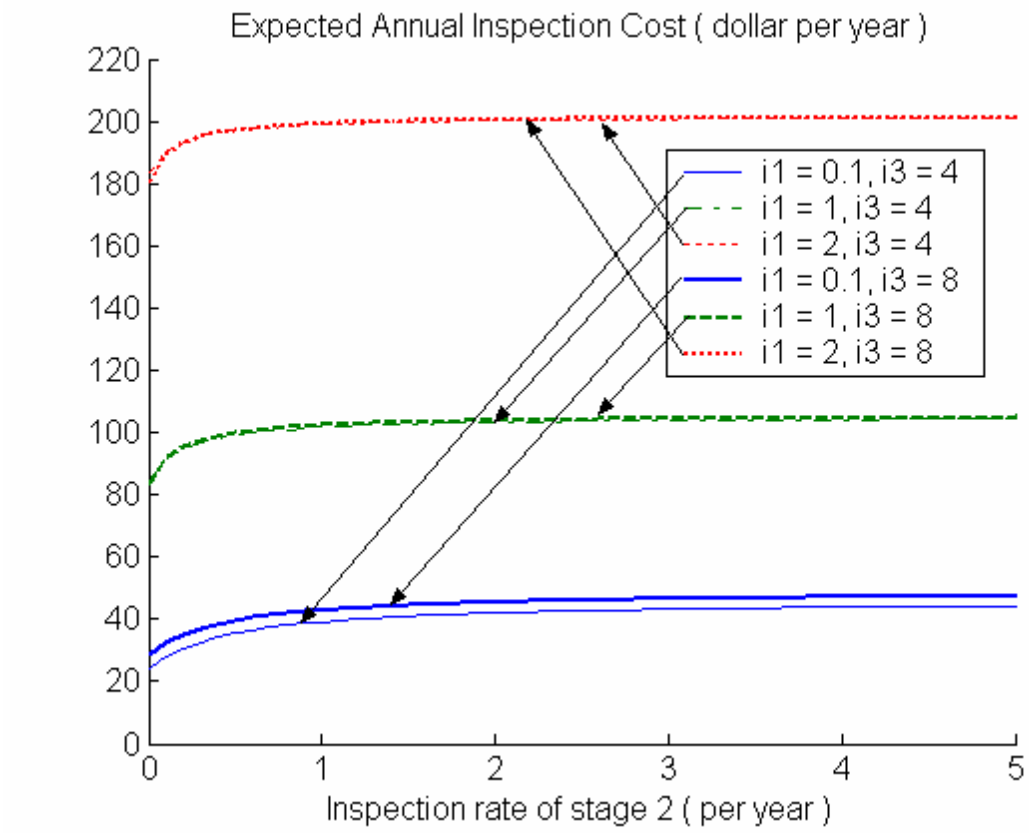


Fig. 7.14 Relationship between Expected Annual Inspection Cost and Inspection Rate of Stage 2

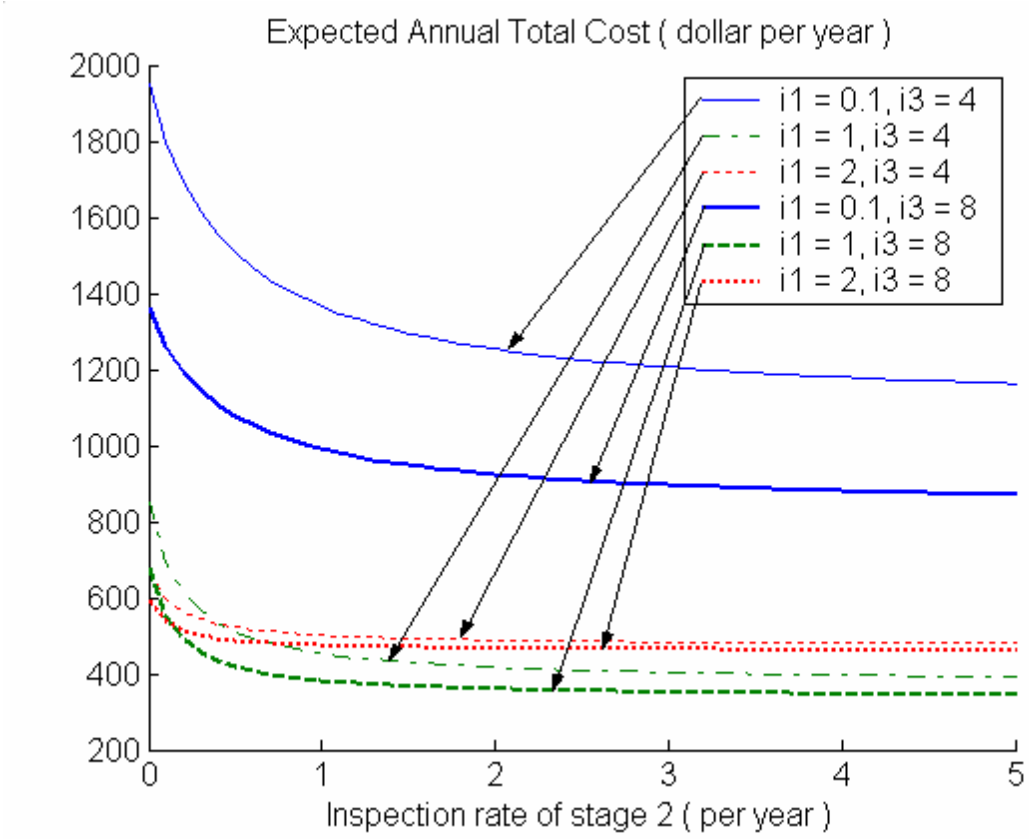


Fig. 7.15 Relationship between Expected Annual Total Cost and Inspection Rate of Stage 2

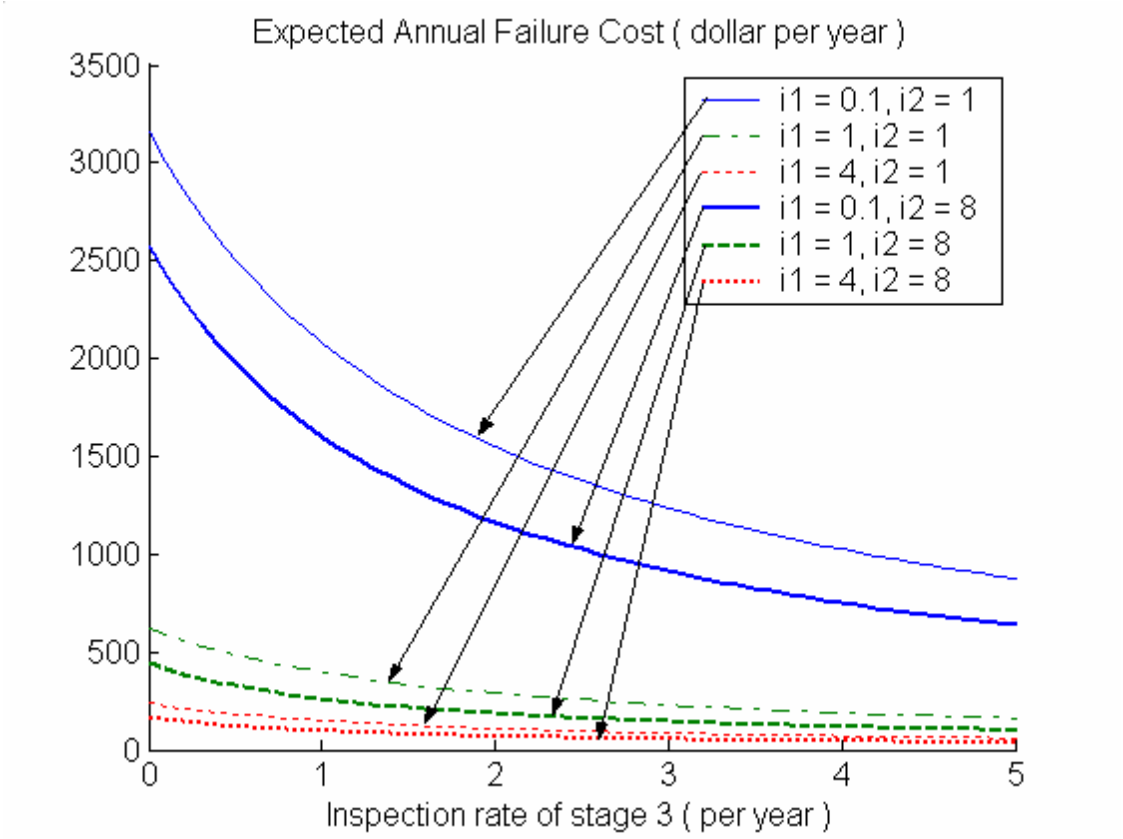


Fig. 7.16 Relationship between Expected Annual Failure Cost and Inspection Rate of Stage 3

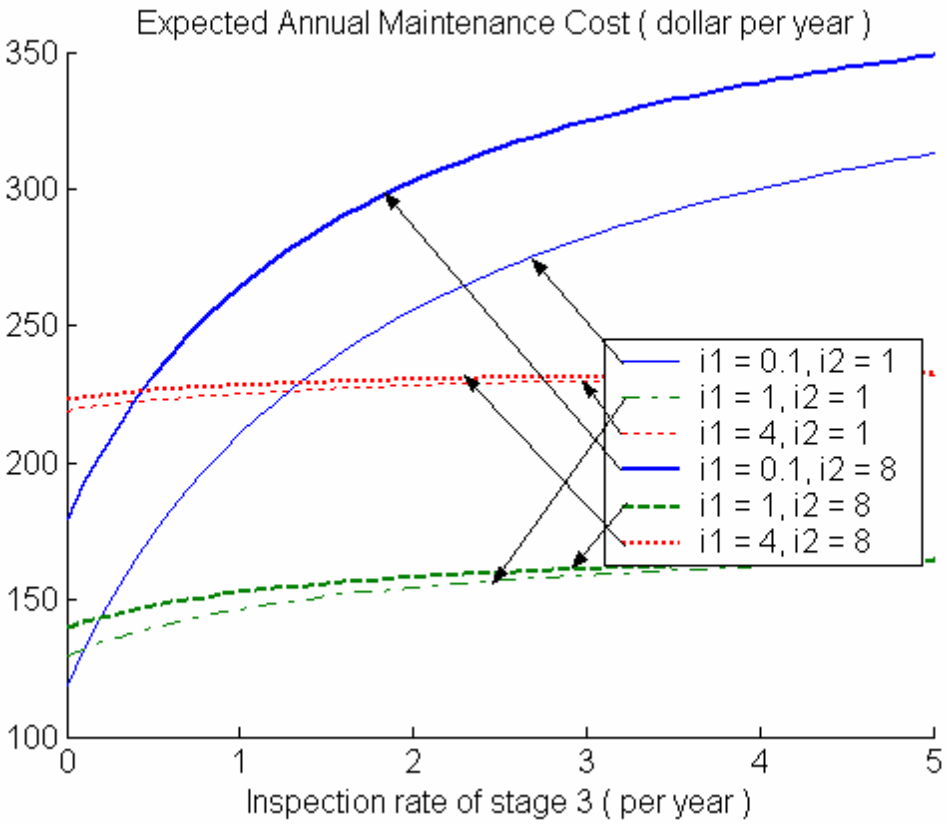


Fig. 7.17 Relationship between Expected Annual Maintenance Cost and Inspection Rate of Stage 3

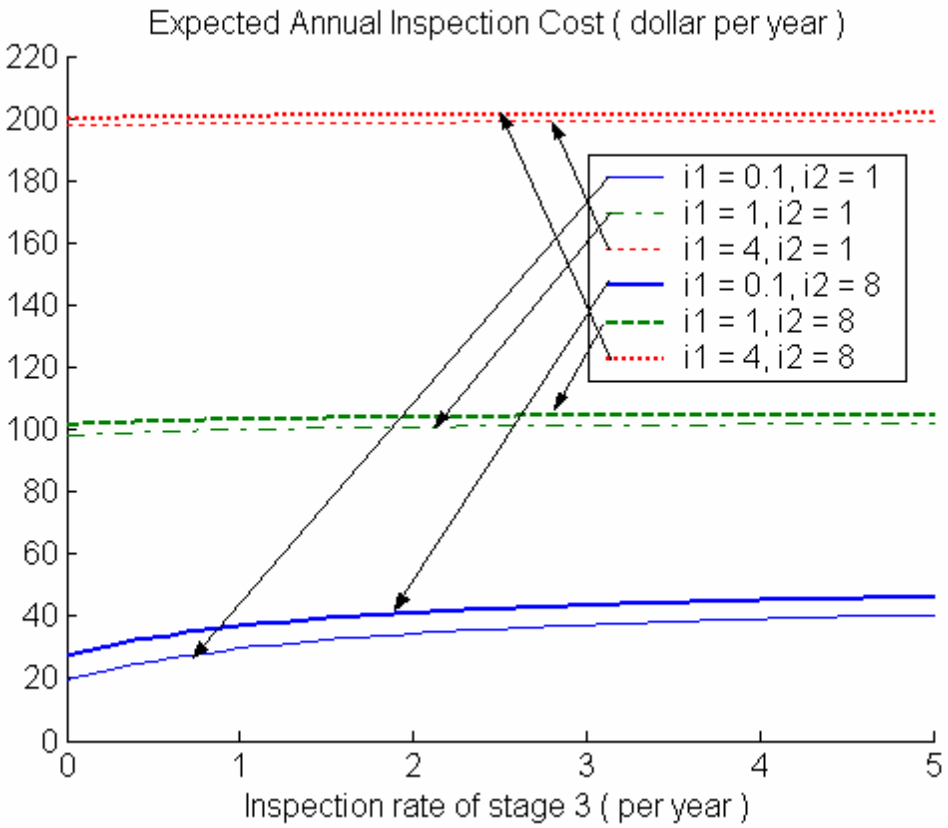


Fig. 7.18 Relationship between Expected Annual Inspection Cost and Inspection Rate of Stage 3

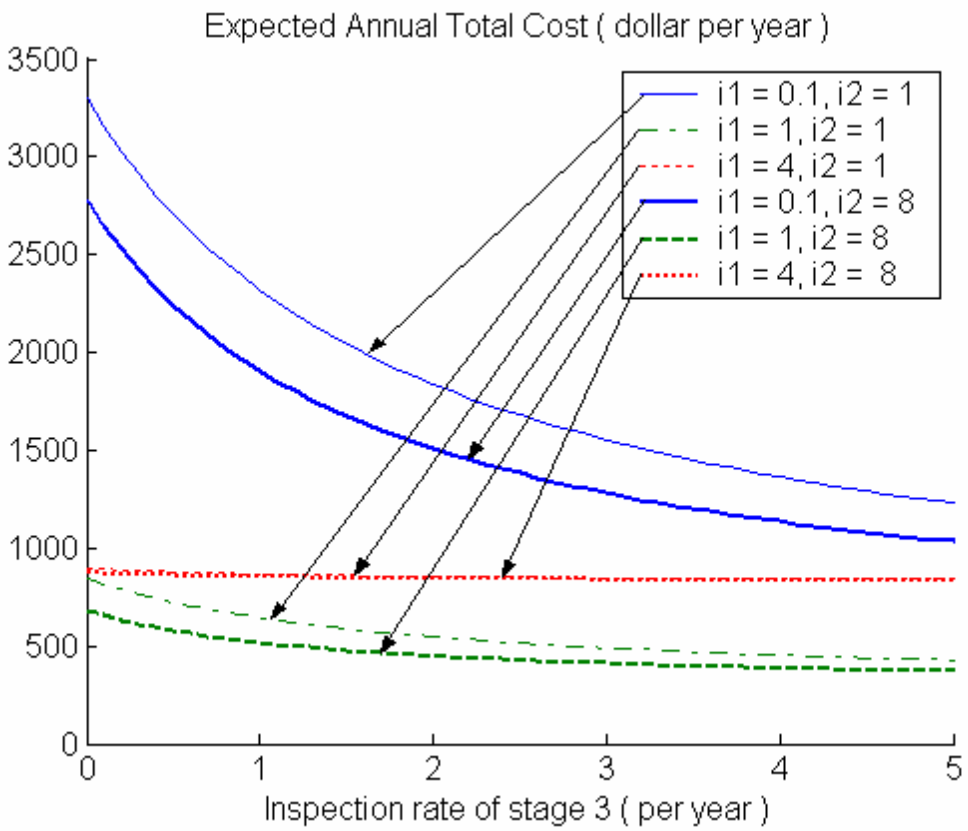


Fig. 7.19 Relationship between Expected Annual Total Cost and Inspection Rate of Stage 3

Simulation results on cost suggest that cost effective maintenance occurs at small inspection rate of D1 and high inspection rate of D2 and D3. In the next section, equivalent mathematical models are presented for simpler analysis. Equations derived from mathematical analysis provide an explicit relationship of each inspection rate with MTTFF and costs.

## 7.4 Equivalent Models for Mathematical Analysis

The proposed equivalent models have 3 discrete stages representing deterioration processes. Maintenance is assumed to be implemented at every inspection, thus, maintenance and inspection rate of each stage are considered to be an equivalent repair rate. Let

D1 = Stage 1

D2 = Stage 2, minor deterioration

D3 = Stage 3, major deterioration

F = Failure stage

$y_1$ = Mean time in stage 1 (year)

$y_2$ = Mean time in stage 2 (year)

$y_3$ = Mean time in stage 3 (year)

$\mu_{21}$ = Repair rate from stage 2 to 1 (/year)

$\mu_{32}$ = Repair rate from stage 3 to 2 (/year)

$\mu_{31}$ = Repair rate from stage 3 to 1 (/year)

In the following, two models are proposed to simplify the transformer maintenance model. The first model assumes that after maintenance is performed, the stage of a device will always be improved. The second model assumes that with some probability, maintenance may accelerate failure of a device. Mathematical equations relating MTTFF and costs to inspection rates in each stage of both models are derived in

the following section. The equivalent models are employed in analyses in the next section, MTTFF and Cost analysis.

### 7.4.1 Perfect Maintenance Model

It is assumed that in the initial stage the transformer is in good working condition that needs no maintenance. Moreover, it is assumed that maintenance improves the device to the previous stage; therefore, repair rate of stage 2 improves the device to stage 1 and repair rate of stage 3 improves the device to stage 2. The model is shown in Fig. 7.20.

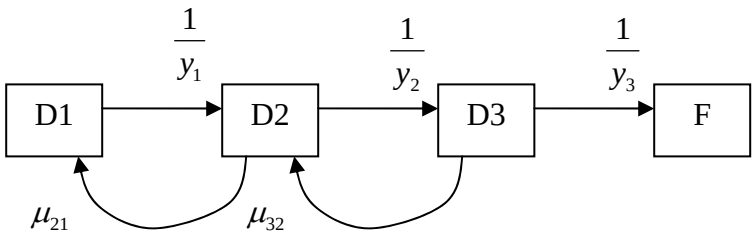


Fig. 7.20 Perfect Maintenance Equivalent Model

### 7.4.2 Imperfect Maintenance Model

This model shown in Fig. 7.21 is slightly different from the model in Fig. 7.20. Transition rate from stage 1 to 3 is introduced ($\lambda_{13}$) to describe an imperfect inspection of stage 1. This model accounts for the probability that inspection of stage 1 might cause the system to transit to stage 3. Note that this model is an equivalent model for

transformer maintenance model in Fig. 7.1 since it accounts for a transition of stage 1 to 3.

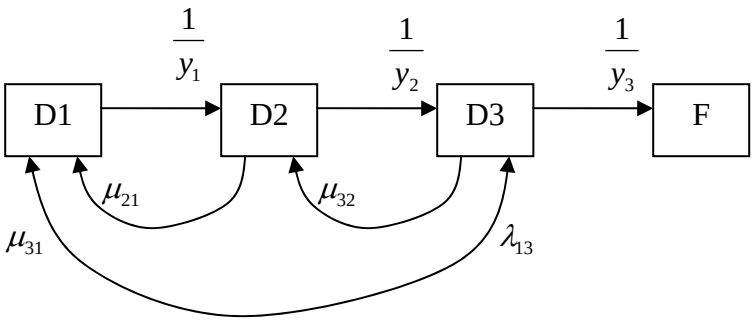


Fig. 7.21 Imperfect Maintenance Equivalent Model

The equivalent models will be employed in analyses in the next section, MTTFF and Cost analysis. The equations obtained from the analyses will be used to verify the simulation results from the previous analyses.

## 7.5 Mean Time to the First Failure Analysis

MTTFF equations are derived using the methodology of first passage time calculation [86]. Cost equations are derived using steady state probability calculation. The cost analyses include failure cost, maintenance cost, and total cost. Maintenance cost in this analysis includes inspection cost based on the assumption of the equivalent model that maintenance is implemented at every inspection. These equations are used to explain the simulation results in Fig. 7.2-7.7.

### 7.5.1 MTTFF for Perfect Maintenance Model

Truncated transitional probability matrix *Q* is constructed by deleting row 4 and column 4 which associated with the absorbing state [86].

$$Q_n = \begin{bmatrix} 1-\frac{1}{y_1} & \frac{1}{y_1} & 0 \\ \mu_{21} & 1-\left(\mu_{21}+\frac{1}{y_2}\right) & \frac{1}{y_2} \\ 0 & \mu_{32} & 1-\left(\mu_{32}+\frac{1}{y_3}\right) \end{bmatrix} \tag{7.1}$$

The expected number of time intervals matrix is calculated from $N = \left[I - Q_n\right]^{-1}$

$$N = \begin{bmatrix} \frac{1}{y_1} & -\frac{1}{y_1} & 0 \\ -\mu_{21} & \mu_{21}+\frac{1}{y_2} & -\frac{1}{y_2} \\ 0 & -\mu_{32} & \mu_{32}+\frac{1}{y_3} \end{bmatrix}^{-1} \tag{7.2}$$

Determination of this matrix is found from (7.3).

$$\det(N) = \frac{\mu_{21}\mu_{32}}{y_1} + \frac{\mu_{21}}{y_1 y_3} + \frac{\mu_{32}}{y_1 y_2} + \frac{1}{y_1 y_2 y_3} - \left(\frac{\mu_{32}}{y_1 y_2} + \frac{\mu_{21}\mu_{32}}{y_1} + \frac{\mu_{21}}{y_1 y_3}\right) = \frac{1}{y_1 y_2 y_3} \tag{7.3}$$

Then,

$$N = y_1 y_2 y_3 \begin{bmatrix} \mu_{21}\mu_{32} + \frac{\mu_{21}}{y_3} + \frac{1}{y_2 y_3} & \mu_{21}\mu_{32} + \frac{\mu_{21}}{y_3} & \mu_{21}\mu_{32} \\ \frac{\mu_{32}}{y_1} + \frac{1}{y_1 y_3} & \frac{\mu_{32}}{y_1} + \frac{1}{y_1 y_3} & \frac{\mu_{32}}{y_1} \\ \frac{1}{y_1 y_2} & \frac{1}{y_1 y_2} & \frac{1}{y_1 y_2} \end{bmatrix}^T = \begin{bmatrix} N(1) & N(2) & N(3) \end{bmatrix}^T \tag{7.4}$$

Mean time to the first failure depends on the starting stage, if the device enters from stage 1, 2, or 3, MTTFF is the summation of matrix $N(1)$, $N(2)$, or, $N(3)$ and is shown in (7.5), (7.6) and (7.7).

$$MTTFF = y_1 + y_2 + y_3 + \mu_{21} y_1 y_2 + \mu_{32} y_2 y_3 + \mu_{21}\mu_{32} y_1 y_2 y_3 \tag{7.5}$$

$$MTTFF = y_2 + y_3 + \mu_{21} y_1 y_2 + \mu_{32} y_2 y_3 + \mu_{21}\mu_{32} y_1 y_2 y_3 \tag{7.6}$$

$$MTTFF = y_3 + \mu_{32} y_2 y_3 + \mu_{21}\mu_{32} y_1 y_2 y_3 \tag{7.7}$$

Let us assume that the system starts at stage 1, MTTFF is (7.5). Let

$T_0$ = Life time without maintenance

$T_E$ = Extended life time with maintenance

Transition rate from D1 to D2, from D2 to D3, and from D3 to F, are given in (7.8), (7.9), and (7.10).

$$\lambda_{12} = \frac{1}{y_1} \tag{7.8}$$

$$\lambda_{23} = \frac{1}{y_2} \tag{7.9}$$

$$\lambda_{3f} = \frac{1}{y_3} \tag{7.10}$$

Then,

$$T_0 = y_1 + y_2 + y_3 \tag{7.11}$$

$$T_E = \frac{\mu_{21}}{\lambda_{12}\lambda_{23}} + \frac{\mu_{32}}{\lambda_{23}\lambda_{3f}} + \frac{\mu_{21}\mu_{32}}{\lambda_{12}\lambda_{23}\lambda_{3f}} \tag{7.12}$$

$$MTTFF = T_0 + T_E \tag{7.13}$$

Notice that the extended time consists of the following terms;

- The first term, $\frac{\mu_{21}}{\lambda_{12}\lambda_{23}}$, is the ratio between the maintenance rate from stage 2 to stage 1 and the failure rate from stage 1 to 2 and 2 to 3.
- The second term, $\frac{\mu_{32}}{\lambda_{23}\lambda_{3f}}$, is the ratio between the maintenance rate from stage 3 to stage 2 and the failure rate from stage 2 to 3 and 3 to failure stage.
- The third term, $\frac{\mu_{21}\mu_{32}}{\lambda_{12}\lambda_{23}\lambda_{3f}}$, is the ratio between the two maintenance rates (from 2 to 1 and from 3 to 2) and the failure rate of all stages.

The extended life time of perfect maintenance model is a summation of all possible combinations of ratios between maintenance rate of the current stage and failure rate of the current and previous stage. Since $T_E$ can only be positive in this model, inspection and maintenance always extend the equipment life time. If the repair rate of each stage is high relative to the transition rate of that stage and the previous stage ($\mu_{21} >> \lambda_{12}\lambda_{23}, \mu_{32} >> \lambda_{23}\lambda_{3f}$), the device will have a very long extended lifetime.

### 7.5.2 MTTFF for Imperfect Maintenance Model

Truncated transitional probability matrix Q is constructed by deleting row 4 and column 4 which associated with the absorbing state [86].

$$Q_n = \begin{bmatrix} 1-\left(\lambda_{13}+\frac{1}{y_1}\right) & \frac{1}{y_1} & \lambda_{13} \\ \mu_{21} & 1-\left(\mu_{21}+\frac{1}{y_2}\right) & \frac{1}{y_2} \\ \mu_{31} & \mu_{32} & 1-\left(\mu_{31}+\mu_{32}+\frac{1}{y_3}\right) \end{bmatrix} \tag{7.14}$$

The expected number of time intervals matrix is calculated from $N = \left[I - Q_n\right]^{-1}$

$$N = \begin{bmatrix} \lambda_{13}+\frac{1}{y_1} & -\frac{1}{y_1} & -\lambda_{13} \\ -\mu_{21} & \mu_{21}+\frac{1}{y_2} & -\frac{1}{y_2} \\ -\mu_{31} & -\mu_{32} & \mu_{31}+\mu_{32}+\frac{1}{y_3} \end{bmatrix}^{-1} \tag{7.15}$$

Determination of this matrix is found from (7.16).

$$\det(N) = \frac{1}{y_1 y_2 y_3} + \frac{\lambda_{13}}{y_2 y_3} + \frac{\lambda_{13}\mu_{21}}{y_3} \tag{7.16}$$

Then,

$$N = \frac{1}{\det(N)} \begin{bmatrix} \frac{1}{y_2 y_3} + \mu_{21}(\mu_{31}+\mu_{32}) + \frac{\mu_{21}}{y_3} + \frac{\mu_{31}}{y_2} & \mu_{21}(\mu_{31}+\mu_{32}) + \frac{\mu_{21}}{y_3} + \frac{\mu_{31}}{y_2} & \mu_{21}(\mu_{31}+\mu_{32}) + \frac{\mu_{31}}{y_2} \\ \frac{1}{y_1 y_3} + \mu_{32}\lambda_{13} + \frac{\mu_{31}}{y_1} + \frac{\mu_{32}}{y_1} & \frac{1}{y_1 y_3} + \mu_{32}\lambda_{13} + \frac{\mu_{31}}{y_1} + \frac{\mu_{32}}{y_1} + \frac{\lambda_{13}}{y_3} & \mu_{32}\lambda_{13} + \frac{\mu_{31}}{y_1} + \frac{\mu_{32}}{y_1} \\ \frac{1}{y_1 y_2} + \frac{\lambda_{13}}{y_2} + \mu_{21}\lambda_{13} & \frac{1}{y_1 y_2} + \frac{\lambda_{13}}{y_2} + \mu_{21}\lambda_{13} & \frac{1}{y_1 y_2} + \frac{\lambda_{13}}{y_2} + \mu_{21}\lambda_{13} \end{bmatrix}^T \tag{7.17}$$

$$= \begin{bmatrix} N(1) & N(2) & N(3) \end{bmatrix}^T$$

Mean time to the first failure depends on the starting stage, if the device enters from stage 1, 2, or 3, MTTFF is the summation of matrix $N(1), N(2),$ or, $N(3)$ and is shown in (7.18), (7.19) and (7.20).

$$MTTFF = \frac{1}{\det(N)}\left(\frac{1}{y_2 y_3} + \frac{1}{y_1 y_3} + \frac{1}{y_1 y_2} + \mu_{21}(\mu_{31} + \mu_{32}) + \frac{\mu_{21}}{y_3} + \frac{\mu_{31}}{y_2} + \mu_{32}\lambda_{13} + \frac{\mu_{31}}{y_1} + \frac{\mu_{32}}{y_1} + \frac{\lambda_{13}}{y_2} + \mu_{21}\lambda_{13}\right) \quad (7.18)$$

$$MTTFF = \frac{1}{\det(N)}\left(\frac{1}{y_1 y_3} + \frac{1}{y_1 y_2} + \mu_{21}(\mu_{31} + \mu_{32}) + \frac{\mu_{21}}{y_3} + \frac{\mu_{31}}{y_2} + \mu_{32}\lambda_{13} + \frac{\lambda_{13}}{y_3} + \frac{\mu_{31}}{y_1} + \frac{\mu_{32}}{y_1} + \frac{\lambda_{13}}{y_2} + \mu_{21}\lambda_{13}\right) \quad (7.19)$$

$$MTTFF = \frac{1}{\det(N)}\left(\frac{1}{y_1 y_2} + \mu_{21}(\mu_{31} + \mu_{32}) + \frac{\mu_{31}}{y_2} + \mu_{32}\lambda_{13} + \frac{\mu_{31}}{y_1} + \frac{\mu_{32}}{y_1} + \frac{\lambda_{13}}{y_2} + \mu_{21}\lambda_{13}\right) \quad (7.20)$$

Let us assume that the system starts at stage 1, then the MTTFF is (7.21).

$$MTTFF = \frac{T_0 + T_E}{1 + \frac{\lambda_{13}}{\lambda_{12}} + \frac{\lambda_{13}\mu_{21}}{\lambda_{12}\lambda_{23}}} \quad (7.21)$$

$$T_E = \frac{\mu_{21}\mu_{31} + \mu_{21}\mu_{32} + \mu_{21}\lambda_{13} + \mu_{32}\lambda_{13}}{\lambda_{12}\lambda_{23}\lambda_{3f}} + \frac{\mu_{21}}{\lambda_{12}\lambda_{23}} + \frac{\mu_{31}}{\lambda_{23}\lambda_{3f}} + \frac{\mu_{31}}{\lambda_{12}\lambda_{3f}} + \frac{\mu_{32}}{\lambda_{23}\lambda_{3f}} + \frac{\lambda_{13}}{\lambda_{12}\lambda_{3f}} \quad (7.22)$$

The following observation is made regarding the relationships of inspection rate of each stage and MTTFF.

- It is possible that inspection and maintenance will reduce MTTFF at very high inspection rate of stage 1 (recall that high inspection in stage 1 will increase $\lambda_{13}$; thus, denominator may be large). This will increase the failure rate from stage 1 to 3; therefore, MTTFF may decrease. This conclusion is verified by the simulation result in Fig. 7.5.
- High inspection rate of stage 2 will increase the repair rate from stage 2 to 1 ($\mu_{21}$). Assuming that this repair rate is very high, MTTFF can be approximated as (7.23). This means that MTTFF will increase to a constant value. This is verified by the simulation result in Fig. 7.6.

$$MTTFF \approx \frac{1 + y_3(\mu_{31} + \mu_{32} + \lambda_{13})}{\lambda_{13}} \tag{7.23}$$

– High inspection rate of stage 3 increases the repair rate from stage 3 to 2 ($\mu_{32}$) and also repair rate of stage 3 to 1 ($\mu_{31}$). These rates are linearly related to MTTFF; therefore, the lifetime increases linearly with inspection rate of stage 3. This is verified by the simulation result in Fig. 7.7.

## 7.6 Cost Analysis

Cost equations are derived using steady state probability calculation. The cost analyses include failure cost, maintenance cost, and total cost. Maintenance cost in this analysis includes inspection cost based on the assumption of the equivalent model that maintenance is implemented at every inspection. These equations explain the simulation results in Fig. 7.8-7.19. Let

$FC$ = Repair cost after failure (dollar/time)

$MC$ = Maintenance cost (dollar/time)

$P(i)$ = Steady state probability of stage $i$, $i$ = 1,2, or 3

$C_F$ = Expected annual failure cost (dollar/year)

$C_M$ = Expected annual maintenance cost (dollar/year)

$C_T$ = Expected annual total cost (dollar/year)

$T_R$ = Repair time (year)

The expected failure cost per year is found from (7.24) and the expected maintenance cost per year is found from (7.25).

$$C_F = FC \times \text{frequency of failure} \tag{7.24}$$

$$C_M = MC \times \text{frequency of maintenance} \tag{7.25}$$

### 7.6.1 Cost Analysis for Perfect Maintenance Model

The transitional probability matrix shown in (7.26) and resulting steady state probability are derived in the following.

$$R = \begin{bmatrix} -\frac{1}{y_1} & \mu_{21} & 0 & \mu_F \\ \frac{1}{y_1} & -\left(\mu_{21} + \frac{1}{y_2}\right) & \mu_{32} & 0 \\ 0 & \frac{1}{y_2} & -\left(\mu_{32} + \frac{1}{y_3}\right) & 0 \\ 0 & 0 & \frac{1}{y_3} & -\mu_F \end{bmatrix} \tag{7.26}$$

Using frequency balance approach, steady state probability is calculated from (7.27).

$$P = \begin{bmatrix} -\frac{1}{y_1} & \mu_{21} & 0 & \mu_F \\ 1 & 1 & 1 & 1 \\ 0 & \frac{1}{y_2} & -\left(\mu_{32} + \frac{1}{y_3}\right) & 0 \\ 0 & 0 & \frac{1}{y_3} & -\mu_F \end{bmatrix}^{-1} \cdot \begin{bmatrix} 0 \\ 1 \\ 0 \\ 0 \end{bmatrix} \tag{7.27}$$

Determination of this matrix is shown in (7.28).

$$\det(P) = -\frac{1}{y_1}\cdot\left[(y_1\mu_{21}+1)\left(\mu_{32}+\frac{1}{y_3}\right)(\mu_F)+(y_1\mu_F+1)\left(\frac{1}{y_2}\right)\left(\frac{1}{y_3}\right)-(-\mu_F)\left(\frac{1}{y_2}\right)\right] \tag{7.28}$$

$$= -\frac{1}{y_1y_2y_3} - \mu_F\left(\frac{1}{y_1y_2}+\frac{1}{y_2y_3}+\frac{1}{y_1y_3}+\frac{\mu_{21}}{y_3}+\frac{\mu_{32}}{y_1}+\mu_{21}\mu_{32}\right)$$

From, $MTTFF = T_0 + \mu_{21}y_1y_2 + \mu_{32}y_2y_3 + \mu_{21}\mu_{32}y_1y_2y_3$, we have

$$\det(P) = -\frac{\mu_F}{y_1y_2y_3}\left(\frac{1}{\mu_F}+MTTFF\right) \tag{7.29}$$

Let $T_R = \frac{1}{\mu_F}$, the repair time (year), then

$$\det(P) = -\frac{\mu_F}{y_1y_2y_3}(T_R+MTTFF) \tag{7.30}$$

The probability of each state is shown in (7.31).

$$P = \frac{1}{(T_R+MTTFF)}\begin{bmatrix} y_1+y_1y_2\mu_{21}+y_1y_2y_3\mu_{21}\mu_{32} \\ y_2+y_2y_3\mu_{32} \\ y_3 \\ T_R \end{bmatrix} \tag{7.31}$$

Failure cost is found from (7.32).

$$C_F = FC\times P(3)\times\frac{1}{y_3} = \frac{FC}{T_R+MTTFF} \tag{7.32}$$

The failure cost is an average cost over lifetime in one cycle of the device. This indicates that as MTTFF increases, the annual failure cost will reduce and it can also reduce to zero. Consider the case of very frequent maintenance, this cost will approach zero. On the other hand, without maintenance; this cost will be an average cost over a total life time (life time without maintenance plus repair time). This indicates that failure

cost will be the highest without maintenance; therefore, maintenance helps reducing failure cost.

Maintenance cost is found from (7.33).

$$C_M = MC \times \left( P(2) \cdot \mu_{21} + P(3) \cdot \mu_{32} \right) = \frac{MC\left( y_2 \mu_{21} + y_3 \mu_{32} + y_2 y_3 \mu_{21} \mu_{32} \right)}{T_R + MTTFF} \tag{7.33}$$

Maintenance cost depends on repair rate of stage 2 and 3. Without maintenance, this cost is obviously zero. Consider the case of very frequent maintenance causing the device to stay in stage 1 longer, maintenance cost is the highest and equal to an average cost over a lifetime in stage 1. Therefore, maintenance cost increases from zero to some constant value.

The expected total cost is a summation of failure and maintenance cost. Clearly, without maintenance the total cost is only a failure cost which is an average cost over a total lifetime. Consider very frequent maintenance, failure cost is zero while maintenance cost is the highest. Thus, total cost is dominated by failure cost at small inspection rate and it is dominated by maintenance cost at high inspection rate. The next question arises as if, at all, we should do the maintenance.

Since maintenance is introduced in order to reduce the total cost, it should be implemented only if the highest possible total cost without maintenance is less than the highest possible total cost with maintenance, i.e.,

$$C_F\left( \mu_{21} = 0, \mu_{32} = 0 \right) < C_M\left( \mu_{21} \neq 0 \middle| \mu_{32} \neq 0 \right) \tag{7.34}$$

$$C_F\left( \mu_{21} = 0, \mu_{32} = 0 \right) = \frac{FC}{T_R + T_0} \tag{7.35}$$

$$C_M\left(\mu_{21}\neq 0 \middle| \mu_{32}\neq 0\right)=\begin{cases} C_M\left(\mu_{21}=0,\mu_{32}\to\infty\right)=\dfrac{MC}{y_2} \\ C_M\left(\mu_{21}\to\infty,\mu_{32}=0\right)=\dfrac{MC}{y_1} \\ C_M\left(\mu_{21}\to\infty,\mu_{32}\to\infty\right)=\dfrac{MC}{y_1} \end{cases} \tag{7.36}$$

Thus, the following inequality (7.37) should be considered.

$$\frac{FC}{T_R+T_0}>\frac{MC}{y_1} \quad or \quad \frac{MC}{y_2} \tag{7.37}$$

Similarly,

$$\frac{FC}{MC}>\frac{T_R+T_0}{y_1} \quad or \quad \frac{T_R+T_0}{y_2} \tag{7.38}$$

This means that if the ratio of failure cost and maintenance cost is higher than a constant value, then the maintenance should be implemented. Intuitively, if the failure cost is not expensive, we would rather replace the device than maintain it.

### 7.6.2 Cost Analysis for Imperfect Maintenance Model

The transitional probability matrix shown in (7.39) and resulting steady state probability are derived in the following.

$$R=\begin{bmatrix} -\left(\dfrac{1}{y_1}+\lambda_{13}\right) & \mu_{21} & \mu_{31} & \mu_F \\ \dfrac{1}{y_1} & -\left(\mu_{21}+\dfrac{1}{y_2}\right) & \mu_{32} & 0 \\ \lambda_{13} & \dfrac{1}{y_2} & -\left(\mu_{31}+\mu_{32}+\dfrac{1}{y_3}\right) & 0 \\ 0 & 0 & \dfrac{1}{y_3} & -\mu_F \end{bmatrix} \tag{7.39}$$

Using frequency balance approach, steady state probability is calculated from (7.40).

$$P=\begin{bmatrix} 1 & 1 & 1 & 1 \\ \frac{1}{y_1} & -\left(\mu_{21}+\frac{1}{y_2}\right) & \mu_{32} & 0 \\ \lambda_{13} & \frac{1}{y_2} & -\left(\mu_{31}+\mu_{32}+\frac{1}{y_3}\right) & 0 \\ 0 & 0 & \frac{1}{y_3} & -\mu_F \end{bmatrix}^{-1} \cdot \begin{bmatrix} 1 \\ 0 \\ 0 \\ 0 \end{bmatrix} \tag{7.40}$$

Determination of this matrix is shown in (7.41).

$$\det(P)=-\frac{\mu_F}{y_1y_2y_3}(T_R+MTTFF)(1+y_1\lambda_{13}+y_1y_2\mu_{21}\lambda_{13}) \tag{7.41}$$

The probability of each state is shown in (7.42).

$$P=\frac{1}{(T_R+MTTFF)}\begin{bmatrix} \frac{y_1+y_1y_2\mu_{21}+y_1y_3\mu_{31}+y_1y_2y_3\mu_{21}\mu_{31}+y_1y_2y_3\mu_{21}\mu_{32}}{(1+\lambda_{13}y_1+\lambda_{13}\mu_{21}y_1y_2)} \\ \frac{y_2+y_2y_3\mu_{31}+y_2y_3\mu_{32}+y_1y_2y_3\lambda_{13}\mu_{32}}{(1+\lambda_{13}y_1+\lambda_{13}\mu_{21}y_1y_2)} \\ y_3 \\ T_R \end{bmatrix} \tag{7.42}$$

Failure cost is found from (7.43).

$$C_F=FC\times P(3)\times\frac{1}{y_3}=\frac{FC}{T_R+MTTFF} \tag{7.43}$$

Failure cost equation of imperfect maintenance model is the same as that of perfect maintenance model; however, MTTFF equation is different. From MTTFF analysis, MTTFF will be greater than the lifetime without maintenance as long as the probability of transferring from stage 1 to 3 is not high which is usually true. Therefore,

failure cost reduces to a constant value as inspection rate of any stage increases. This conclusion is verified by simulation results in Fig. 7.8, 7.15 and 7.19.

Without any maintenance, $C_F = \frac{FC}{T_R + T_0}$ is the highest possible value. If the failure rate from stage 1 to stage 3 is significantly smaller than failure rate from stage 1 to stage 2 ( $\lambda_{13} << \lambda_{12}$ ) and failure rate from stage 2 to stage 3 ( $\lambda_{13} << \lambda_{23}$ ), then MTTFF increases and $C_F$ decreases as repair rates of any stages ( $\mu_{12}$ , $\mu_{31}$ , or $\mu_{32}$ ) increase. On the other hand, if the failure rate from stage 1 to stage 3 is slightly larger (or slightly smaller) than the failure rate from stage 1 to 2 ( $\frac{\lambda_{12}}{\lambda_{13}} \approx 1$ ), then MTTFF can be possibly small. If MTTFF is low relative to $T_R$ , then $C_F$ will converge to $C_F = \frac{FC}{T_R}$ .

Maintenance cost is found from (7.44).

$$C_M = MC \times \left( P(1) \cdot \lambda_{13} + P(2) \cdot \mu_{21} + P(3) \cdot \left( \mu_{31} + \mu_{32} \right) \right) \tag{7.44}$$

If the probability of transferring from stage 1 to stage 3 is insignificant then the analysis is the same as in perfect maintenance model. Maintenance cost will increase from zero to some constant value when inspection rates of D2 and D3 increase. This is verified by simulation results in Fig. 7.13 and Fig. 7.17. However, when inspection rate of stage 1 increases (probability of transferring from stage 1 to 3 is higher), maintenance cost could increase to infinity. This is verified by the simulation result in Fig. 7.9. It might be the case that the device condition gets worse and worse with every inspection and maintenance.

In terms of total cost, failure cost dominates total cost at small inspection rate while maintenance cost dominates total cost at high inspection rate. Total cost will be lowest at optimum region of inspection rate of stage 1 and high inspection rate of stage 2 and 3. This conclusion is verified by simulation results in Fig. 7.11, Fig. 7.15, and Fig. 7.19.

Note that in this cost analysis, the inspection cost is accounted in the maintenance cost. However, if the inspection is used only to determine the stage of the device then the inspection cost need to be addressed in the model separately.

## 7.7 Inspection Model

An inspection stage is added to the perfect maintenance model. The model is shown in Fig. 7.22. Note that the inspection stage has no transition rate to other stage under an assumption of perfect inspection that the device after inspection stays in the same stage.

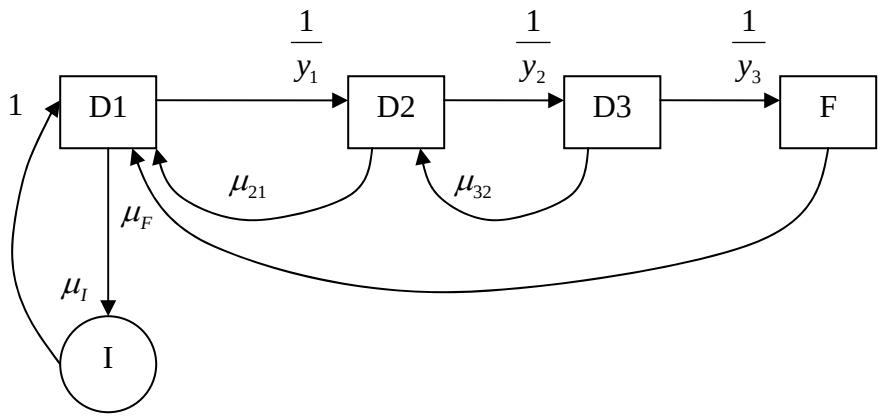


Fig. 7.22 Inspection Model

Transitional probability matrix and resulting steady state probability are derived in the following. Truncated transitional probability matrix Q is constructed by deleting row 4 and column 4 which associated with the absorbing state [86].

$$Q_n = \begin{bmatrix} 1-\left(\mu_I + \frac{1}{y_1}\right) & \frac{1}{y_1} & 0 & \mu_I \\ \mu_{21} & 1-\left(\mu_{21} + \frac{1}{y_2}\right) & \frac{1}{y_2} & 0 \\ 0 & \mu_{32} & 1-\left(\mu_{32} + \frac{1}{y_3}\right) & 0 \\ 1 & 0 & 0 & 0 \end{bmatrix} \tag{7.45}$$

The expected number of time intervals matrix is calculated from $N = \left[I - Q_n\right]^{-1}$.

$$N = \begin{bmatrix} \mu_I + \frac{1}{y_1} & -\frac{1}{y_1} & 0 & -\mu_I \\ -\mu_{21} & \mu_{21} + \frac{1}{y_2} & -\frac{1}{y_2} & 0 \\ 0 & -\mu_{32} & \mu_{32} + \frac{1}{y_3} & 0 \\ -1 & 0 & 0 & 1 \end{bmatrix}^{-1} \tag{7.46}$$

Determination of this matrix is shown in (7.47).

$$\det(N) = \frac{1}{y_1 y_2 y_3} \tag{7.47}$$

Assume that the device first entered from stage 1,

$$N(1) = \begin{bmatrix} y_1 + y_1 y_2 \mu_{21} + y_1 y_2 y_3 \mu_{21} \mu_{32} \\ y_2 + y_2 y_3 \mu_{32} \\ y_3 \\ \mu_I \left(y_1 + y_1 y_2 \mu_{21} + y_1 y_2 y_3 \mu_{21} \mu_{32}\right) \end{bmatrix}^T \tag{7.48}$$

Then, Mean time to the first failure is the time spent in stage 1, 2 and 3,

$$MTTFF = y_1 + y_2 + y_3 + \mu_{21} y_1 y_2 + \mu_{32} y_2 y_3 + \mu_{21}\mu_{32} y_1 y_2 y_3 \tag{7.49}$$

The transitional probability matrix and the resulting steady state probabilities are derived in the following. Transitional probability matrix is shown in (7.50).

$$R = \begin{bmatrix} -\left(\mu_I + \frac{1}{y_1}\right) & \mu_{21} & 0 & \mu_F & 1 \\ \frac{1}{y_1} & -\left(\mu_{21} + \frac{1}{y_2}\right) & \mu_{32} & 0 & 0 \\ 0 & \frac{1}{y_2} & -\left(\mu_{32} + \frac{1}{y_3}\right) & 0 & 0 \\ 0 & 0 & \frac{1}{y_3} & -\mu_F & 0 \\ \mu_I & 0 & 0 & 0 & -1 \end{bmatrix} \tag{7.50}$$

Using frequency balance approach, steady state probability is calculated from (7.51).

$$P = \begin{bmatrix} 1 & 1 & 1 & 1 & 1 \\ \frac{1}{y_1} & -\left(\mu_{21} + \frac{1}{y_2}\right) & \mu_{32} & 0 & 0 \\ 0 & \frac{1}{y_2} & -\left(\mu_{32} + \frac{1}{y_3}\right) & 0 & 0 \\ 0 & 0 & \frac{1}{y_3} & -\mu_F & 0 \\ \mu_I & 0 & 0 & 0 & -1 \end{bmatrix}^{-1} \cdot \begin{bmatrix} 1 \\ 0 \\ 0 \\ 0 \\ 0 \end{bmatrix} \tag{7.51}$$

Determination of this matrix is shown in (7.52).

$$\det(P) = \frac{\mu_F}{y_1 y_2 y_3}\left(T_R + T_I + MTTFF\right) \tag{7.52}$$

where $T_I$ is time in inspection stage and is given in (7.53).

$$T_I = \mu_I\left(y_1 + \mu_{21} y_1 y_2 + \mu_{21}\mu_{32} y_1 y_2 y_3\right) \tag{7.53}$$

Then, probability in each stage is given in (7.54).

$$P = \begin{bmatrix} \dfrac{y_1 + y_1y_2\mu_{21} + y_1y_2y_3\mu_{21}\mu_{32}}{T_R + T_I + MTTFF} \\ \dfrac{y_2 + y_2y_3\mu_{32}}{T_R + T_I + MTTFF} \\ \dfrac{y_3}{T_R + T_I + MTTFF} \\ \dfrac{T_R}{T_R + T_I + MTTFF} \\ \dfrac{\mu_I\left(y_1 + y_1y_2\mu_{21} + y_1y_2y_3\mu_{21}\mu_{32}\right)}{T_R + T_I + MTTFF} \end{bmatrix} \tag{7.54}$$

The conditional probabilities of stage 1, 2 and 3 given that the stages are in working stages (excluding time spent in inspection stage) is found from (7.55), (7.56), and (7.57) correspondingly. The steady stage probability for each stage is as follow.

$$P(1) = \frac{\dfrac{y_1 + y_1y_2\mu_{21} + y_1y_2y_3\mu_{21}\mu_{32}}{T_R + T_I + MTTFF}}{1 - \dfrac{\mu_I\left(y_1 + y_1y_2\mu_{21} + y_1y_2y_3\mu_{21}\mu_{32}\right)}{T_R + T_I + MTTFF}} = \frac{y_1 + y_1y_2\mu_{21} + y_1y_2y_3\mu_{21}\mu_{32}}{T_R + MTTFF} \tag{7.55}$$

$$P(2) = \frac{\dfrac{y_2 + y_2y_3\mu_{32}}{T_R + T_I + MTTFF}}{1 - \dfrac{\mu_I\left(y_1 + y_1y_2\mu_{21} + y_1y_2y_3\mu_{21}\mu_{32}\right)}{T_R + T_I + MTTFF}} = \frac{y_2 + y_2y_3\mu_{32}}{T_R + MTTFF} \tag{7.56}$$

$$P(3) = \frac{\dfrac{y_3}{T_R + T_I + MTTFF}}{1 - \dfrac{\mu_I\left(y_1 + y_1y_2\mu_{21} + y_1y_2y_3\mu_{21}\mu_{32}\right)}{T_R + T_I + MTTFF}} = \frac{y_3}{T_R + MTTFF} \tag{7.57}$$

Notice that the MTTFF equation in (7.49) is the same as that of the model without inspection. Moreover, the steady state probability equations (7.55), (7.56), and (7.57) are the same as those of perfect inspection model.

Intuitively, inspection by itself should not improve operating lifetime of the device since it is introduced only to determine the stage of the device. However, in this case the inspection has no transition rate to other stage because we assume perfect inspection that the device after inspected will stay in the same stage. Clearly, the inspection does not affect the failure and maintenance cost.

Inspection cost is analyzed as follow. Let

$IC$ = Inspection cost (dollar/time)

$C_I$ = Expected inspection cost (dollar/year)

The expected annual inspection cost is given in (7.58) and (7.59).

$$C_I = IC \times P(1) \times \mu_I \tag{7.58}$$

$$C_I = IC \times \frac{\mu_I \left( y_1 + y_1 y_2 \mu_{21} + y_1 y_2 y_3 \mu_{21} \mu_{32} \right)}{T_R + MTTFF} \tag{7.59}$$

Inspection cost is a linear function of inspection rate and probability of being in stage 1; therefore, high inspection rates and repair rates of going from any stage to stage 1 increase the inspection cost.

Obviously, inspection increases the total cost. However, inspection is intended to determine the stage of the device which is a crucial issue. Inspection is neither introduced to extend the device lifetime nor to reduce the cost. As long as the inspection does not cause the system to transit to higher stages, it should be implemented

## 7.8 Discussion and Conclusions

A probabilistic model for transformer maintenance optimization is proposed using the concept of representing the deterioration process by the device of stages. Analysis of inspection rate of each stage on MTTFF, failure cost, maintenance cost and inspection cost are investigated in the study. Simulation results from MATLAB are shown and verified by mathematical equations of the equivalent model. The study suggests the criteria of implementing maintenance by comparing the failure and maintenance cost. In addition, inspection model has been constructed for inspection cost analysis. The analysis suggests the inspection is introduced only to determine the stage of device.

# CHAPTER VIII

# CONCLUSIONS

## 8.1 Conclusions

Electric market deregulation is a driving force for efficient power system operation. The competitive environment demands high system reliability with the least cost. The need for optimizing available resources to maximize system reliability has assumed an increased importance. This dissertation examines two optimization problems involving power system reliabilty analysis, namely multi-area power system adequacy planning and transformer maintenance optimization.

Chapter II proposes a new simulation method for power system reliability evaluation. A sampling technique called Discrete Latin Hypercube Sampling (DLHS) is proposed. The proposed method provides both reliability indexes and their distributions and requires less computational time and memory than Latin Hypercube Sampling (LHS) in the sampling process. Comparative study shows that DLHS and LHS predict reliability indexes and distributions better than Monte Carlo simulation (MC). This contribution is beneficial to a wide-range of problems that involve integration of reliability assessment and optimization.

Chapters III to IV propose several solution methods to the multi-area power system adequacy planning problem. The first method proposed in Chapter III employs sensitivity analysis with Monte Carlo simulation. This method can be used as a guideline to quantify the effectiveness of additional generation to each area. The procedure is

simple yet effective enough to provide relationship between reliability indexes and additional capacity after one Monte Carlo simulation.

The second proposed method in Chapter IV applies scenario analysis with a state-space decomposition approach called Global Decomposition. The comparative algorithm allows efficient reliability evaluation which need not be performed completely in order to obtain optimal planning policy. The analysis applies to both generation, and transmission lines planning using loss of load probability as a reliability index of interest. The algorithm can also be extended to compute other reliability indexes such as frequency of loss of load.

After Global Decomposition, system reliability equation is derived which leads to the development of the third method using Dynamic programming presented in Chapter V. Using system loss of load probability (LOLP) as a reliability index, a dynamic programming approach based on LOLP simplified analytical formulation is developed. The equation relating LOLP to additional capacity in the system is derived. With reasonable assumptions, this complex function is approximated into a separable structure to which dynamic programming is effectively applied. Due to the approximation, the solution obtained is considered near optimal. Heuristic search is then applied to obtain optimal solution.

The fourth method presented in Chapter VI is in the stochastic programming framework. A two-stage recourse model is proposed to formulate the problem with expected unserved energy (EUE) cost as a reliability index. Unit avaiability of a generator is also included in the formulation. The L-shaped algorithm is applied to the

problem; however, the algorithm performs poorly with a large test system due to the dimensionality of system state space. Sample Average Approximation technique is employed to reduce computational time using two sampling techniques, namely Monte Carlo simulation and Latin Hypercube Sampling. The promising results from LHS are proved to be effective and better than those from MC.

In addition to the planning problem, Chapter VII discusses transformer maintenance optimization using a probabilistic model to devise the optimal maintenance schedule. A probabilistic maintenance model is proposed where mathematical equations relating maintenance practice and equipment lifetime and cost are derived. These closed-form expressions insightfully explain how the transformer parameters relate to reliability. This mathematical model facilitates an optimum, cost-effective maintenance scheme for the transformer.

## 8.2 Suggestions of Future Work

Simulation methods proposed in Chapter II are implemented on single area power system reliability analysis. The methods can be extended to a multi area power system level. Area load and generation correlations should also be addressed in the sampling process. In terms of planning problem, both LOLP and EUE can be integrated using probabilistic constrained stochastic programming. Although both indexes seem to be similar in the sense that they are probabilistic, LOLP is a discrete index while EUE is a continuous index in the optimization state space. Therefore, each index requires distinct approach to maneuver the solution algorithm, which is computationally

expensive. This challenge may be achieved by exploiting sampling techniques and introducing novel scenario selection schemes. The proposed methods for planning problem can be applicable to other power system optimization problems such as security and operation.

# REFERENCES

[1] P. Jirutitijaroen and C. Singh, "Comparison of Simulation Methods for Power System Reliability Indexes and their Distributions," *IEEE Transactions on Power Systems*, 2007, to be published.

[2] P. Jirutitijaroen and C. Singh, "Stochastic Programming Approach for Unit Availability Consideration in Multi-Area Generation Expansion Planning," in *Proceedings of the 2007 PES General Meeting*, Tempa, Florida, June 2007.

[3] M. Liefvendahl and R. Stocki, "A Study on Algorithms for Optimization of Latin Hypercubes," *Journal of Statistical Planning and Inference*, vol. 136, no. 9, pp. 3231-3247, September 2006.

[4] P. Jirutitijaroen and C. Singh, "Multi-Area Generation Adequacy Planning Using Stochastic Programming," in *Proceedings of the 2006 IEEE PES Power Systems Conference and Exposition*, Atlanta, Georgia, October 2006.

[5] P. Jirutitijaroen and C. Singh, "A Hybrid Method for Multi-Area Generation Expansion using Tabu-search and Dynamic Programming," in *Proceedings of the 2006 International Conference on Power System Technology*, Chongqing, China, October 2006.

[6] P. Jirutitijaroen and C. Singh, "Reliability and Cost Trade-Off in Multi-Area Power System Generation Expansion Using Dynamic Programming and Global Decomposition," *IEEE Transactions on Power Systems*, vol. 21, no. 3, pp. 1432-1441, August 2006.

[7] P. Jirutitijaroen and C. Singh, "A Method for Generation Adequacy Planning in Multi-Area Power Systems Using Dynamic Programming and Global Decomposition," in *Proceedings of the 2006 PES General Meeting*, Montreal, Quebec, Canada, June 2006.

[8] P. Jirutitijaroen and C. Singh, "A Global Decomposition Algorithm for Reliability Constrained Generation Planning and Placement," in *Proceedings of the 9th International Conference on Probabilistic Methods Applied to Power Systems*, Stockholm, Sweden, June 2006.

[9] J. T. Linderoth, A. Shapiro, and S. J. Wright, "The Empirical Behavior of Sampling Methods for Stochastic Programming," *Annals of Operations Research*, vol. 142, no. 1, pp. 215-241, February 2006.

[10] A. S. D. Braga and J. T. Saraiva, "A Multiyear Dynamic Approach for Transmission Expansion Planning and Long-Term Marginal Costs Computation," *IEEE Transactions on Power Systems*, vol. 20, no. 3, pp. 1631-1639, August 2005.

[11] S. Kannan, S. M. R. Slochanal and N. P. Padhy, "Application and Comparison of Metaheuristic Techniques to Generation Expansion Planning Problem," *IEEE Transactions on Power Systems*, vol. 20, no. 1, pp. 466-475, February 2005.

[12] J. Choi, A. A. El-keib, and T. Tran, "A Fuzzy Branch and Bound-Based Transmission System Expansion Planning for the Highest Satisfaction Level of the Decision Maker," *IEEE Transactions on Power Systems*, vol. 20, no. 1, pp. 476-484, February 2005.

[13] P. Jirutitijaroen and C. Singh, "The Effect of Transformer Maintenance Parameters on Reliability and Cost: A Probabilistic Model," *Electric Power System Research*, vol. 72, no. 3, pp. 213-224, December 2004.

[14] M. O. Buygi, G. Balzer, H. M. Shanechi, and M. Shahidehpour, "Market-Based Transmission Expansion Planning," *IEEE Transactions on Power Systems*, vol. 19, no. 4, pp. 2060-2067, November 2004.

[15] N. S. Rau and F. Zeng, "Adequacy and Responsibility of Locational Generation and Transmission – Optimization Procedure," *IEEE Transactions on Power Systems*, vol. 19, no. 4, pp. 2093-2101, November 2004.

[16] A. A. Chowdhury, B. P. Glover, L. E. Brusseau, S. Hebert, F. Jarvenpaa et al., "Assessing Mid-Continent Area Power Pool Capacity Adequacy Including Transmission Limitations," in *Proceedings of the 8th International Conference on Probabilistic Methods Applied to Power Systems*, Ames, Iowa, September 2004.

[17] N. Samaan, "Reliability Assessment of Electric Power Systems Using Genetic Algorithms," Ph.D. Dissertation, Texas A&M University, College Station, Texas, August 2004.

[18] X. Yu and C. Singh, "Expected Power Loss Calculation Including Protection Failures Using Importance Sampling and SOM," in *Proceedings of the 2004 IEEE PES General Meeting*, Denver, Colorado, June 2004.

[19] E. P. Zafiropoulos and E. N. Dialynas, "Reliability and Cost Optimization of Electronic Devices Considering the Component Failure Rate Uncertainty," *Reliability Engineering & System Safety*, vol. 84, no. 3, pp. 271-284, June 2004.

[20] P. Weng and R. Billinton, "Reliability Assessment of a Restructured Power System Considering the Reserve Agreement," *IEEE Transactions on Power Systems*, vol. 19, no. 2, pp. 972-978, May 2004.

[21] J. Bushnell, T. E. Mansur, and C. Saravia, "Market Structure and Competition: A Cross-Market Analysis of U.S. Electricity Deregulation," Center for the Study of Energy Market, University of California Energy Institute, Berkeley, California, 2004.

[22] L. Lawton, M. Sullivan, K. V. Liere, A. Katz, and J. Eto, "A Framework and Review of Customer Outage Costs: Integration and Analysis of Electric Utility Outage Cost Surveys," November 2003 [Online] Available: http://repositories.cdlib.org/lbnl/LBNL-54365

[23] P. Weng and R. Billinton, "Reliability Assessment of a Restructured Power System Using Reliability Network Equivalent Techniques," *IEE Proceedings-Generation, Transmission and Distribution*, vol. 150, no. 5, pp. 555-560, September 2003.

[24] N. Alguacil, A. L. Motto, and A. J. Conejo, "Transmission Expansion Planning: A Mixed-Integer LP Approach," *IEEE Transactions on Power Systems*, vol. 18, no. 3, pp. 1070-1077, August 2003.

[25] J. Bushnell, "Looking for Trouble: Competition Policy in the U.S. Electricity Industry," Paper presented at conference on Electricity Deregulation: Where from Here?, Bush Presidential Conference Center, Texas A&M University, July 2003.

[26] P. Joskow, “The Difficult Transition to Competitive Electricity Markets in the U.S.,” Paper presented at conference on Electricity Deregulation: Where from Here?, Bush Presidential Conference Center, Texas A&M University, July 2003.

[27] K. A. Klevorick, “The Oversight of Restructured Electricity Markets,” Paper presented at conference on Electricity Deregulation: Where from Here?, Bush Presidential Conference Center, Texas A&M University, July 2003.

[28] J. C. Helton, F. J. Davis, “Latin Hypercube Sampling and the Propagation of Uncertainty in Analyses of Complex Systems,” *Reliability Engineering & System Safety*, vol. 81, no. 1, pp. 23-67, July 2003.

[29] B. Verweij, S. Ahmed, A. J. Kleywegt, G. Nemhauser, and A. Shapiro, “The Sample Average Approximation Method Applied to Stochastic Routing Problems: A Computational Study,” *Computational Optimization and Applications*, vol. 24, pp. 289-333, February 2003.

[30] Federal Energy Regulatory Commission, “Office of Market Oversight and Investigations Energy Market Assessment 2003,” 2003, [Online] Available: www.ferc.gov/legal/ferc-regs/land-docs/fall2003-part1.pdf

[31] H. M. Khodr, J. F. Gomez, L. Barnique, J. H. Vivas, and P. Paiva et al., “A Linear Programming Methodology for the Optimization of Electric Power–Generation Schemes,” *IEEE Transactions on Power Systems*, vol. 17, no. 3, pp. 864-869, August 2002.

[32] H. T. Firmo and L. F. L. Legey, "Generation Expansion Planning: An Iterative Genetic Algorithm Approach," *IEEE Transactions on Power Systems*, vol. 17, no. 3, pp. 901-906, August 2002.

[33] B. Zhaohong and W. Xifan, "Studies on Variance Reduction Technique of Monte Carlo Simulation in Composite System Reliability Evaluation," *Electric Power Systems Research*, vol. 63, no. 1, pp. 59-64, August 2002.

[34] R. Kamat and S. Oren, "Multi-settlement System for Electricity Markets: Zonal Aggregation under Network Uncertainty and Market Power," in *Proceedings of the 35th Hawaii International Conference on System Sciences*, January 2002.

[35] IEEE/PES Task Force on Impact of Maintenance Strategy on Reliability of the Reliability, Risk and Probability Applications Subcommittee, "The Present Status of Maintenance Strategies and the Impact of Maintenance on Reliability," *IEEE Transactions on Power Systems*, vol. 16, no. 4, pp. 638-646, November 2001

[36] V. Wasserberg, H. Borsi, and E. Gockenbach, "An Innovation Online Drying Procedure for Liquid Insulated High Voltage Apparatus," in *International Symposium on Electrical Insulating Materials*, pp. 587 -590, November 2001.

[37] M. D. Wilkinson and P. Dyer, "Continuous Moisture Management: Extending Transformer Service Life," in *Proceedings of the 16th International Conference and Exhibition Publication on Electricity Distribution Part 1: Contributions. CIRED*, vol. 1, pp. 66, June 2001.

[38] S. Binato, G. C. de Oliveira, and J. L. de Araujo, “A Greedy Randomized Adaptive Search Procedure for Transmission Expansion Planning,” *IEEE Transactions on Power Systems*, vol. 16, no. 2, pp. 247-253, May 2001.

[39] J. F. Swidzinski and C. Kai, “Nonlinear Statistical Modeling and Yield Estimation Technique for Use in Monte Carlo Simulations [Microwave Devices and ICs],” *IEEE Transactions on Microwave Theory and Techniques*, vol. 48, no. 12, pp. 2316-2324, December 2000.

[40] IEEE Trial-Use Guide for Detection of Acoustic Emissions from Acoustic Emissions from Partial Discharges in Oil-Immersed Power Transformers, IEEE Std. C57.127-2000.

[41] D. Lieber, A. Nemirovskii, and R. Y. Rubinstein, “A Fast Monte Carlo Method for Evaluating Reliability Indexes,” *IEEE Transactions on Reliability*, vol. 48, no. 3, pp. 256-261, September 1999.

[42] N. S. Rau, “Assignment of Capability Obligation to Entities in Competitive Markets – The Concept of Reliability Equity,” *IEEE Transactions on Power Systems*, vol. 14, no. 3, pp. 884-889, August 1999.

[43] J. Mitra and C. Singh, “Pruning and Simulation for Determination of Frequency and Duration Indices of Composite Power Systems,” *IEEE Transactions on Power Systems*, vol. 14, no. 3, pp. 899-905, August 1999.

[44] A. de Pablo, “Furfural and Ageing: How Are They Related,” in *IEE Colloquium on Insulating Liquids*, pp. 5/1-5/4, May 1999.

[45] M. Keramat and R. Kielbasa, "Modified Latin Hypercube Sampling Monte Carlo (MLHSMC) Estimation for Average Quality Index," *Analog Integrated Circuits and Signal Processing*, vol. 19, no. 1, pp. 87-98(12), April 1999.

[46] W. K. Mak, D. P. Morton, and R. K. Wood, "Monte Carlo Bounding Techniques for Determining Solution Quality in Stochastic Programs," *Operations Research Letters*, vol. 24, pp. 47-56, February 1999.

[47] J. Lapworth and T. McGrail, "Transformer failure modes and planned replacement," in *IEE Colloquium on Transformer Life Management*, pp. 9/1-9/7, October 1998.

[48] C. Singh, A. D. Patton, A. Lago-Gonzalez, A. R. Vojdani, A.R., G. Gross et al., "Operating Considerations in Reliability Modeling of Interconnected Systems – an Analytical Approach," *IEEE Transactions on Power Systems*, vol. 3, no. 3, pp. 1119-1126, August 1998.

[49] A. White, "A Transformer Manufacturer's Perspective of Condition Monitoring Systems," in *IEE Colloquium on Condition Monitoring and Associated Database Handling Strategies*, pp. 4, June 1998.

[50] J. Endrenyi, G.J. Anders, and A.M. Leite da Silva, "Probabilistic Evaluation of The Effect of Maintenance on Reliability – An Application," *IEEE Transactions on Power Systems*, vol. 13, no. 2, pp. 576-583, May 1998.

[51] R. C. G. Teive, E. L. Silva, and L. G. S. Fonseca, "A Cooperative Expert System for Transmission Expansion Planning of Electrical Power Systems," *IEEE Transactions on Power Systems*, vol. 13, no. 2, pp. 636-642, May 1998.

[52] C. Myers, “Transformers-Conditioning Monitoring by Oil Analysis Large or Small; Contentment or Catastrophe,” in *Proceedings of the 1st IEE/IMechE International Conference on Power Station Maintenance - Profitability Through Reliability*, pp. 53-58, April 1998.

[53] S. H. Sim and J. Endrenyi, “Optimal Preventive Maintenance with Repair,” *IEEE Transactions on Reliability*, vol. 37, no. 1, pp. 92-96, April 1998.

[54] H. Salehfar and S. Trihadi, “Application of Perturbation Analysis to Sensitivity Computations of Generating Units and System Reliability,” *IEEE Transactions on Power Systems*, vol. 13, no. 1, pp. 152-158, February 1998.

[55] J. Mitra and C. Singh, “Capacity Assistance Distributions for Arbitrarily Configured Multi-Area Networks,” *IEEE Transactions on Power Systems*, vol. 12, no. 4, pp. 1530-1535, November 1997.

[56] J. Zhu and M. Chow, “A Review of Emerging Techniques on Generation Expansion Planning,” *IEEE Transactions on Power Systems*, vol. 12, no. 4, pp. 1722-1728, November 1997.

[57] V. A. Levi and M. S. Calovic, “A New Decomposition Based Method for Optimal Expansion Planning of Large Transmission Networks,” *IEEE Transactions on Power Systems*, vol. 6, no. 3, pp. 937-943, August 1997.

[58] C. Singh and J. Mitra, “Composite System Reliability Evaluation Using State Space Pruning,” *IEEE Transactions on Power Systems*, vol. 12, no. 1, pp. 471-479, February 1997.

[59] R. Billinton and A. Jonnavithula, "Composite System Adequacy Assessment Using Sequential Monte Carlo Simulation with Variance Reduction Techniques [Power Networks]," in *Proceedings of the IEE Generation, Transmission and Distributions*, vol. 144, no. 1, pp. 1-6, January 1997.

[60] J. R. Birge and F. Louveaux, *Introduction to Stochastic Programming*, 1st Edition, Duxbury Press, Belmont, California, 1997.

[61] C. Singh and N. Gubbala, "An Efficient Decomposition Approach for Multi-Area Production Costing," *Electric Power and Energy Systems*, vol. 18, no. 4, pp. 259-270, May 1996.

[62] J. L. Higle and S. Sen, *Stochastic Decomposition: A Statistical Method for Large Scale Stochastic Linear Programming*, Kluwer Academic Publishers, Dordrecht, The Netherlands, 1996.

[63] G. C. Oliveira, A. P. C. Costa, and S. Binato, "Large Scale Transmission Network Planning Using Optimization and Heuristic Techniques," *IEEE Transactions on Power Systems*, vol. 10, no. 4, pp. 1828-1834, November 1995.

[64] A. C. G. Melo and M. V. F. Pereira, "Sensitivity Analysis of Reliability Indices with respect to Equipment Failure and Repair Rates," *IEEE Transactions on Power Systems*, vol. 10, no. 2, pp. 1014-1021, May 1995.

[65] S. S. Oren, P. T. Spiller, P. Varaiya, and F. Wu, "Nodal Prices and Transmission Rights: A Critical Appraisal," *The Electricity Journal*, pp. 24-35, April 1995.

[66] N. V. M. Gubbala, "Realistic and Viable Methodologies for Reliability Evaluation of Multi-Area Interconnected Power Systems," Ph.D. Dissertation, Texas A&M University, College Station, Texas, December 1994.

[67] R. Romero and A. Monticelli, "A Zero-One Implicit Enumeration Method for Optimizing Investments in Transmission Expansion Planning," *IEEE Transactions on Power Systems*, vol. 9, no. 3, pp. 1385-1391, August 1994.

[68] M. M. Ahmad, A. Debs, and Y. Wardi, "Estimation of the Derivatives of Generation System Reliability Indices in Monte Carlo Simulation," *IEEE Transactions on Power Systems*, vol. 8, no. 4, pp. 1448-1454, November 1993.

[69] A. C. G. Melo, M. V. F. Pereira, and A. M. Leite da Silva, "A Conditional Probability Approach to the Calculation of Frequency and Duration Indices in Composite System Reliability Evaluation," *IEEE Transactions on Power Systems*, vol. 8, no. 3, pp.1118-1125, August 1993.

[70] A. D. Patton and S. K. Sung, "A Transmission Network Model for Multi-Area Reliability Studies," *IEEE Transactions on Power Systems*, vol. 8, no. 2, pp. 459-465, May 1993.

[71] G. Infanger, *Planning Under Uncertainty: Solving Large-Scale Stochastic Linear Programs*, Boyd & Fraser, Danvers, Massachusetts, 1993.

[72] Z. Deng and C. Singh, "A New Approach to Reliability Evaluation of Interconnected Power Systems Including Planned Outages and Frequency Calculations," *IEEE Transactions on Power Systems*, vol. 7, no. 2, pp. 734-743, May 1992.

[73] S. Sung, “Multi-Area Power System Reliability Modeling,” Ph.D. Dissertation, Texas A&M University, College Station, Texas, May 1992.

[74] J. H. Pickles, I. H. Russel, and J. F. Macqueen, “Importance Sampling for Power System Security Assessment,” in *Proceedings of the Probabilistic Methods Applied to Electric Power Systems*, 47-52, July 1991.

[75] C. Marnay and T. Strauss, “Effectiveness of Antithetic Sampling and Stratified Sampling in Monte Carlo Chronological Production Cost Modeling [Power Systems],” *IEEE Transactions on Power Systems*, vol. 6, no. 2, pp. 669-675, May 1991.

[76] C. Singh and Z. Deng, “A New Algorithm for Multi-Area Reliability Evaluation – Simultaneous Decomposition—Simulation Approach,” *Electric Power Systems Research*, vol. 21, pp. 129-136, 1991.

[77] IEEE Guide for the Interpretation of Gases Generated in Oil-Immersed Transformers, IEEE Std. C57.104-1991.

[78] A. Lago-Gonzalez and C. Singh, “The Extended Decomposition Simulation Approach for Multi-Area Reliability Calculations,” *IEEE Transactions on Power Systems*, vol. 5, no. 3, pp. 1024-1031, August 1990.

[79] A. Santos Jr., P. M. Franca, and A. Said, “An Optimization Model for Long-Range Transmission Expansion Planning,” *IEEE Transactions on Power Systems*, vol. 4, no. 1, pp. 94-100, February 1989.

[80] C. Singh and A. Lago-Gonzalez, "Improved Algorithm for Multi-Area Reliability Evaluation Using the Decomposition-Simulation Approach," *IEEE Transactions on Power Systems*, vol. 4, no. 1, pp. 321-328, February 1989.

[81] J. Endrenyi and S.H. Sim, "Availability Optimization for Continuously Operating Equipment with Maintenance and Repair," in *Proceedings of the 2nd International Conference on Probabilistic Methods Applied to Power Systems*, September 1988.

[82] IEEE Standard Test Procedure for Thermal Evaluation of Oil-Immersed Distribution Transformers, IEEE Std. C57.100-1986.

[83] P. Clancy, G. Gross, and F. F. Wu, "Probabilistic Flows for Reliability Evaluation of Multi-Area Power System Interconnection," *Electrical Power and Energy Systems*, vol. 5, no. 2, pp. 101-114, April 1983.

[84] D. Patton and C. Singh, "Operating Considerations in Generation Reliability Modeling – An Analytical Approach," *IEEE Transactions on Reliability*, May 1981.

[85] M. D. McKay, R. J. Beckman, and W. J. Conover, "A Comparison of Three Methods for Selecting Values of Input Variables in the Analysis of Output from a Computer Code," *Technometrics*, vol. 21, pp. 239-245, 1979.

[86] C. Singh and R. Billinton, *System Reliability Modeling and Evaluation*, Hutchinson Educational, London, 1977.

[87] P. Doulliez and E. Jamoulle, “Transportation Networks with Random Arc Capacities,” *Reveu Francaise d’Automatique, Informatique et Recherche Operationelle*, vol. 3, pp. 45-66, 1972.

[88] C. Singh, “Reliability Modeling and Evaluation in Electric Power Systems,” Ph.D. Dissertation, University of Saskatchewan, Saskatoon, Saskatchewan, Canada, August 1972.

[89] L. L. Garver, “Effective Load Carrying Capability of Generating Units,” *IEEE Transactions on Power Apparatus and Systems*, vol. PAS-85, no. 8, pp. 910-919, August 1966.

# APPENDIX A

## TWELVE AREA POWER SYSTEM DATA

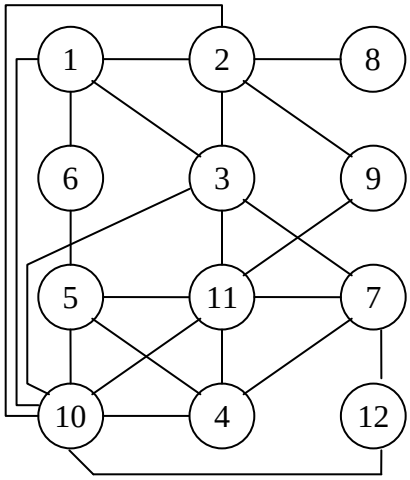


Fig. A.1 A Twelve Area Power System

Table A.1 A Twelve Area Generating Units Statistic

| Capacity Range(MW) | Number of Unit in Area | | | | | | | | |
|---|---|---|---|---|---|---|---|---|---|
| | 1 | 2 | 3 | 4 | 5 | 9 | 10 | 11 | 12 |
| 5-20 | - | - | 1 | - | - | 1 | 10 | 1 | - |
| 21-50 | 4 | - | 1 | - | 2 | 5 | 2 | 4 | - |
| 51-100 | 5 | 2 | 1 | - | 1 | 1 | - | 2 | - |
| 101-200 | 2 | 4 | 2 | - | 4 | 4 | 1 | 5 | 1 |
| 201-300 | 1 | 5 | 2 | 1 | - | 1 | - | 3 | 1 |
| 301-500 | 3 | 8 | 6 | 5 | - | - | 2 | 3 | 1 |
| 501-1000 | - | 8 | 6 | 1 | - | 1 | 2 | 1 | - |
| > 1000 | - | 6 | 4 | - | - | - | - | - | - |
| Total | 13 | 32 | 23 | 7 | 7 | 13 | 17 | 19 | 3 |

Table A.2 A Twelve Area Peak Load and Reliability Indexes

| Area | Peak Load (MW) | LOLP | EUE (MW) |
|---|---|---|---|
| 1 | 1900 | 0.0114 | 1.9866 |
| 2 | 18300 | 0.0026 | 2.4017 |
| 3 | 10250 | 0.0009 | 0.5176 |
| 4 | 2200 | 0.0109 | 2.2592 |
| 5 | 60 | 0.0027 | 0.1504 |
| 9 | 1200 | 0.0151 | 1.7049 |
| 10 | 2400 | 0.0701 | 17.935 |
| 11 | 2850 | 0.0034 | 0.5762 |
| 12 | 850 | 0.1435 | 21.285 |

Table A.3 A Twelve Area Cluster Load Data

| Cluster | Cluster Value ( times Peak Load) | Probability |
|---|---|---|
| 1 | 1.3309 | 0.0482 |
| 2 | 1.2198 | 0.1097 |
| 3 | 1.1178 | 0.1125 |
| 4 | 1.0140 | 0.1407 |
| 5 | 0.9206 | 0.1532 |
| 6 | 0.8144 | 0.1414 |
| 7 | 0.7204 | 0.1719 |
| 8 | 0.6145 | 0.1225 |

Table A.4 A Twelve Area Load Equivalent Transition Rates (Per Year)

| $\lambda_l^{ij}$ | j | | | | | | | |
|---|---|---|---|---|---|---|---|---|
| i | 1 | 2 | 3 | 4 | 5 | 6 | 7 | 8 |
| 1 | 0 | 1536 | 0 | 0 | 0 | 0 | 0 | 0 |
| 2 | 629 | 0 | 1441 | 82 | 0 | 0 | 0 | 0 |
| 3 | 44 | 1271 | 0 | 1662 | 780 | 0 | 0 | 0 |
| 4 | 0 | 135 | 1251 | 0 | 2047 | 313 | 0 | 0 |
| 5 | 0 | 0 | 359 | 1684 | 0 | 0 | 1965 | 183 |
| 6 | 0 | 0 | 0 | 216 | 1507 | 0 | 2440 | 7 |
| 7 | 0 | 0 | 0 | 0 | 506 | 1605 | 0 | 1221 |
| 8 | 0 | 0 | 0 | 0 | 0 | 90 | 1633 | 0 |

# APPENDIX B

## THIRTEEN AREA POWER SYSTEM DATA

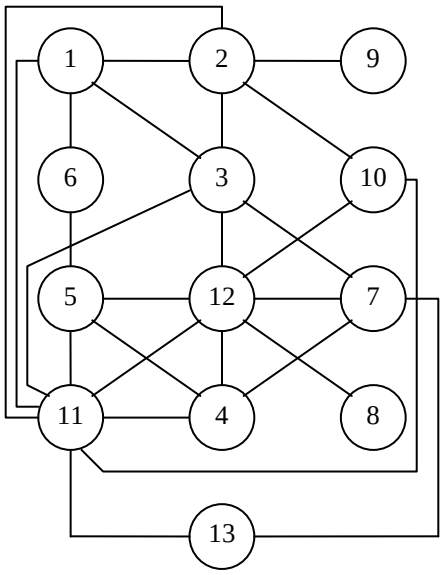


Fig. B.1 A Thirteen Area Power System

Table B.1 A Thirteen Area Installed Capacity and Peak Load

| Area | Installed Capacity (MW) | Peak Load (MW) |
|---|---|---|
| 1 | 2240 | 2024 |
| 2 | 22743 | 19144 |
| 3 | 14610 | 12573 |
| 4 | 2920 | 3087 |
| 5 | 79 | 301 |
| 6 | 468 | 0 |
| 7 | 3000 | 0 |
| 8 | 83 | 149 |
| 9 | 346 | 0 |
| 10 | 1785 | 1358 |
| 11 | 2595 | 1525 |
| 12 | 3546 | 3443 |
| 13 | 815 | 1613 |

Table B.2 A Thirteen Area Transfer Capability

| From Area | To Area | Installed Capacity (MW) |
|---|---|---|
| 1 | 2 | 3674.1 |
| 1 | 3 | 329.8 |
| 1 | 6 | 117.8 |
| 1 | 11 | 152.3 |
| 2 | 3 | 1064.9 |
| 2 | 9 | 159.7 |
| 2 | 10 | 708.1 |
| 2 | 11 | 393.9 |
| 3 | 7 | 384.2 |
| 3 | 11 | 203.1 |
| 3 | 12 | 55.3 |
| 4 | 5 | 37.9 |
| 4 | 7 | 334.9 |
| 4 | 11 | 181.9 |
| 4 | 12 | 110 |
| 5 | 6 | 358.9 |
| 5 | 11 | 35.2 |
| 5 | 12 | 590.4 |
| 7 | 12 | 334.7 |
| 7 | 13 | 799.6 |
| 8 | 12 | 129.1 |
| 10 | 11 | 99.6 |
| 10 | 12 | 118.4 |
| 11 | 12 | 140.7 |
| 11 | 13 | 117.8 |

# APPENDIX C

## THREE AREA POWER SYSTEM DATA

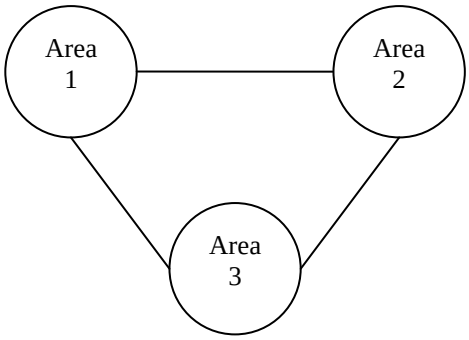


Fig. C.1 A Three Area Power System

Table C.1 Three Area Power System Generation Cumulative Probability

| State of Cap. Arc | Area 1 | | Area 2 | | Area 3 | |
|---|---|---|---|---|---|---|
| | Cap (MW) | Cum. Prob. | Cap (MW) | Cum. Prob. | Cap (MW) | Cum. Prob. |
| 7 | | | 600 | 1.000000 | | |
| 6 | 500 | 1.00000 | 500 | 0.737856 | 500 | 1.00000 |
| 5 | 400 | 0.67232 | 400 | 0.344640 | 400 | 0.67232 |
| 4 | 300 | 0.26272 | 300 | 0.098880 | 300 | 0.26272 |
| 3 | 200 | 0.05792 | 200 | 0.016960 | 200 | 0.05792 |
| 2 | 100 | 0.00672 | 100 | 0.001600 | 100 | 0.00672 |
| 1 | 0 | 0.00032 | 0 | 0.000064 | 0 | 0.00032 |

Table C.2 A Three Area Transfer Capability

| State of Cap. arc | Tie-line | | | | | |
|---|---|---|---|---|---|---|
| | 1-1 | | 1-2 | | 1-3 | |
| | Cap (MW) | Cum. Prob. | Cap (MW) | Cum. Prob. | Cap (MW) | Cum. Prob. |
| 2 | 100 | 1 | 100 | 1 | 100 | 1 |
| 1 | 0 | 0.1 | 0 | 0.1 | 0 | 0.1 |

Table C.3 A Three Area Load Parameters

| Load State | Area 1 (MW) | Area 2 (MW) | Area 3 (MW) | Probability |
|---|---|---|---|---|
| 1 | 500 | 600 | 500 | 0.028257 |
| 2 | 400 | 500 | 400 | 0.275288 |
| 3 | 300 | 400 | 300 | 0.436651 |
| 4 | 200 | 300 | 200 | 0.259803 |

Table C.4 A Three Area Generation Equivalent Transition Rates

| Area 1 | | | Area 2 | | | Area 3 | | |
|---|---|---|---|---|---|---|---|---|
| Cap (MW) | $\lambda^{+}_{g_1}$ | $\lambda^{-}_{g_1}$ | Cap (MW) | $\lambda^{+}_{g_2}$ | $\lambda^{-}_{g_2}$ | Cap (MW) | $\lambda^{+}_{g_3}$ | $\lambda^{-}_{g_3}$ |
| | | | 600 | 0.6 | 0 | | | |
| 500 | 0.5 | 0 | 500 | 0.5 | 1 | 500 | 0.5 | 0 |
| 400 | 0.4 | 1 | 400 | 0.4 | 2 | 400 | 0.4 | 1 |
| 300 | 0.3 | 2 | 300 | 0.3 | 3 | 300 | 0.3 | 2 |
| 200 | 0.2 | 3 | 200 | 0.2 | 4 | 200 | 0.2 | 3 |
| 100 | 0.1 | 4 | 100 | 0.1 | 5 | 100 | 0.1 | 4 |
| 0 | 0 | 5 | 0 | 0 | 6 | 0 | 0 | 5 |

Table C.5 A Three Area Transmission Lines Equivalent Transition Rates

| From Area - To Area | | | | | | | | |
|---|---|---|---|---|---|---|---|---|
| 1-2 | | | 1-3 | | | 2-3 | | |
| Cap (MW) | $\lambda^{+}_{t_{12}}$ | $\lambda^{-}_{t_{12}}$ | Cap (MW) | $\lambda^{+}_{t_{13}}$ | $\lambda^{-}_{t_{13}}$ | Cap (MW) | $\lambda^{+}_{t_{23}}$ | $\lambda^{-}_{t_{23}}$ |
| 100 | 0.0274 | 0 | 100 | 0.0274 | 0 | 100 | 0.0274 | 0 |
| 0 | 0 | 3 | 0 | 0 | 3 | 0 | 0 | 3 |

Table C.6 A Three Area Load Equivalent Transition Rates

| $\lambda^{ij}_{l}$ | Load state, j | | | |
|---|---|---|---|---|
| Load state, i | 1 | 2 | 3 | 4 |
| 1 | 0 | 1.3429 | 0.0206 | 0 |
| 2 | 0.3394 | 0 | 1.9753 | 0.0278 |
| 3 | 0.0085 | 1.3399 | 0 | 2.1036 |
| 4 | 0 | 0.0452 | 2.2370 | 0 |

# APPENDIX D

## TRANSFORMER MODEL PARAMETERS

Model parameters are given below.

| | | |
|---|---|---|
| Inspection cost | = | 100 $ |
| Oil filtering cost | = | 1,000 $ |
| Oil replacement cost | = | 10,000 $ |
| Failure cost | = | 100,000 $ |
| Mean time in D1 | = | 10 years |
| Mean time in D2 | = | 7 years |
| Mean time in D3 | = | 3 years |

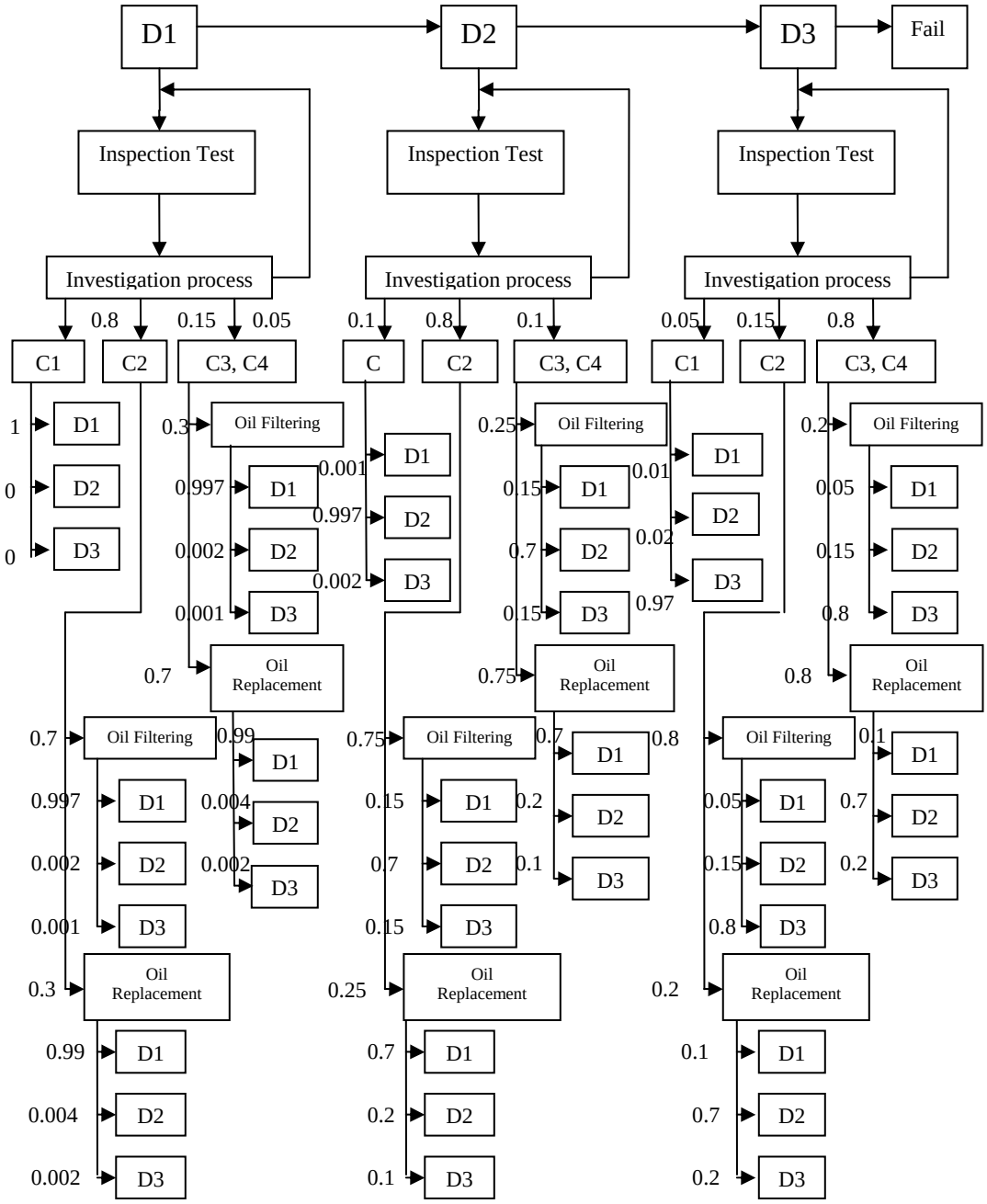


Fig. D.1 Transformer Model Parameters

# VITA

Panida Jirutitijaroen received the B.Eng. degree in electrical engineering from Chulalongkorn University, Bangkok, Thailand, in 2002. She earned a Ph.D. degree in electrical engineering at Texas A&M University. Her research interests include power system reliability and optimization methods applied to power system. She can be reached through Dr. Chanan Singh, Department of Electrical Engineering, Texas A&M University, College Station, TX 77843